Chemical, physical and mineralogical properties associated with the hardening of some South African fly ashes

A.E. Campbell
Chemistry B.Sc. Hons.
(University of Western Ontario)

Submitted in partial fulfilment of the
requirements for the degree of
Master of Science in Environmental Geochemistry

In the
Department of Geological Sciences
University of Cape Town

January, 1999

To James,

May his beautiful disposition never falter,
for what he has given me as a brother and a friend
is worth more than I can truly quantitate.

Acknowledgements

There are a number of people and institutions I would like to thank. without their help and encouragement this thesis would not have developed to the extent that it did:

Assoc. Professor Martin Fey and Assoc. Professor James Willis are congratulated for their excellent supervision and support during this dissertation. Their creative input, constant enthusiasm and support have made this academic exercise more rewarding than my wildest expectations. They truly are one of a kind;

Martin Ginster at Sasol, for his instrumental development of this project and the enthusiasm he has provided;

Sasol, for the generous bursary that has enabled me to fulfil this chapter of my academic career;

ESKOM, for the financial support of this course;

Dane Gerneke for patient and arduous time spent on the SEM and the great product that he produces;

Harro vonBlottnitz in the Department of Chemical Engineering, for arranging the use of the modulus of rupture instrument and his continued enthusiasm. Also in the Department of Chemical Engineering I must thank Hellen Divey for her assistance;

Dr. Richard Kruger (Ash Resources) and Prof. Mark Alexander (Dept of Civil Engineering, UCT), for providing valuable sources of literature that I could not have been able to obtain otherwise;

Patrick Sieas and Antoinette Upton, for general assistance in the laboratory;

David Wilson for preparing the fly ash polished thin sections;

To all of my fellow classmates, who endured the same road that I have recently travelled and had no hesitation relating to my problems and triumphs;

Portia Ceruti, for providing constant intellectual and moral support, belief in my abilities and endless encouragement;

Finally, my brother James and parents Sue and Graham for their constant support during this dissertation, albeit from afar, and belief in my abilities and consistent encouragement. I could not have done it without them.

Abstract

Coal combustion for power generation is relied on heavily in South Africa. The main residue from the combustion process is fly ash, with about 22 million tons being produced in 1994, of which only about 1 million tons is utilised. the remainder requiring disposal as waste. Various environmental impacts are associated with the disposal of fly ash in surface impoundments, including loss of usable land, contamination of groundwater, production of wind-blown particulates, effects on vegetation and aesthetic impacts. Ultimately the disposal of fly ash in the mined-out underground workings is highly sought after, as it may limit many of the impacts which fly ash induces on the environment.

The main purpose of this study was to assess the degree of hardening of four South African fly ashes from power stations at Kriel, Lethabo, Matla and Sasol in terms of their chemical, physical and mineralogical properties. Samples were taken of fresh and unweathered ashes from each power station.

Unweathered ash samples analysed by XRFS were found to have high contents of SiO_2 (49.9-56.3%), Al_2O_3 (27.2-31.5%), CaO (4.2-8.6%) and Fe_2O_3 (3.1-3.9%) with varying contributions from loss on ignition (L.O.I.) (0.4-4.4%) and MgO (1.1-2.2%). The major mineral phases detected in unweathered ash by XRD include quartz, mullite and glass, with smaller contributions from hematite and lime. Laser particle size analysis and liquid limit determination (Atterberg tests) were also conducted. The exceptionally high L.O.I of Sasol ash (4.4%) was attributed to the presence of partially burned coal, based on DTA and TGA investigation.

Modulus of rupture experiments were conducted on briquettes (dimensions 7.0 x 3.5 x 1.0 cm) of unweathered ash from Kriel, Matla, Lethabo and Sasol, which were wetted to their liquid limit and cured for 24 h under ambient conditions. The tests indicated that there is a strong linear relationship between total Ca content and the modulus of rupture for 3 of the 4 unweathered ashes. The fly ash from Kriel deviates from this relationship, providing evidence that other chemical (e.g. form of Ca) and physical factors (e.g. particle size) may also play a role in hardening.

Investigation by SEM of the morphology of weathered, hardened fly ash samples from Kriel, Matla and Sasol revealed contrasting abundances and types of secondary minerals. Although no secondary minerals were detected under SEM (maximum magnification 8000x) in Sasol fly ash, calcite was positively identified by XRD. Weathered Matla and Kriel fly ash contained an abundance of secondary minerals forming extensive inter-particle bridges. The presence of exfoliation layers on fly ash cenospheres in samples taken on the sides of the Kriel ash dam suggests that dissolution of the spheres occurs as weathering proceeds. Ettringite ($Ca_6Al_2(SO_4)_3.32H_2O$) and calcite ($CaCO_3$) were identified by XRD in samples from Kriel and Matla. No gypsum ($CaSO_4.2H_2O$) was detected in any fly ash sample.

Investigation of secondary minerals by SEM-EDXRF in hardened, weathered ash from Kriel and Matla indicated that they are enriched in Ca, Al and S with respect to both the bulk chemical analysis and also compared with underlying and surrounding phases. No enrichment of Si in the secondary minerals was found. This suggests a Ca-Al-SO_4 secondary phase such as ettringite.

Weathered ash from Kriel has a much higher total CaO content (10.8%) than unweathered ash (7.7%). This increase in Ca content corresponds to the appearance of calcite on the XRD pattern. It was postulated that such accumulation of calcite may occur predominantly as a surface crust by processes analogous to those involved in pedogenic calcrete formation.

Saturated paste and dilute aqueous extracts were prepared from three unweathered ashes and their composition changes monitored over a 24-hour period. Sasol pastes showed a sharp rise in both Ca concentration and pH within 5 minutes, whereas Matla took 6 hours for solution pH to reach a plateau of about 12.7, and Ca concentrations also increased gradually. During the later part of the equilibration period, pH remained high but Ca, SO_4 and other ions (including Na and Cl) showed steadily decreasing concentrations to as little as one-third of their earlier levels. Behaviour of the wetted Kriel ash was intermediate between that of

Sasol (fast) and Matla (slow reaction). The final solution composition showed indications of levelling off at a composition representing slight supersaturation with respect to gypsum. The co-precipitation of Na and Cl with the Ca and SO_4 suggests formation of a more complex secondary solid than gypsum, such as ettringite which is stable at high pH and which is structurally more amenable to accommodating impurities. The markedly differing rates of dissolution-precipitation reactions upon wetting the different ashes points to a possible explanation of differential hardening in terms of the classical relationship between strength and setting time documented in the cement technology literature.

The addition of between 1 and 5% CaO (as $Ca(OH)_2$) to unweathered Sasol fly ash produced a linear increase in the modulus of rupture of 24-hour fly ash briquettes, the increase having the effect of keeping the treated Sasol ash on the original trend line relating briquette strength to CaO content in Sasol, Lethabo and Matla (but not Kriel) ashes.

Observations made in the field and those made from laboratory experiments reveal certain inconsistencies in mineralogical data and in long-term (field-observed) hardening versus short-term (24 hour) experimental hardening, suggesting that a means for predicting ash hardening remains elusive. Nevertheless, there are some indications that further investigation may be very fruitful if field studies are expanded and if hardening experiments are conducted over longer periods than those used here.

Table of contents

List of figures

List of tables

Abbreviations and acronyms

ASTM	American Society of Testing and Materials
DTA	Differential thermal analysis
EC	Electrical conductivity
EDXRFS	Energy dispersive X-ray fluorescence spectrometry
IAP	Ion activity product
IC	Ion chromatography
K/A*10	$(K_2O/Al_2O_3)*10$
L.O.I.	Loss on ignition
μ	Ionic strength
OPC	Ordinary Portland cement
PAI	Pozzolanic activity index
PFA	Pulverised fly ash
PPI	Pozzolanic potential index
P_z	Pozzolanic index
SEM	Scanning electron microscopy
SI	Saturation index
TGA	Thermogravimetric analysis
XRD	X-ray diffractometry
XRFS	X-ray fluorescence spectroscopy

Chapter 1: Introduction

Industrialisation on a global scale coupled with population growth has resulted in a world demand for cheap fuel sources. Coal combustion inevitably has been the answer in many countries, of which South Africa is no exception considering the abundance of raw material that the nation possesses. As of 1997, South Africa's production of coal reached 206 Mt, with the majority being exported making South Africa the world's largest exporter of steam coal (Morris, 1997). The remainder, 60 to 80 Mt, is used for power generation within the country, constituting the most important power-generating source. Combustion of coal for power generation produces a variety of residues, the most abundant of which is pulverised fuel ash (PFA or fly ash). Eskom, South Africa's largest power producing company, generated 22 Mt of fly ash in 1994.

Fly ash is the combustion residue which enters the flue gas stream. The fly ash is removed from the coal combustion system by a series of electrostatic precipitators and, more recently, bag filters which remove sequentially finer particle size fractions before eventual release of the gas stream into the atmosphere. Fly ash is made up predominantly from the alterations that the pulverised coal has undergone during heating, combustion, melting, and vaporisation. The result of the transformation of coal to the ash is a fine-grained material consisting predominantly of spherical, glassy particles. The majority of fly ash produced is disposed of in ash dams or tailing ponds, the former gaining popularity due to increased disposal regulation in most industrialised countries, coupled with the increased costs for liners associated with wet disposal. Ultimately the ideal disposal method would be to return the ash back to the underground working from which the coal was harnessed. This however requires an improved knowledge of the hardening properties of fly ash.

Dry fly ash disposal is currently being carried out at several of South Africa's power stations. The disposal of South African fly ash into dams is unlikely to decline due to

the vast amounts of ash produced from coal combustion. The method of dry disposal is fairly new to the power generating industry in South Africa, resulting in several key questions that remain to be answered concerning the long-term disposal of the ash, as well as factors which affect hardening of the ash. Many of these types of disposal questions are the same as those yet to be answered definitively concerning the methods of wet ash disposal. This may stem from the fact that each ash is unique. Depending on the parent coal from which the fly ash was derived, combustion produces differing chemical and physical attributes of the fly ash.

Fly ashes exhibit hardening properties as well as pozzolanic properties. At first glance the two terms may appear the same, however, the property that the ash exhibits depends entirely on the system which it is used within. A pozzolan is an additive used within the cement industry to enhance the setting and hardening properties of the cement to which it is combined. The term pozzolan, pozzolanic activity and pozzolanicity are all applicable when discussing the use of fly ash within the cement industry or in a cement medium. However, when discussing the reactions that are responsible for the hardening of fly ash within its dump, the term pozzolan or any of its derivatives is not applicable, nor is it correct. Although the reactions that may be taking place during hardening and pozzolanic reactions may be similar and, in some cases identical, the use of the term pozzolan, or any derivation therein, will not be used within this dissertation unless specifically discussing previous studies that have utilised the term. However, a discussion and understanding of the pozzolanic activity will be presented as it provides insight into the hardening properties of fly ash.

Fly ashes, when added to a cement matrix, exhibit pozzolanic activity. When in a finely divided form and in the presence of moisture, the particles react chemically with $Ca(OH)_2$ at ambient temperatures to form compounds possessing cementicious properties. Essential requirements for pozzolanicity are that the material should be siliceous, glassy and finely divided. Lea (1971) suggests that the pozzolanic activity

of fly ash is indicative of the lime-pozzolan reaction but emphasises that the reaction is not very well understood.

Study of the hardening properties of fly ash has been limited around the world and especially in South Africa, whereas the pozzolanic activity of fly ash has been studied extensively. Globally most of the studies have been concentrated on the addition of fly ash as an admixture to ordinary Portland cement (OPC) and on how the fly ash alters the hydration products and affects the hardening of the end product cement. Little attention has been paid to the hardening activity of fly ash outside of its use as a pozzolan in cement. The cementation of fly ash, especially the secondary minerals formed as a result of hardening, is of fundamental importance not only in terms of responsible environmental disposal, but also in understanding the process of hardening and in manipulating this property to find further uses for the ash.

Disposal of fly ash must take on a broader spectrum if it is to be utilised effectively. Some of the further uses of ash include higher proportions of ash being used as a pozzolan in concrete structures and especially in road paving. Fly ash as a soil amendment has been researched for possible uses especially in the agricultural sector. The co-disposal of fly ash is an area that more research needs to be aimed because preliminary studies (Smit, 1998) have shown that stabilisation of soluble waste in fly ash bricks is probable and possible. All of these applications, however, require an increased understanding of the hardening reactions that fly ash undergoes outside of an OPC matrix.

The strategy of the present investigation into the cementation of fly ash was based on sampling a suite of South African coal burning power stations; Sasol, Matla, Kriel, and Lethabo. The stations were chosen based on the degree of hardening exhibited by the ash dams and whether the fly ash was known to possess cementitious activity. A series of samples were taken from each power station to try and achieve a range of weathering periods ranging from fresh fly ash collected from the hopper to highly weathered ash on old sections of the dumps. In embarking on this research

several questions evolved which were of importance and relevance in understanding not only the factors which affect the hardening of fly ashes, especially the secondary minerals produced as a result, but also to achieve a better understanding of South African fly ashes and their possibilities for enhanced underground disposal. This study was formulated to aid in the understanding of:

- The extent of hardening exhibited by a suite of South African fly ashes.
- The secondary minerals formed as a result of the hardening reactions.
- The factors which control the cementation (alkalinity of pore water, atmospheric CO_2 concentrations, chemical composition).
- Controlling factors which can be applied to produce cementation in samples which lack significant hardening properties, or conversely inhibit hardening in samples which possess the property.

The knowledge of the physical and chemical factors which determine the activity of fly ash is essential to the full exploitation of the combustion residue, both economically and environmentally. This thesis consists of three main sections starting with a comprehensive investigation of the recent and applicable literature on the subject. The physical, mineralogical and chemical components of fly ash will be reviewed in the literature review in addition to the factors which contribute to the hydration of pozzolans. The studies which have investigated the correlation between the pozzolanic activity of fly ash in terms of its crushing or compressive strength, and the factors which potentially contribute to its cementicious property will also be reported. An additional chapter is allocated to the results and discussions of the chemical and mineralogical characterisation of the ash samples, fly ash cementation and modulus of rupture, followed by a chapter on conclusions of the study.

Chapter 2: Chemical, mineralogical, and physical characteristics of fly ash and their effects on hardening – a literature review

2.1 Introduction

Fly ash, as defined by the American Society for Testing and Materials (ASTM) (1993), is the "finely divided residue that results from the combustion of ground or powdered coal and is transported from the boiler by flue gas". Fly ash must be distinguished from the coarser ash that collects at the bottom of the furnace, called bottom ash, because of physical and chemical differences. The general primary mineralogy and chemical composition of South African fly ash is well described and documented by Willis (1987), Lesch (1987), Lesch and Cornell (1987), and Bosch (1990). The chemical composition of fly ash is determined by the inorganic and organic constituents of the coal from which it was derived. Bituminous coal comprises 98% of South African production (Morris, 1997) and gives the ashes produced in South Africa their characteristic physical, mineralogical, and chemical attributes.

2.2 History and background

The term pozzolan has a rooted history with Roman builders, who along with the Greeks, recognised that certain volcanic deposits, if finely ground and mixed with lime and sand, yielded a mortar possessing superior strength. The best variety of the red or purple tuff used by the Roman builders was obtained from Pozzoli or Pozzuoli and the material acquired the name pozzolana. The definition today has been broadened. The term pozzolan is used to describe natural materials as well as some calcined clays and shales. Artificial pozzolans include fly ash, boiler slag and precipitated silica.

The major use of fly ash is as a pozzolan in cement, that is, it is used to assist in forming compounds possessing cementitious properties. Hubbard *et al.* (1985) define

PFA to have "compounds which, while having no direct cementitious properties, will react with Ca^{2+} ions released in cement hydration to form low solubility compounds of cementitious character". Thus, the pozzolanic activity constitutes the reactions, rate of reactions and the products of the pozzolan that form in a system to which it has been mixed.

The original materials used by the Greeks and the Romans were added to lime and sand to create a mortar, as are the modern day pozzolans added to cement. The term pozzolan, apart from implying that the material is siliceous or alumino-siliceous and finely divided, implies that the material is an additive. The red or purple volcanic tuff used by the Romans only became a pozzolan once it was added to the lime/sand mortar, and remained a volcanic tuff up to that point. Similarly, fly ash is a pozzolan and undergoes pozzolanic reactions when it is added to a cement system, but fly ash by itself outside of the realm of cement is not a pozzolan, it is fly ash.

Several authors (Fourie *et al.* (1997); Hodgson and Grobbelaar (1994)) have used the term pozzolanic activity to describe the reactions occurring in an ash dam or dump. It is my interpretation that the term is inappropriate, misleading and misused to describe reactions that are taking place in a single-phase system constituting fly ash by itself.

2.3 Physical and mineralogical characteristics of fly ash

Early studies by Watt and Thorne (1965) characterised the presence of eight different fly ash particle types by microscopic examination based on shape, colour and some physical characteristics (Table 2.1). The fineness of fly ash particles depends largely on the combustion temperature, the grinding size of introduced coal, and whether the resultant particle is spherical or irregular (Figure 2.1). Watt and Thorne (1965) showed by the production of synthetic fly ashes, and comparing them to 14 industrial ashes, that each primary fly ash particle is produced by the burning out of a single coal particle containing at most two mineral species. By contrast, the model adopted by the Centre for Civil Engineering Research and Codes (1992)

implies that many fly ash particles are derived from a solitary coal particle. Due to the high temperature reached during the instantaneous burning of coal, most of the mineral components in the coal melt and form small fused drops. Generally the ash particles produced vary in size from 1.0 to 300 microns and are frequently (70%) finer than 74 microns (no. 200 mesh), and averaging 50 microns in diameter (Helmuth, 1987).

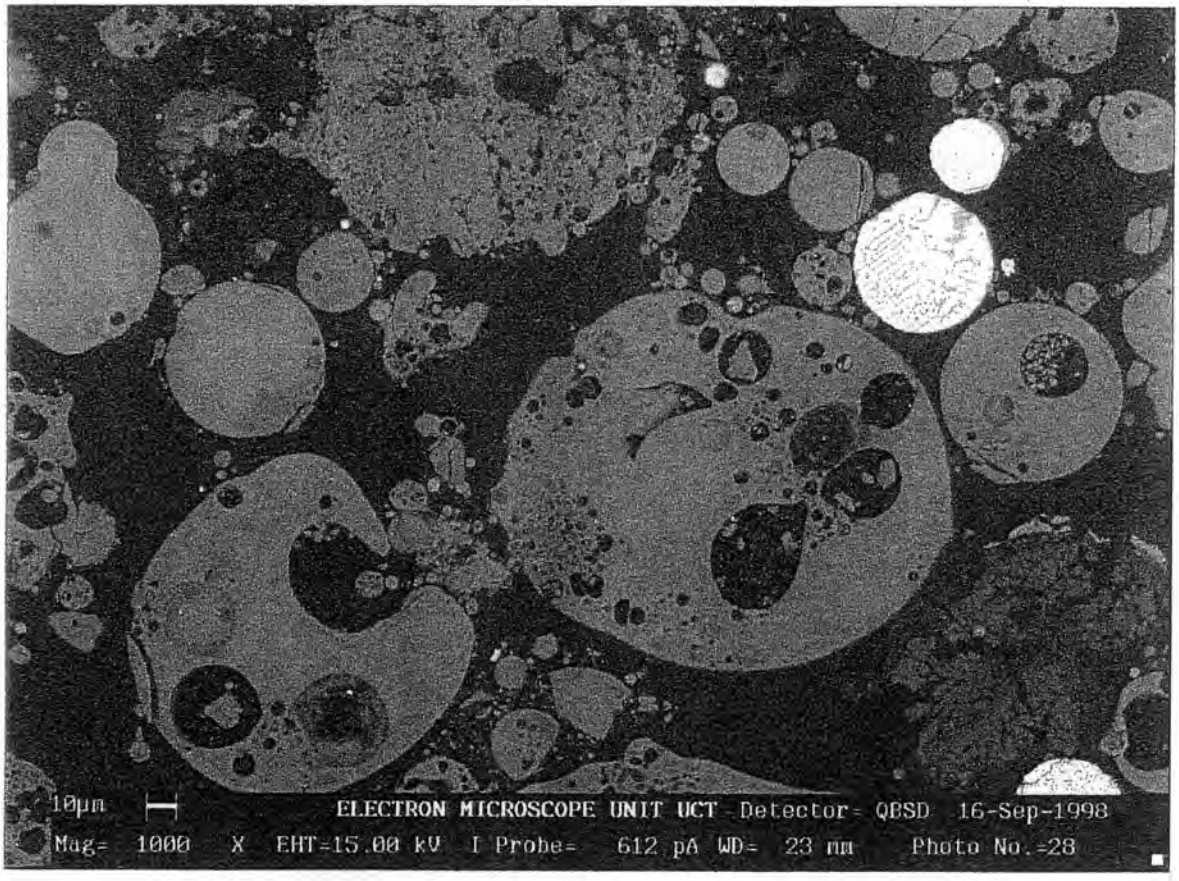

Figure 2.1: SEM image of a polished thin section of Matla fly ash, displaying contrasting spherical and angular nature of the particles and their different size fractions.

Table 2.1: Types of fly ash particles identified by microscopic examination (after Watt and Thorne, 1965)

Type	Shape	Colour	Crystallinity and texture	Characteristic diameter (μm)*	Comments
1	Spherical and rounded	Colourless	(a) Glassy, clear, solid (b) Glassy, containing small bubbles	0 – 20	
			(c) Glassy, with crystal traces	10 – 50	
			(d) Predominantly crystalline		
2	Spherical and rounded	Light brown to black	Lighter coloured ones; glassy; all solid	5 – 30	Increasing iron content
3	Rounded	White in reflected light	Glassy, spongy	10 – 200	Cenospheres
4	Irregular	Light brown	Partly crystalline, solid	10 – 100	Irregularity
5	Irregular	Varicoloured in reflected light	Partly crystalline, solid	50 – 500	Contains red particles
6	Irregular	Black	Solid or porous	20 – 200	Burnt coal
7	Angular	Colourless	Crystalline, solid	10 – 100	Quartz
8	Angular	Red	Crystalline, solid	5 – 50	Hematite

* The characteristic size range when the study was conducted may not reflect the same particle range observed in fly ashes today as a result of smaller mean particle sizes due to technological advancements.

Mehta (1994) found that fly ash particles containing higher amounts of CaO are finer than those containing lower quantities. The free CaO content is an important parameter because it will dissolve into solution at a faster rate than will the calcium contained within the glass matrix, which has implications towards the pH of the pore space and hence hardening reactions. Studies by Mather (1984) on the glass content in four low-calcium fly ashes from the eastern United States indicated that most of the glass particles were spheres in the 1-20 micron range. The finest fractions of fly ash are richest in glass, while carbon is most abundant in the coarsest fraction (Luke, 1961).

The crystallography of PFA varies depending on the parent material. Due to the rapid cooling of the fly ash from the flue gas, particles are composed chiefly (50-90%) of mineral matter in the form of glassy particles (Weshe, 1991). Quartz is the one mineral which survives the combustion process from coal, with a slight reduction in concentration from coal to ash (Hubbard *et al.*, 1984). Willis (1987) noted that the quartz content of South African fly ashes vary considerably from different precipitators at the same power station. This is speculated by Willis (1987) to be due to the quartz in the coal having a limited grain-size range and thus being associated with concentrations of fly ash which have similar grain size. The major mineralogical phases of South African fly ash include glass, mullite, and quartz (Willis, 1987; Lesch and Cornell, 1987). Other mineral phases in South African fly ash detected by Bosch (1990) in a study of the mineralogy and chemistry of fly ash from three coal burning power stations included lime, portlandite, and the Fe oxides hematite, maghemite and magnetite. The iron minerals magnetite and hematite, as well as K_2SO_4 and $CaSO_4$, may be present as smaller particles adhering to the surfaces of the spheres. The iron oxides and quartz also occur as separate angular particles.

Diamond (1983) found that the position of the X-ray diffraction maximum for glass in fly ash shifts progressively to higher 2θ angle values with increasing CaO content of the ash. This result was speculated by Diamond (1983) to be due to the presence of a calcium aluminate glass with ashes containing CaO contents

close to 20 percent, while higher amounts of silicate glass occur at lower CaO abundance.

A classification scheme with eleven morphological classes based on particle shape and opacity was developed by Fisher and Natusch (1979). Two classes of glassy spheres produced, cenospheres and plerospheres, dominate (67-95%) the morphology in the smaller particle size fraction of fly ash. Hubbard *et al.* (1985) suggest that the cenospheres are the most abundant type of sphere and that they must be considered the prime pozzolana or reactive phase. The clay minerals, predominantly kaolinite and illite, of the parent coal impurity are the source of the reactive components of fly ash as they are the components that produce the cenospheres. Illite contains up to 6% potash (K_2O) while kaolinite is essentially potash free which dramatically alters their transformations during combustion (Hubbard *et al.*, 1985). Raask (1968) described the process of cenosphere formation and described it to be due to the efficient fluxing capacity of potash in conjunction with CO_2 evolution during combustion that leads to the development of the cenosphere glass froth. Fisher *et al.* (1975) suggest that the crystals contained within the plerospheres may preferentially concentrate heavy metals, which may in turn influence the interaction of the sphere during hardening of the ash.

Much like the other physical parameters of fly ash, the specific gravity varies depending on the rank of coal from which it was derived. Cabrera *et al.* (1986) measured the specific gravity of 18 fly ashes from the United Kingdom and found that the range of specific gravity was 1.97-2.58 g/cm^{-3}. Malhotra and Ramezanianpour (1994) suggest that specific gravity values of about 3 are representative of iron-rich ashes, while values of about 2 tend to indicate the presence of hollow spheres. Separation of spheres into particle size fractions based on density differences may not be as efficient as other techniques due to the presence of hollow spheres.

2.4 Chemical properties of fly ash

Many of the physical properties of fly ash are related and attributed to the chemical components of the fly ash particles. The chemical composition of fly ash depends on the composition of the coal burned, but even fly ash from a single source may vary greatly over a relatively short (daily) time interval (Jarrige, 1971). Adriano *et al.* (1980) considered fly ash to be a ferro-alumino-silicate mineral with the elements Si, Al, Fe, Ca, K, and Na being predominant within the matrix. Spectrometric techniques show that SiO_2, Al_2O_3, Fe_2O_3, and CaO are the major constituents in most fly ashes. Studies of South African ash by Willis (1987) and Bosch (1990) showed high levels of Ti and P within the fly ash matrix compared with fly ashes from other coal burning nations.

Adriano *et al.* (1980) indicate that all naturally occurring elements are contained within fly ash and for the most part are concentrated with respect to the parent coal. The exceptions to increased concentration include the volatile elements which may be lost during the combustion process, that is if they do not condense on the surfaces of fly ash particles. Bosch (1990) noted that there was a tendency for higher concentrations of trace elements in PFA to be associated with smaller particle sizes. Coles (1979) recognised three classes of elements based on their enrichment as a function of particle size. The three classes are: elements which have little or no enrichment in the smaller particle size (Al, Ca, Fe, K, Mg, Mn, Na, Rb, Ti, Ce, La, and Nd); elements which are enriched in the smaller particle size (As, Ga, Mo, Pb, Se, W, and Zn); and elements the behaviour of which is intermediate between the two groups (Ba, Sr, Cr, Cu, Ni, U and V).

The additions of conditioning agents such as sulphur trioxide, sodium carbonate and bicarbonate, ammonium, and sodium sulphate, to improve the collection efficiency of electrostatic precipitators may affect fly ash composition. However, one of the more popular additives for enhanced electrostatic precipitation in South Africa is SO_3, of which very little is added to the flue gas stream and will unlikely alter the chemical makeup of the ash particles exiting the precipitation process.

Loss on ignition (LOI) of fly ash when burned at about 1000°C is due to the presence of carbonates, combined water in residual clay minerals and combustion of free carbon. In addition to a weight loss, an increase in weight on heating the sample may be due to oxidation of S and Fe compounds. Wesche (1991) indicates that carbon is the most important component of loss on ignition because it is the component which is important in determining the water requirement for mortars. The amount of water necessary to obtain a paste of normal consistency is greater when the carbon content is high, however factors such as fineness and specific surface area should not be discounted.

Comparisons of low-calcium and high-calcium fly ashes show that high-calcium fly ashes usually contain smaller amounts of unburned carbon (<1%) (Mehta, 1994). Complete removal of carbon in low-calcium fly ash is rare; the presence of 2-10% carbon is quite common. Carbon may be encapsulated in glass, but a major portion occurs as cellular particles which have large specific surface areas which can be detrimental to the pozzolanic activity of fly ashes. Surface enrichment of elements such as sulphur and volatile heavy metals on particle surfaces most likely occurs via condensation from the vapour phase. Hullett *et al.* (1980) suggest that the surface enrichment can also occur by diffusion from inside the particle during re-crystallisation and compositional differences and gradients resulting from re-crystallisation could affect the pozzolanic activity.

Hubbard *et al.* (1985) found a correlation between the K_2O/Al_2O_3 ratio and the concentration of amorphous aluminosilicate in fly ashes from the United Kingdom. Taylor (1997) indicates that it is the aluminosilicate phase which overwhelmingly takes part in pozzolanic activity and that the K_2O/Al_2O_3 ratio proposed by Hubbard *et al.* (1985) might be used as a pozzolanic potential index (PPI) to evaluate the use of fly ash in cement.

The classification of fly ash based on its chemical characteristics may be partitioned into one of two classes from the ASTM standards (1993); Class F and Class C (Table 2.2). Class F fly ash is normally produced from bituminous or anthracite coal and exhibits pozzolanic properties. Class C fly ash is normally

produced from burning sub-bituminous coal, which in addition to having pozzolanic properties also possesses some cementitous properties. Most SA fly ashes are Class F. In addition to the properties outlined for the two classifications of fly ash, the Class C ash contains higher levels of calcium. The higher level of calcium in the Class C fly ash with respect to the Class F fly ash has resulted in an alternative terminology; high-calcium and low-calcium fly ash.

Table 2. 2: ASTM standards classification of fly ash (ASTM, 1993)

	Class F	Class C
$SiO_2 + Al_2O_3 + Fe_2O_3$, min %	70.0	50.0
SO_3, max %	5.0	5.0
Moisture content, max %	3.0	3.0
LOI, max %	6.0	6.0
Available alkalis, as Na_2O, max %	1.5	1.5

2.5 Concrete and cement chemistry

Concrete is a concentrated suspension of particulate material of widely differing densities, particle sizes, and chemical compositions in a solution of lime and other components. The system is not static. As soon as the cement and water mix, reactions commence which ultimately produce the binder which consolidates the concrete mass. New particles are formed, and the original particles dissolve or are coated with cementitous products. ASTM (1993) defines a cementitious material as "a material which, when mixed with water, with or without aggregate, provides the plasticity and the cohesive and adhesive properties necessary for placement, and the formation of a rigid mass". The implication is that forces other than weak electrostatic van der Waal's forces are operative.

In many instances, the term 'cement' is used to describe ordinary Portland cement (OPC). In the context of this thesis, however, the term 'cement' will be applied in the broader sense. The chemistry of OPC has been reviewed extensively by Taylor (1997). A brief account of the hydration products involved in OPC is

covered here, which may aid in understanding more fully the bonding involved in fly ash.

2.5.1 Mineralogy and chemical reactions of OPC

Portland cement consists primarily of compounds of calcium and silicon with smaller amounts of iron and aluminium compounds. An accepted simplification to the complex chemistry of Portland cement is that it consists of four main compounds which react with water, producing reaction products involved in cementation reactions. The four reactants are tricalcium silicate (alite; Ca_3SiO_5), dicalcium silicate (belite; Ca_2SiO_4), tricalcium aluminate ($Ca_3Al_2O_6$), and tetracalcium aluminoferrite ($Ca_4Al_2Fe_2O_{10}$). Some of the more important hydration reactions are presented in equations 2.1 to 2.6.

$$2Ca_3SiO_5 + 6H_2O \rightarrow Ca_3Si_2O_7.3H_2O + 3Ca(OH)_2 \quad (2.1)$$

$$2Ca_2SiO_4 + 4H_2O \rightarrow Ca_3Si_2O_7.3H_2O + Ca(OH)_2 \quad (2.2)$$

$$Ca_3Al_2O_6 + 3CaSO_4.2H_2O + 26H_2O \rightarrow Ca_6Al_2O_6(SO_4)_3.32H_2O \quad (2.3)$$

$$Ca_3Al_2O_6 + CaSO_4.2H_2O + 10H_2O \rightarrow Ca_4Al_2O_6SO_4.12H_2O \quad (2.4)$$

$$Ca_3Al_2O_6 + Ca(OH)_2 + 18H_2O \rightarrow Ca_4Al_2O_7.19H_2O \quad (2.5)$$

$$Ca_4Al_2O_7Fe_2O_3 + 2Ca(OH)_2 + 10H_2O \rightarrow Ca_6Al_2Fe_2O_{12}.12H_2O \quad (2.6)$$

Tricalcium and dicalcium silicate compounds together comprise 70 to 80 percent of OPC and contribute most to the overall bonding of the cement (Eglington, 1987). The hydration of tricalcium silicate begins very early with a moderate evolution of heat up to a time of 28 days, at which point the hydration is all but complete (Wesche, 1991). While the hydration of tricalcium silicate contributes to the early strength of the cement, dicalcium silicate hydrates much more slowly and contributes to the strength of the cement at a later stage.

Tricalcium aluminate sets almost instantaneously. The rapid setting of the compound evolves a considerable amount of heat. The extent of heat release can be retarded by the addition of gypsum within the mix which forms the reaction product tricalcium sulphoaluminate, better known as the mineral ettringite

($Ca_6Al_3(SO_4)_2.32H_2O$). Ettringite is soluble in the pore water of the cement and forms coatings over the aluminate particles, which delays their hydration.

Tetracalcium aluminoferrite contributes very little to the strength of the cement as it hydrates very slowly. Very little heat is evolved during the formation of the reaction products.

2.5.2 Ettringite

An important mineral associated with the pozzolanic activity of Portland cements is ettringite. In a study by Bezuidenhout (1995), a possible solution to the decreased sulphate concentration observed in the leachate through an ash dam relative to the ash water, was the formation of ettringite. Hassett (1988, cited in Schwab, 1995) indicated that a decrease in the concentration of anions in weathered fly ash may be due to the formation of ettringite coupled with a group of chemically analogous isostructural compounds in which other oxyanions are substituted for sulphate [e.g. $As(OH)_3$, $H_2AsO_4^{2-}$, $B(OH)_3$, CrO_4^{2}, MoO_4^{2-}, SeO_3, SeO_4^{2-}, and $H_2VO_4^{2-}$].

Ettringite is only stable at high pH which is characteristic of fresh (unweathered) ash. Schwab (1995) indicated that ettringite will dissolve incongruently to gypsum, calcite and gibbsite as weathering proceeds and the pH decreases. It is probable that ettringite plays a substantial role in the early stages of hardening of fly ash. Joshi and Rosauer's (1973) study on the pozzolanic activity of synthetic fly ash identified, by X-ray diffraction analysis, the presence of ettringite in fly ash mortars within one week of reaction. After eight weeks of mortar curing the ettringite previously identified, ($Ca_6Al_2O_6(SO_4)_3.32H_2O$), had converted to the monosulphate form ($Ca_4Al_2O_6SO_4.12H_2O$) and it was speculated by Joshi and Rosauer (1973) that subsequent dissolution occurred to form calcite, gypsum and gibbsite.

Watt and Thorne (1966), Thorne and Watt (1965), and Joshi and Rosauer (1973) suggest that the reaction rate up to a period of 8-10 weeks is largely reaction controlled. Joshi and Rosauer (1973) indicate that after a period of eight weeks

each reacted ash particle contained a reaction product coating which allowed any further pozzolanic reaction to proceed only after available $Ca(OH)_2$ diffused through the reaction coating. This reaction coating may have been ettringite. It is suggested that after a period of 8 weeks the reaction rate shifts from being reaction-controlled to diffusion-controlled.

Ettringite formation in Portland cement plays havoc with the setting of the paste. Sulphates react with the hydrated aluminate products from tricalcium aluminate to give the high-sulphate tricalcium sulphoaluminate. Ettringite occupies more than twice the molecular volume of the reactant aluminate and expansive forces can exceed the tensile strength of the hardened mortar accompanying its formation.

2.6 Pozzolanic activity

Fly ash exhibits pozzolanic activity. A pozzolan is defined as a "siliceous or siliceous and aluminous material which in itself possesses little or no cementicious value but which will, in finely divided form and in the presence of moisture, chemically react with $Ca(OH)_2$ at ambient temperatures to form compounds possessing cementicious properties" (ASTM, 1993).

There is confusion with respect to the use of the term "pozzolanic reactivity". Takemoto and Uchikawa (1980) use the term to indicate the degree of the chemical reaction of the pozzolan and water with calcium hydroxide, or material which produces calcium hydroxide in water. Clifton *et al.* (1978; cited in Helmuth, 1987) use the term for the rate of reaction to produce strength giving phases. ISO uses the term "pozzolanicity" for the results obtained in tests to determine the reduction of the concentration of calcium dissolved in the liquid cement suspensions. Helmuth (1987) indicates that the degree of reaction is evidently inadequate unless a reaction time and test condition is specified, and if a specification is made then the term implies an average rate of reaction. Helmuth (1987) also states that the "degree of reaction" implies the ability to determine the 100% reacted state, or the ultimate degree of reaction. In addition, it may be difficult to determine, or even define, the "degree of reaction" because there are several different reactions taking place and these may occur at different rates.

The pH of ash varies depending on the S content. High-S coals produce acidic ashes as low as pH 4.5 while low-S coals, similar to those found in South Africa, produce alkaline ashes (pH 12) (Adriano *et al.*, 1980). Fresh (unweathered) ashes have pH values greater than 11 (Townsend and Gillham, 1975; Dudas, 1981) and as a consequence of weathering and leaching, stabilise at pH values of 7.8 (Dudas, 1981). Hodgson and Grobbelaar (1996) suggest two possibilities by which a drop in the pH of fly ash can occur under dry ash disposal conditions. They are:

- All or most of the calcium oxide has been converted to calcium carbonate, because of periodic carbon dioxide ingress into the ash, reacting with the calcium oxide and water.
- All or most of the calcium oxide is leached from the ash, because the ash is saturated with water.

Because of the dry ash disposal conditions involved in the study, the latter suggestion is not plausible, as the ash is not saturated with respect to water. Hodgson and Grobbelaar (1996) proposed that the CaO reacts with CO_2 at the atmosphere-ash boundary to form $CaCO_3$. Additionally, they suggested that the combination of calcium and sulphate precipitates gypsum ($CaSO_4.2H_2O$) to form a durable layer with calcite which comprises, what they defined as, the pozzolanic layer. The indication was that calcite and gypsum are the dominant minerals contributing to the hardness of fly ash dumps. However, very little chemical or mineralogical analyses were provided to substantiate the hypothesis. Malhotra and Ramezanianpour (1994) suggest that the pozzolanic activity of fly ash involved in cement reactions is mostly related to the reaction between the reactive silica of the pozzolan and $Ca(OH)_2$, which produces calcium silicate hydrate.

It is unlikely, as Hodgson and Grobbelaar (1996) suggest, that the CaO in fly ash (typically < 10%) would react to form enough calcite to be the most predominant cementing mineral phase. Malhotra and Ramezanianpour (1994) suggest that ettringite, monosulphoaluminate hydrate, and calcium silicate hydrate cause

hardening of fly ash when mixed with water, and make no mention of calcite (it was not stated however whether or not the reaction products were within an OPC matrix). This is not to say that calcite is not present in ash dam hardening. Bezuidenhout (1995) indicated the presence of mullite and quartz as the main mineral phases in an ash dam core, with smaller quantities of gypsum and calcite. It is possible that the calcite plays a major role in older highly weathered ashes and is not a factor in the early stages of hardening reactions within the ash dam.

2.6.1 Fly ash hydration reactions

Malhotra and Ramezanianpour (1994) indicate that high calcium fly ashes have self hardening properties caused by reactions of fly ash when added to water through formation of ettringite, monosulphoaluminate hydrate and a calcium silicate hydrate gel (indefinite composition). The early stages of hydration reactions determine the initial pozzolan microstructure as well as set the stage for the later strength which the hardened ash exhibits in a cement mortar. The reactivity of the glassy spheres depends on the alkali content in solution; high alkalinity should increase the rate of reaction of the spheres while pore water with lower alkalinity would be expected to slow the reaction rate.

2.6.2 Factors affecting hardening properties of fly ashes

Many characteristics have been studied with respect to attempting to establish a relationship between fly ash composition and pozzolanic properties in the cement paste. Characteristics including fineness, specific surface area, density, glass content, calcium content, carbon content, silica and silica plus alumina content. Watt and Thorne (1995, 1966) and Thorne and Watt (1995) utilised 14 fly ashes in an attempt to identify the most important physical and chemical characteristics which determine the pozzolanic activity of fly ash as indicated by strength tests in fly ash mortars. Joshi and Rosauer (1973) and Cabrera and Gray (1973) also attempted to establish the effects of variations in chemical composition, degree of crystallinity, and specific surface area on the pozzolanic activity of fly ashes. Ravina (1980) studied the correlation between the pozzolanic activity of eight low-calcium fly ashes and their fineness as determined by the amount retained on a 45-micron sieve, and found a linear relation between the specific surface area of

PFA and its pozzolanic activity index. Although Malhotra and Ramezanianpour (1994) indicate that high calcium fly ashes have self-hardening properties, Joshi and Rosauer (1973) found no clear relation between calcium content and pozzolanic strength of fly ash in cement pastes.

Watt and Thorne (1966) developed a theoretical relationship between the specific surface area of an ash and its activity. Assuming that all parts of the surface of a fly ash sphere are attacked at the same rate, the volume of the reacting layer (V) at any time will be;

$$v = \int_{r_o}^{r_o - d} 4r^2 \, dr \qquad \text{Equation 2.2}$$

(where d is the thickness of the reacted surface layer, and r_o is the initial radius). The curve obtained from the theoretical approach represents the course of reaction of the ash on an arbitrary time scale. The calculated values agree with those obtained experimentally confirming a relationship between particle size and the degree of reaction. Joshi and Rosauer (1973) and Ravina (1980) confirmed, using synthetic fly ash mortars, that the compressive strength values were directly proportional to specific surface area. Thorne and Watt (1965) reported correlations between crushing strength of mortars at 365 days in relation to SiO_2 and SiO_2 plus Al_2O_3 content of fly ash. They noted that fly ashes produced mortars which developed strengths at different rates, but not in any systematic way. Contrary to Thorne and Watts' findings, many studies found little agreement between the total silica plus alumina content present in fly ash, and pozzolanic activity. This can be attributed to the various mineral forms that the silica and alumina can occur as, which will alter the reaction matrix of the ash.

Joshi and Rosauer (1973) demonstrated the presence of iron, other than incorporated in an aluminosiliceous form, reduced strength development substantially. Most iron oxides in fly ash are present as non-reactive hematite and magnetite, and only perturb the reactivity of fly ash when they are present within the glass. Joshi and Rosauer (1973) also found that magnetic benefication only slightly increased pozzolanic strength.

2.7 Assessment of pozzolanic activity in relation to cement

Many studies have utilised modulus of rupture as an index of the strength of fly ash briquettes or to determine the probable breaking load on a beam. The modulus of rupture is expressed as the maximum stress in the material when failure occurs in bending. For a beam of rectangular cross section, such as that which will be used in this dissertation, the modulus of rupture, S, is given by the equation;

$$s = \frac{3FL}{2bd^2} \qquad \text{Equation 2.2}$$

where F = the breaking force applied at the centre of the briquette beam span, L= the distance between the briquette and supports, b = the width of the briquette, and d = the depth or thickness of the briquette (Reeve, 1982).

Thorne and Watt (1965) conducted crushing strength tests on lime mortars to try and establish relationships between the strength of the mortar and carbon content, glass content, silica and alumina content, density, and specific surface area. They concluded that for short periods of curing there was no obvious correlation between parameters tested and the crushing strength. Joshi and Rosauer (1973) also used modulus of rupture tests to establish that the pozzolanic activity of synthetic fly ash is influenced more by the amount of glassy phase than by particle size.

To establish what role CO_2 plays in the hardening of South African fly ash, Fourie *et al.* (1997) subjected mortars to curing in 100% CO_2 and N_2 environments followed by modulus of rupture experiments. The results of these sets of experiments showed an increase in the breaking force (hardening) over time for Matla fly ash mortars under a 100% CO_2 environment, while no change was observed under 100% N_2. Fourie *et al.* (1997) attributed the increased strength to calcite production in the mortar, however they were working under the premise which $CaCO_3$ was the major binding agent. In addition to the strength increase for Matla fly ash under a 100% CO_2 environment, Duvha fly ash under the same

conditions exhibited a decrease in strength. The results and experiments conducted warrant repetition. The attempt to relate the properties of fly ash to the pozzolanic activity has been almost entirely focussed for its use as an admixture in cement. Raask and Bhaskar (1975) found that the rate of dissolution of pure silica in HF was directly proportional to the surface area and that the rate coefficient defined as the 'pozzolanic index' (P_z) could be used to select PFA for its use in concrete mixes. Another index created to try to establish a relationship was by Hubbard *et al.* (1985) who developed the pozzolanic potential index (PPI) which allows compositional characterisation of PFA for use in concrete.

No studies have been found relating the characteristics of fly ash to the strength that it will achieve when placed in an ash dump. It is quite probable that many of the tests and methods utilised to analyse fly ash for use in concrete will be inappropriate for testing the strength of fly ash outside of its use in concrete.

2.8 Conclusions

Generation of electricity using coal-burning power stations is not likely to decrease in South Africa due to the amplitude of high-grade coal seams within the country. The most abundant coal combustion residue is fly ash. At the present time the fly ash produced has found little application outside of Portland cement admixtures, not nearly enough to substantially decrease the quantities being disposed of in ash dumps. Disposal of fly ash has been in the wet form as a slurry with water or dry ash disposal in ash dams. Environmental contamination from fly ash disposal on terrestrial ecosystems include leaching of potentially toxic substances, vegetation and food chain effects (Carlson and Adriano (1993), as well as groundwater contamination from ash dam leachate (Bezuidenhout, 1995), air pollution (Linton *et al.*,1977) from wind blown particulates and aesthetic pollution. In addition to surface disposal, an alternative is to return the ash as a slurry back to the underground workings from where the coal originated.

Examination of the literature has revealed that the characterisation of South African fly ash with respect to chemistry, primary mineralogy, and physical characteristics have been well documented. What is lacking in the literature is a comprehensive study of what happens to the chemical and mineralogical properties of fly ash once it has been incorporated into a slurry and allowed to harden in an ash dam.

There are conflicting opinions worldwide as to the pozzolanic activity of fly ash and the mechanism by which it hardens. From a host of papers it would seem as though the term "pozzolanic activity" has been broadened and ill defined to such an extent that the term may have become redundant and somewhat misleading, certainly within the realm of ash dam hardening. The term has found to be inappropriate when discussing fly ash hardening outside of a cement context. Factors which have been studied in relation to pozzolanic activity are extensive but yet no direct confirmation and agreement of a correlation has been achieved. A common trend throughout the literature is the disagreement as to the physical, chemical, and mineralogical factors which can be used to assess the pozzolanic activity and it would follow that these same factors may not relate to hardening of ash dams.

Most studies have been limited to assessing the pozzolanic activity of fly ash associated in an OPC matrix. The study by Fourie *et al.* (1997) does address fly ash hardening out of an OPC network but is lacking a comprehensive chemical analysis to accompany the physical components of the study. In addition, the study warrants repeat due to the superficial coverage of the topic and the lack of any in depth data to support the proposed findings. The study by Bezuidenhout (1995) touches on the secondary minerals within a South African ash dump and is the springboard for the work contained within this thesis. Few studies have been encountered concerning the secondary minerals produced in South African as a result of the reaction of fly ash in an alkaline environment.

Chapter 3: Materials and methods

Fly ash, whether disposed dry or in an ash dam or pond, varies with respect to the hardness it attains over a specific weathering and setting period. South African ash dumps display a variety of setting strengths and for this reason a suite of fly ash dams has been sampled. The coal burning power stations that were sampled for fly ash include Kriel, Lethabo, Matla, and Sasol. The locations of the above mentioned sampling sites on the South African Highveld are displayed in Figure 3.1. The reasoning behind choosing the various power stations to sample is outlined in the following chapter, coupled with brief descriptions of the methods used to characterise them:

3.1 Sampling strategy

The choice of sampling Lethabo, Kriel, Matla and Sasol was specific in order to obtain a range of fly ashes displaying hardened properties of varying degrees, some showing a high setting strength as well as those displaying weak strength. Lethabo and Sasol display, at best, poor hardening within the ash dam, while Matla, and especially Kriel, display concrete-like hardening. Of the four power stations sampled Sasol is the only coal burning power station that is not part of ESKOM's national electricity grid. The power plant at Sasol is used for production of electricity within the organisation for manufacturing and conversion of petroleum by-products.

Lethabo and Matla were chosen for two reasons. Firstly, their respective disposal methods, dry ash disposal in a dump at Lethabo and wet disposal in a dam at Matla, exhibited contrasting hardening properties. Lethabo lacks significant hardening while Matla displays high strength. The pair of samples provided an opportunity to compare and contrast the two disposal methods. Secondly, they are the two power stations that produce fly ashes currently being marketed, by Ash Resources Ltd., for use as a pozzolan within the cement manufacturing sector. Lethabo is sought after for its apparent small mean particle size and its close

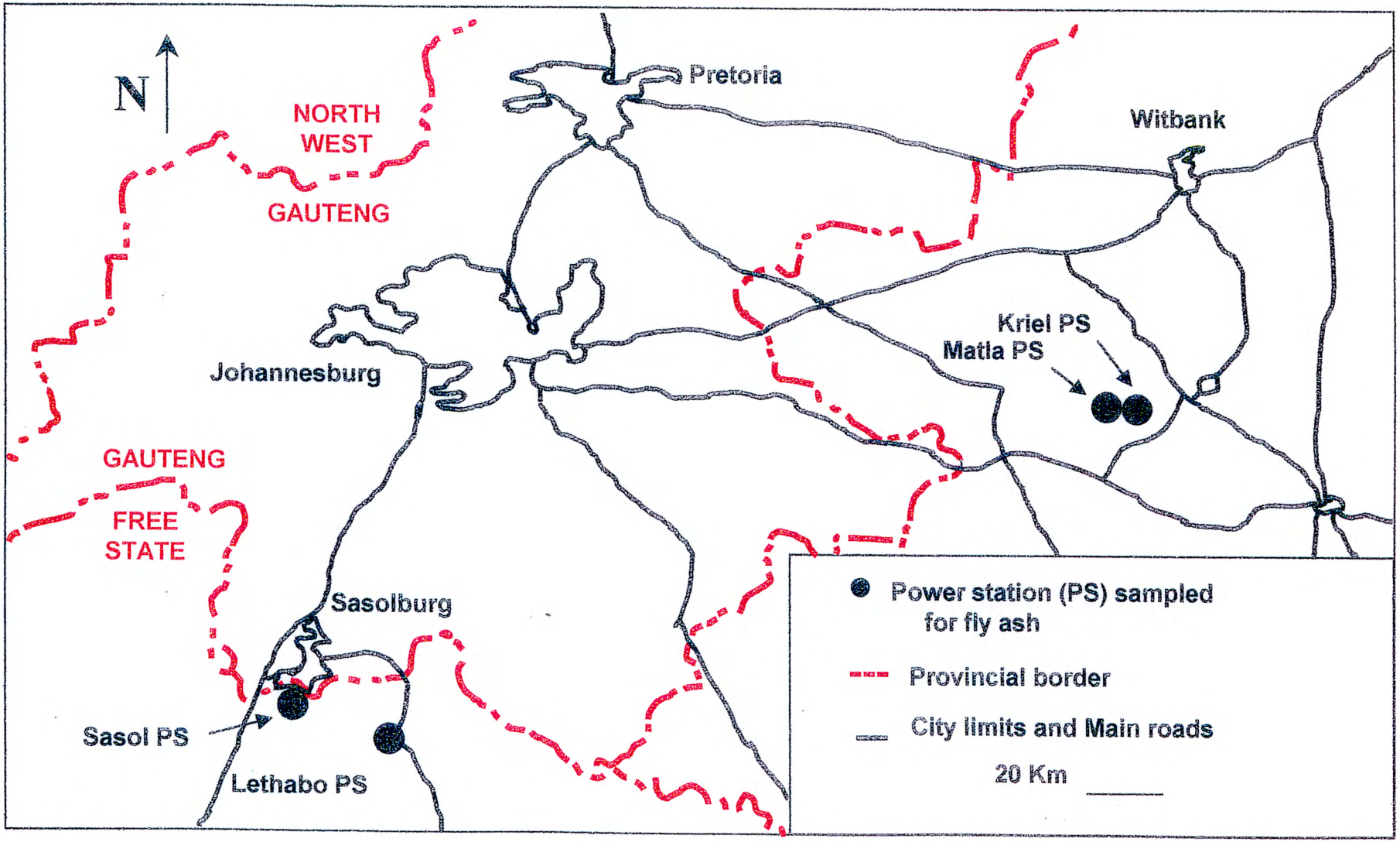

Figure 3.1: Locations of the coal burning power stations sampled for fly ash

proximity to the major industrial centre of Johannesburg, which make it highly marketable. The relatively high CaO content of the fly ash from Matla places it in high demand in South Africa. Matla and Kriel are within kilometres of each other and extract coal from the same seam. However, Kriel extracts the coal in an underground working whereas the coal used in Matla is strip-mined. Matla and Kriel were sampled due to their close proximity to one another, but also due to the fact that their fly ash may show varying degrees of hardening.

Each site was sampled in a way that established a progression in degree of weathering of fly ash, from unweathered fly ash to highly weathered older ash dumps. In addition, each series of fly ash samples was taken in the same manner to allow comparative analysis between ash samples from each power station. The samples consisted of a fresh fly ash sample from the hopper, as well as a moistened conveyor belt sample (where relevant) of fly ash being transported from the hopper towards the dump. In addition to the unweathered samples a minimum of two weathered samples from the ash dam were taken in an attempt to get a representative suite of samples at a relatively early stage of weathering (up to one year) and a highly weathered sample (greater than three years).

Descriptions of the samples taken from each of the South African coal burning power stations are given in Table 3.1. The sample names listed are the same as those used throughout the thesis and are accompanied with a brief sampling description.

Bosch (1990) noted that there was a trend for higher concentrations of trace elements in PFA to be associated with smaller particle sizes. Willis (1987) found concentrations of trace metals increased in fly ash from sequential precipitators within the same power station. This is partly due to the increase in specific surface area associated with smaller particle sizes from sequential precipitators. Consequently, the fresh fly ash taken from one of the hoppers at each power station represents only a spot sample, as it was not possible to sequentially sample the full series of fly ash from all hoppers and thereby form a composite sample. ASTM (1993) standards define the important oxides associated with the use of fly ash as a pozzolan as the SiO_2, Al_2O_3, and Fe_2O_3 content.

Table 3.1: Description of fly ash samples taken from four South African coal burning power stations

Power Station	Sample Name	Location and Description
Sasol	Sasol	Unweathered fly ash from the hopper at Sasol Power Station.
	SasolBot	A weathered fly ash sample from one of the main ash dumps at Sasol. The sample was taken at the lower section of the ash dam that was of higher cemented strength than the upper section of the ash dam. Vegetation of the lower slopes of the ash dam, where the sample was taken, had been established although the cover was still very sparse. See Figure 3.2.
	SasolTop	A weathered sample from the upper slopes of the same ash dam from which the sample SasolBot was taken. Vegetation had been established although struggling to take hold. The degree of stabilisation on the upper slope of the dump was poor and the "hardened" ash crumbled to the touch.
Kriel	Kriel	Unweathered fly ash from the hopper at Kriel Power Station.
	KrielCbt	Fly ash sample from the conveyor belt. The sample had been slightly moistened for the purpose of dust suppression during transport from the hopper to the ash dump.
	KrielTop	Sample from the top of one of the larger Kriel ash dumps. The sample was less than a year old, most likely as young as a month old, as it was still moist and had not achieved an advanced setting strength.
	KrielStp	The strongest sample taken from Kriel or any of the other ash dams. Taken from the lower steps of the same ash dump as sample KrielTop. A geological hammer was required to chip away at the sampling point as it had established strength similar to that of concrete. See Figure 3.3.
Matla	Matla	Unweathered fly ash from the hopper at Matla Power Station.
	Matla4dy	A weathered fly ash sample as recent as four days old on the ash dam. The sample had not yet hardened but had settled into a firm state. High water content.
	MatlaDam	A weathered fly ash sample from an ash dam estimated to be about 4 years old. Had reached a solid state that required a geological hammer but not as much force as required for the KrielStp sample.
	MatlaFlr	A small pile of hardened fly ash on the floor under the hoppers was noticed, the result of spraying the floor with water to establish a clean working area. The small pile, not more than 10 centimetres high and a metre wide, had achieved a very strong hardened state and was sampled with a geological hammer.
Lethabo	Lethabo	Unweathered fly ash from the hopper at Lethabo Power Station.
	LethaCbt	Fly ash sample from the conveyor belt. The sample had been moistened slightly for the purpose of dust suppression during transport from the hopper to the ash dump.
	Letha1yn	Vegetation on the ash dams at Lethabo occurs quite quickly and for his reason the weathered ash samples were the most difficult to obtain. This sample was taken from a section of the ash dam that was in the process of being habilitated. The ash dam was speculated to be approximately one year old.
	Letha5yn	Located under a vegetated section, the loose sample was extracted using a spade after clearing the overburden.

Figure 3.2: Sampling location of SasolBot on the sparsely vegetated ash dam

Figure 3.3: Sampling location of KrielStp

Since it is these phases that may correlate with the pozzolanic activity of fly ash (Watt and Thorne, 1966; Thorne and Watt, 1965; Joshi and Rosauer, 1973), it is anticipated that the major chemical constituents are the largest contributors to the hardening properties of fly ashes, and the trace elements should be of little consequence.

Samples of fresh fly ash at each power station were sampled and placed in small buckets that were filled to the top and sealed with a tightly fitting lid. Care was taken to limit the flow of atmospheric CO_2 into the fresh sample as reaction of the CaO content to form $CaCO_3$ may have limited the reactivity of the ash. The conveyor belt samples were also placed within closed containers during transport and remained within the closed containers for the remainder of the study. None of the other samples from any of the ash dams were placed in sealed containers, as they were sampled under ambient conditions and had already been exposed, in some cases for years, to CO_2 ingress.

3.2 Experimental procedures

Apart from a few select types of analyses of the weathered samples, which included XRFS, XRD, SEM and SEM EDXRF, all experimental work has been conducted on fresh unweathered fly ash from the hopper of each coal burning power station. Table 3.2 summarises the chemical and physical techniques utilised, and for which range of fly ash samples they were applied to.

Chemical analysis was performed on two types of samples, the fly ash, and a liquid phase consisting of extracts from fly ash/water experiments. In addition to quantitative analysis of the chemical nature of the fly ashes, many physical analyses were also performed on the ash samples. The methods and analytical parameters used are presented in the following sections. Detailed descriptions of the analytical procedures and instrument settings are given where appropriate.

3.2.1 Solution analyses

Aqueous extracts from fly ash were collected using two different techniques: a saturated paste extraction and a more dilute extract obtained by shaking and centrifugation.

Table 3.2: Summary of the physical and chemical techniques used to characterise both weathered and unweathered fly ash samples.

Chemical analysis	Samples analysed	Physical analysis	Samples analysed
XRD	Both*	SEM	Weathered
XRFS	Both	Stress tests	Unweathered
SEM EDXRF	Weathered	Liquid limit	Unweathered
IC	Unweathered	Particle size	Unweathered
		DTA-TGA	Unweathered

* Both refers to analyses performed on unweathered and weathered fly ash samples

3.2.1.1 Saturated paste extracts

A saturated paste extract of the fresh unweathered fly ash from each power station was prepared following the method outlined by Rhoades (1996) in Methods of Soil Analysis, SSSA.

A 500 g fly ash sample was utilised because of the low extract yield from a paste when a trial run was performed using a 250 g sample. De-ionised water was added to the fly ash in a 500 mL polypropylene container. The paste was kept for 24 hours (except were stated otherwise) with a well-fitted lid to prevent evaporative loss and CO_2 ingress, preventing subsequent reaction with the CaO content of the ash. After the equilibration period, a small (several millilitres) addition of further de-ionised water was required to return the fly ash/water mixture to a state representing saturation. The thixotropic nature of the ash caused complications when trying to reach the recommended plastic state of the saturated state.

The saturated paste was filtered through Whatman no. 50 paper on a Buchner funnel. Low saturated paste extract yields were obtained due to the solid state the paste obtains when slightly undersaturated with respect to water. The saturated paste extract was kept in a screw-cap plastic bottle that was sealed with Parafilm to prevent any CO_2 ingress into the container and stored in a refrigerator maintained at approximately 4°C.

Saturated paste extracts were also performed on unweathered fly ash from each power station in which the extract was collected from separate containers after 5 min, 10 min, 30 min, 60 min, 6 hours, and 12 hours of equilibration. The further addition of de-ionised water after each equilibration time (apart from 24 hours) was not necessary.

3.2.1.2 Dilute aqueous extracts

A method was designed for the purpose of evaluating the water-soluble ions in unweathered fly ash at short intervals of reaction (less than 15 minutes). A 5-gram sample of unweathered fly ash was weighed into a polypropylene centrifuge tube. Milli-Q de-ionised water was immediately added to the fly ash and stoppered. A series of ash/water mixes were placed on a reciprocating shaker for periods of 0.5, 1, 2, 5, 7.5, 10 and 15 minutes. The relevant sample was removed at the given interval and immediately transferred to an IEC Centra-CL centrifuge where the sample was spun for 30 seconds at 4000 revolutions per minute. The supernatant was collected and filtered through a 0.45 μm filter using Millipore apparatus and stored in a screw cap bottle. The filtered solutions were immediately analysed for pH and EC to avoid any inaccuracy due to neutralisation of the solution through CO_2 ingress. Major ions from the leaching tests were determined by IC. Samples were stored in a refrigerated system kept at approximately 4°C.

Actual contact time of fly ash with the aqueous phase (e.g. 1, 2, 5 minutes) is longer than is noted. The contact tiem is expressed as the time the mixture spent shaking, however, transferring from the reciprocating shaker to the centrifuge and centrifuge to the filter adds to the overall contact time. The contribution of transfer

time can be disregarded as the procedure was performed in the same manner in all cases and the small contributions of transfer time can be considered constant.

3.2.1.3 Electrical conductivity and pH

Electrical conductivity (EC) and pH of both the saturated paste and dilute aqueous extracts were measured. Electrical conductivity was measured using a Crison Micro CM 2201 conductivity meter equipped with a temperature probe for sequential temperature readings. The pH was measured using a Metrohm 691 pH meter with a KCl (3M) glass reference electrode. Calibration of the instrument was performed using pH 4, 7 and 10 buffer solutions. Samples were opened one at a time, and only after the instruments were ready to be operated, to prevent reaction of the highly basic solutions with atmospheric CO_2. Accuracy of measurements of 0.01 pH units can be expected at pH values below 10. Determination of values above pH 10 is based on an extrapolation of the calibration curve and accuracy is uncertain above this value.

3.2.1.4 Major ions by ion chromatography (IC)

The concentrations of the major cations and anions in the extracts (except carbonate/bicarbonate) were determined using ion chromatography. Prior to analysis, samples were filtered through 0.45 μm filters using Millipore apparatus and diluted, according to the EC of the sample, so as to give a value <100 μS/cm. The concentrations of the major cations (Li^+, Na^+, K^+, NH_4^+, Mg^{2+}, Ca^{2+}, Sr^{2+}) were determined using a Dionex 300 series instrument equipped with an IonPac CG12A guard column and a CG12A separator column with H_2SO_4 (10 mM) as the mobile phase. The separation of major anions (F^-, Cl^-, Br^-, NO_3^-, PO_4^{3-}, SO_4^{2-}) were determined using a Dionex 300 series instrument by passing the solution through an IonPac AS4A guard column and an AS14 separator column with 3.5 mM Na_2CO_3/1.0 mM $NaHCO_3$ as the eluent.

Calibration lines of the standards run before all analyses contained r-squared values greater than 0.97 in all cases. The accuracy of the determinations of ion

concentration present is within 3% while the majority of determinations lie within 1%. Determination of the precision of analyses on the suite of Matla saturated paste extracts at 4 different times over 9 days had RSD values between 0.2 – 10%.

3.2.2 Chemical analysis of the solid state

3.2.2.1 Total element concentrations

Sample preparation of unweathered fly ash consisted of air drying the samples and grinding the fresh fly ash in an agate mortar and pestle, as the samples were already very fine. Weathered fly ash samples were air dried and then milled for approximately three minutes in a carbon steel Siebtechnik swing mill to reduce the grain size to less than 50 μm diameter. Fusion discs of both weathered and unweathered fly ash were prepared according to the method of Norrish and Hutton (1969). Major and minor elements in the fly ash were analysed using a Philips PW X'Unique II (PW1480) wavelength dispersive X-ray fluorescence (XRFS) spectrometer. Elemental concentrations reported as SiO_2, TiO_2, Al_2O_3, Fe_2O_3, MnO, MgO, CaO, K_2O, P_2O_5, and SO_3 were determined as weight percentage in fusion discs. The fusion discs were analysed within the Department of Geological Sciences, UCT on a wavelength dispersive XRFS spectrometer with a Mo/Sc x-ray tube. Powder briquettes were prepared for analysis of Na_2O.

3.2.2.2 Mineralogical phases

All of the samples taken at the power stations were analysed by X-ray diffractometry (XRD). Prior to analysis, samples were ground in an agate mortar and pestle to obtain a uniform degree of fineness and to ensure that any weathered samples were completely homogeneous. The ground fly ash was back-filled into a powder mount and pressed against filter paper to ensure a relative degree of random orientation. The powder mounts were analysed with a Philips PW 1390 X-ray diffractometer and data collected with Philips X'Pert Data Collector software Version 1.1b. Scanning was done over a range of 4 to 60°2θ at a rate of 0.025 degrees-2θ per second using CuKα radiation.

XRD analysis was also used to determine the mineral phases after evaporation and crystallisation of the 24-hour saturated paste extracts from Kriel, Lethabo, Matla and Sasol. Approximately 1mL aliquots of saturated paste extract were placed on a glass slide with a Pasteur pipette and allowed to evaporate. A slight film crystallised on the slide after the sample was allowed to evaporate under ambient conditions, at which point a second layer was applied to ensure an acceptable count rate in the diffractometer of the precipitate relative to the glass of the slide. The glass slide was placed directly into the diffractometer and analysed under the same parameters as the powder mounts.

3.2.3 Physical analyses of fly ash

3.2.3.1 Atterberg limits

When dealing with soils the liquid limit is defined as the moisture content at the boundary between the liquid and plastic states. Although fly ash is not a soil, the liquid limit apparatus is applicable for use on fly ash, and especially in determining the ideal water content for preparing pastes. Liquid limits, or Atterberg limits, were determined following the methods outlined in Standard Test Methods (1979) and ASTM (1993b).

The methods make use of an Atterberg cup. The liquid limit determined using the cup corresponds to the moisture content when 25 taps (raised to a height of 10 mm and lowered) are required to close a specific groove between two equal portions of fly ash paste within the Atterberg cup. The moisture content was determined on a 2 to 3 gram sub-sample dried in an oven at 110°C for 24-hours.

3.2.3.2 Particle size analysis

Particle size analysis was performed by laser diffraction size analysis (Singer *et al.* 1988; Bayvel, 1986). Due to the presence of cenospheres and plerospheres amongst solid fly ash particles, particle size analysis was not carried out by SediGraph or hydrophotometer methods because they make use of settling techniques in the determination of particle size for which hollow spheres are not ideal. Analysis was performed on all four unweathered fly ash samples on a

Malvern Mastersizer High Resolving Particle Size Analyser. Sonication of samples within the aqueous medium was performed to disperse any spheres that may have had tendencies to stick together via weak inter-particle electrostatic forces.

Using Laser diffraction analysis, the determination of the particle size is based on the principle that particles of a given size diffract light through a given angle, with the angle increasing with decreasing particle size (Singer *et al.*, 1988). The particle size was determined by passing a monochromatic light through a dilute fly ash/water mixture through a volume of known dimension. The detector senses the angular distribution of scattered light intensity. The sample and system details are as follows:

Operating parameters: 70% pump, 50% stirrer, 50% ultrasound
Input density: 2.5 g/cm^3
Range lens: 300RF mm Beam length: 2.40 mm
Sampler: MS17 Analysis model: Polydisperse

3.2.3.3 Modulus of rupture

The method applied for testing the strength of fly ash briquettes was adapted from Reeve (1982). The method is an index of the strength of materials and can also be used for comparing the binding strength of structural materials such as fly ash. Samples were prepared by mixing 200 grams of dry unweathered fly ash with enough distilled water to reach the liquid limit as determined using the Atterberg limit test (section 3.2.3.1). The quantity of each fly ash paste prepared was enough to pour moulds for 5 briquettes. The paste was mixed thoroughly for 5 minutes with a metal spatula and poured into Plexiglas frames with dimensions of length, 7.0 cm; width, 3.5 cm; height 1.0 cm. The instrument used for the rupture of modulus tests was an INSTRON (Figures 3.4 and 3.5). The blade used to fracture the samples was applied at a rate of 0.25 mm/min and the resistive force that the briquette was applying to the moving blade was measured in Newtons (N). The briquettes were broken with the same orientation of the top of the drying surface exposed to the moving blade. Before pouring the paste into the moulds, fine silicon lubricant spray was administered on the setting surface as well as the

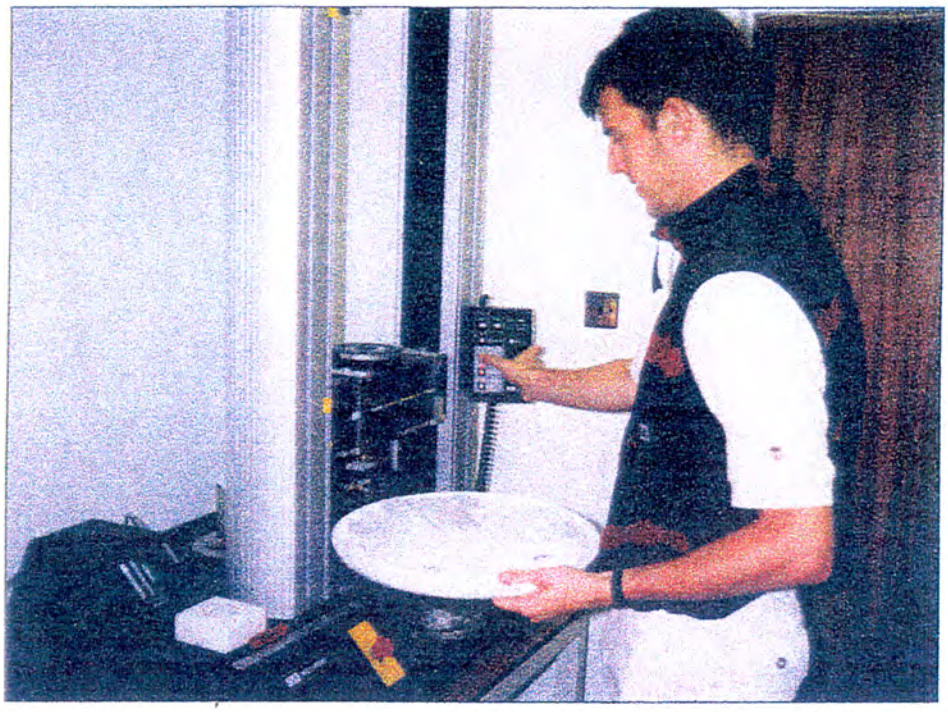

Figure 3.4: Modulus of rupture instrument (Instron) used to assess the hardening property of fly ash briquettes

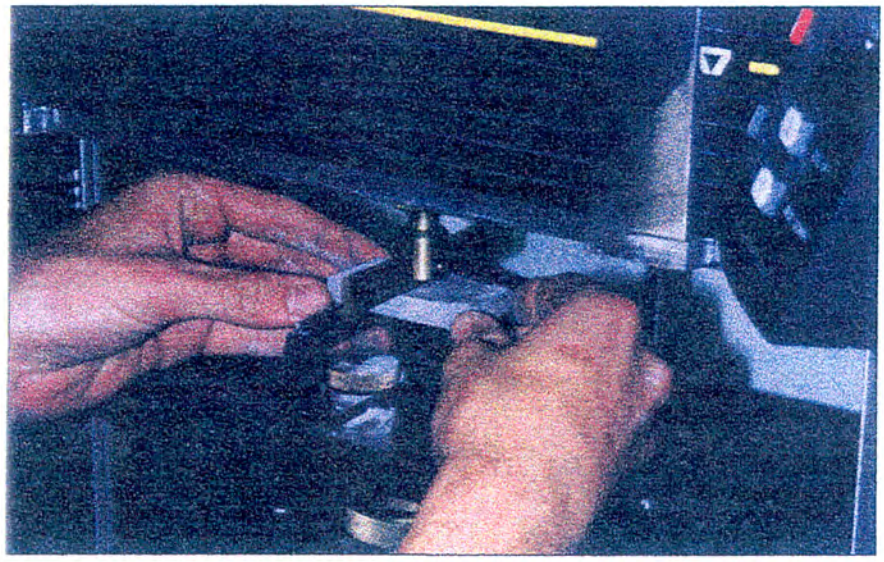

Figure 3.5: Close-up view of the blade used to fracture the briquettes, the fly ash briquette and the mounts. The mounts were placed at a distance of 5 cm from one another and centred with respect to the moving blade.

walls of the frame to avoid any sticking of the sample. To ensure a uniform smooth filling in the mould a glass slide was used to tap the sides of the frame to cause slight reorganisation within the mould and to aid in spreading the sample to create a level surface. Excess fly ash paste was wiped from the mould using the glass slide. The samples were allowed to set for 3 hours at which point they were removed from the frames and allowed to continue curing for 21 hours (a total setting time of 24 hours) without the frame walls confining the side of the briquette from atmospheric contact and unequal curing. The expansive nature of some of the pastes was the initiative behind removal of the briquettes from the frames at an early stage, as it was discovered that samples left in the frames for the complete curing period were not easily removed without being broken.

3.2.3.4 Thermal analysis

In order to determine the composition associated with the loss on ignition (LOI) of the unweathered fly ash samples, differential thermal analysis (DTA) and thermogravimetric analysis (TGA) were performed in the Department of Chemical Engineering, UCT. Further analysis on the individual components of the LOI was carried out at the Council for Geosciences in Pretoria, SA. Carbon and S were determined on a Leco CS 244 analyser on a 0.3 g sub-sample of fly ash. Samples were burnt at a temperature of approximately 1700°C in a RF furnace and analysed in an oxygen atmosphere. The Leco standard 4841 was used for calibration. The water content of the LOI was analysed on a Leco RC 412 analyser on a 0.5 g sub-sample. Samples were analysed in a nitrogen atmosphere at two temperature stages. The first stage (H_2O-) was analysed at 25 to 120°C and the second stage (H_2O+) at 120 to 950°C. NIM-L was used as a calibration standard.

3.2.4 SEM analysis

Weathered fly ash samples from Kriel, Matla, and Sasol (Lethabo was omitted due to monetary and time constraints) were analysed with scanning electron microscopy (SEM). Three signals were used during analysis: secondary electrons, backscattered electrons, and X-rays.

Sample preparation was conducted on large blocks of solidified weathered ash. Samples were cleaved to achieve a suitable size and oriented with the freshly cleaved surface towards the incident beam during analysis. Samples were fastened to the sample holder (stub) with special glue mixed with carbon and subsequently coated with carbon to produce sample conductance. In addition to carbon coated cleaved samples, polished thin sections of samples KrielStp, KrielTop, MatlaDam, and MatlaFlr were prepared. Blocks of sample were sliced and mounted on glass slides, impregnated with resin, and polished using diamond powder. The thin section samples were prepared in the Department of Geological Sciences, UCT. Before sample analysis, silver dag was placed on the glass slide from the polished thin section to the edge of the slide and the sample was then carbon-coated to enable conduction of charge away from the sample during analysis. Samples were stored in an evacuated desicator.

The morphology of cleaved samples and investigation of polished samples was achieved using a Cambridge S200 SEM. Secondary and backscattered electron detectors were operated on both sample types with the electron gun at the following settings:

EHT: 15.00 kV
Beam current: 11 pA
Working distance (WD): 17 mm

Semi-quantitative SEM EDXRF analysis of cleaved fly ash samples was conducted using a LEICA StereoScan 440 SEM EDXRF system run at the following parameters:

EHT: 15.00 kV
WD: 25 mm
Beam current: 111 pA
Take-off angle: 35.0 degrees
Sample tilt angle: 0.0 degrees

Error involved with EDXRFS analysis is discussed in detail by Potts (1992). The uncertainty in the analysis of the chosen spot sites is large as many of the

analyses involve small crystals of unknown thickness. The contribution to the signal from surrounding matrices is unknown, which results in the data being semi-quantitative at best. Further discussion on the uncertainties involved in the analyses is outlined in Section 4.3.1.4.1.

Chapter 4: Results and discussion

Previous investigations into the hardening properties of South African fly ashes (Fourie *et al.*, 1997; Hodgson and Grobbelaar, 1996) have identified differing degrees of hardening associated with weathered ash dams. Sampling of the ash samples used in this study was based primarily on the hardening properties that the fly ashes exhibited within the ash dump. Although fly ashes in South Africa have been noted to possess differing degrees of hardening, no studies have been found that has assessed the degree of hardening of the fly ashes to their chemical, physical and mineralogical properties. The secondary minerals associated with hardening of ash dams are also undocumented.

An assessment of the degree of hardening of the fly ash samples used in this study, by means of modulus of rupture experiments, has been performed and is used as a starting point for this chapter. The reasoning in terms of the chemical, mineralogical and physical attributes of both the weathered and unweathered fly ashes will be discussed/presented in the following sections. Treatment of unweathered fly ash to enhance the hardening property of fly ash will also be discussed.

4.1 Modulus of rupture of untreated ash

4.1.1 Crack propagation and hardening

There are many different bond types that can contribute to the solid nature and hardening of fly ashes. The type of bonding can be divided into two broad categories, which include (i) forces of attraction between particles and (ii) bridges formed by a matrix that holds the particles together. Forces of attraction, or molecular and atomic forces, include van der Waals, ionic, metallic, covalent and electrostatic forces. These forces are short range (negligible at distances greater than 1 μm) and generally weak when isolated. When taken communally, however, they can be significant contributing forces to inter-particle strength.

In terms of fly ash hardening, formation of bridges of secondary minerals between particles becomes the primary contributing bond to strength development (Cohen, 1997). Bridges of a liquid nature will contribute to hardening of a system through forces which hold the particles together as a result of the pressure deficiency or suction created within the liquid (Rumpf, 1977: cited in Cohen, 1997). As the secondary minerals develop, change from liquid bridges to solid bridges with mechanical interlocking between particles is most likely to occur. Solid bridges include products of chemical reactions and crystallisation of dissolved material, while mechanical interlocking includes interlocking of fibrous, flat and bulky particles that may be a result of crystallisation (Cohen ,1997).

The strength of fly ash is an indication of the extent to which varying types of bonds form within the fly ash as it proceeds from its initial state towards a hardened state. A method used to experimentally assess the strength of the fly ash is to manufacture a fly ash briquette and subject the material to an increasing load until failure (permanent deformation) occurs. In order for a crack to propagate through the fly ash briquette, a critical applied energy is required to initiate cracking.

4.1.2 Strength assessment of fly ash briquettes

To assess the setting strength of a paste or mortar, the force (Newtons) required to break a briquette of known dimension is often used to calculate the modulus of rupture. Fly ash briquettes were made to assess the short-term setting strength. The briquette was supported with no constraint on a pair of blades situated 1 cm from each end of the briquette and loaded to failure with a load concentrated at the centre of the briquette (Figure 3.5). When the dimensions of the briquette are applied to the equation (eq. 2.2 of section 2.7) for modulus of rupture (s) for a beam of rectangular cross section the equation simplifies to:

$$s = \frac{3F(7.0)}{2(3.5)(1.0)^2} = 3F$$

where F is the breaking force (in Newtons) applied at the centre of the fly ash briquette.

Data for the modulus of rupture required to break replicate fly ash briquettes made from unweathered ash cured for 24 hours is presented in Table 4.1. Lethabo ash briquettes were very fragile, and sample manipulation of Lethabo briquettes would often cause fractures and breakage at the slightest touch of hand. Matla possesses high short-term curing strength while Sasol and Kriel are intermediate.

Table 4.1: Modulus of rupture for fly ash briquettes cured for one day

Fly Ash Sample	CaO (%)	Modulus of Rupture (N/cm^2)						
		N	Mean	S.D.	Min	Max	Median	± 95% CI
Lethabo	4.23	15	6.39	2.32	2.94	9.63	6.24	3.76
Sasol	6.40	23	18.82	2.72	13.05	23.85	18.69	3.56
Kriel	7.66	20	12.76	2.47	9.93	20.07	12.60	3.46
Matla	8.57	15	30.72	6.38	23.71	44.58	27.24	10.3

Massazza (1998) defines the term 'pozzolanic activity' to include two parameters. They are the maximum amount of lime with which a pozzolan can combine and the rate at which such combination occurs. Other authors such as Aitcin *et al.* (1985) stress that attention should be drawn to the SO_4 and lime present in the fly ash, since these two components are suggested to enhance pozzolanic hardening. Thus, the lime content would seem to play a major role in the setting strength of fly ashes, and in Figure 4.1 the setting strength of fly ash briquettes has been plotted against the total calcium content of the ash.

The Kriel fly ash deviates significantly from a very strong linear correlation plotted for the other three fly ashes. The results obtained do not agree with the qualitative observations made in the field as to the degree of hardening within each ash dump. Kriel was observed to be the hardest of all the fly ash dumps. Based on the hardness of Kriel fly ash in the field the trend may not be appropriately plotted for the samples. It must be realised that with four groups of samples, each representing a series of replicates, the Kriel ash may be the normal group and the samples from Matla, Lethabo and Sasol are deviating from

the actual trend. Similarly, the trend may actually lie, for example, between Kriel and Lethabo with Matla and Sasol being the deviants.

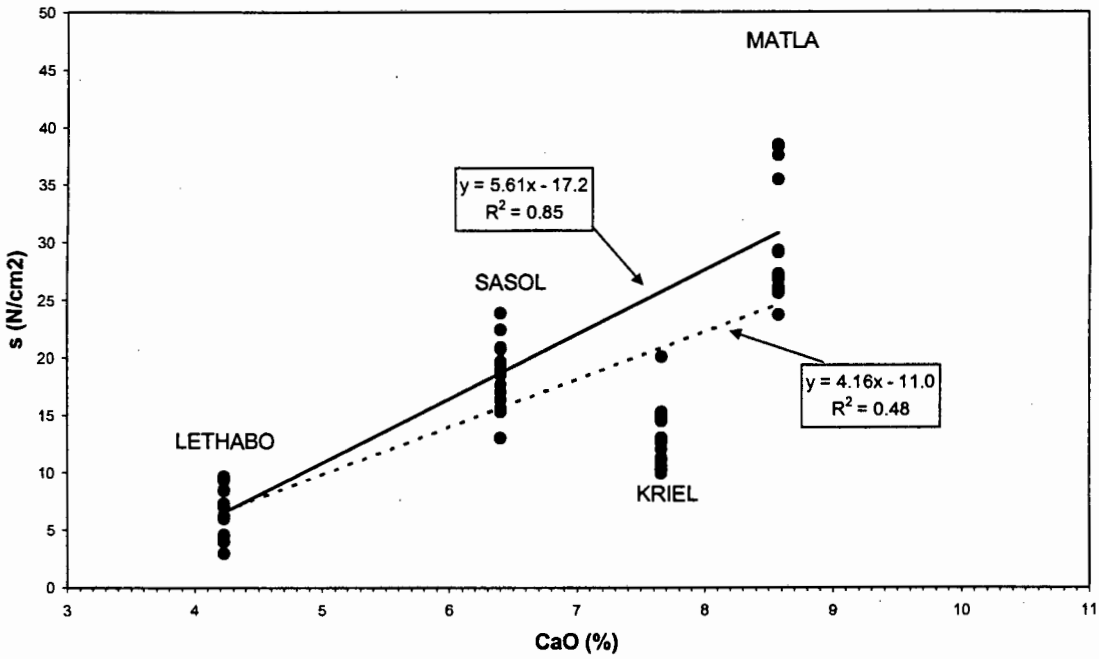

Figure 4.1: Modulus of rupture (s) of fly ash briquettes made from unweathered fly ash plotted against CaO content. The solid line excludes the Kriel samples.

Possible explanations for why the Kriel fly ash does not conform to the relationship in Figure 4.1 is that the unweathered fly ash sample may have different physical properties (although the chemical composition is similar) from that used in the past (Willis, 1987), or that the short-term setting strength of this ash is different from the long-term strength. Clearly, however, the chemical, physical and mineralogical attributes of the fly ashes, both in their weathered and unweathered state, need to be investigated in detail to better understand their hardening behaviour.

4.2 Characteristics of unweathered fly ash

4.2.1 Chemical properties

The importance of understanding the chemical and physical properties of fly ash cannot be emphasised enough with respect to tackling the problems associated with hardening characteristics and the reactions that occur once fly ash comes into contact with moisture. For this reason, the following sections have been

devoted to chemically and physically characterising the four unweathered hopper fly ash samples from Kriel, Lethabo, Matla and Sasol.

The composition of fly ash is dependent on a number of factors with the most critical being the composition of the parent coal. In addition to the parent coal, the boiler parameters will directly affect the amount of unburned coal and the particle morphology of the resultant fly ash. During cooling, inorganic species contained in the vapour phase, such as alkali sulphates, begin to condense as thin coatings on particles and in so doing possibly affect the fly ash reactivity. The condensed coatings on particles may be readily soluble when mixed with a liquid medium. The composition of fly ash may also be altered during collection from the electrostatic precipitators. The S content of the ash affects the efficiency of the precipitators. If the S content is too low then ash loss through the stack may occur. To enhance electrostatic precipitation, conditioning agents such as SO_3, Na_2CO_3, $NaHCO_3$, $NaSO_4$, ammonia, and MgO are added to the ash which may alter the fly ash composition depending on the quantity added (Malhotra and Ramezanianpour, 1994).

4.2.1.1 XRFS analysis

The mean values and standard deviations of duplicate determinations of major element oxides in unweathered fly ash are presented in Table 4.2. Also presented in Table 4.2 are similar data from two previous studies on South African fly ash (Willis, 1987; Fourie *et al.*, 1997). Trace element analysis was not conducted on the ashes because literature on the subject of pozzolanic activity indicates that the major elements are far more important than the trace constituents, which will not significantly alter the hardening properties of the fly ash.

From the data obtained in this study it can be seen that the composition of fly ash from Kriel and Matla fall within the range quoted in the literature by Willis (1987) on fly ash from the same power stations from up to 10 years ago. Willis (1987) found that Matla PFA collected over a two year period showed only small compositional differences. The similar results obtained over a longer time frame can be attributed to the fact that the power stations are "tied" to a particular

colliery and may still be using the same coal seam. Although slight variations from day to day may be anticipated, the general matrix of the coal, and hence the fly ash, remains relatively constant.

The fly ash analysed from Lethabo is similar to that studied by Fourie *et al.* (1997), which suggests that the fly ash has changed little over the past four years at the power station. The main difference is a higher SiO_2 content, which results in lower concentrations of the other oxides. Differences in the SiO_2 are probably due to higher concentrations of quartz in the coal.

Silica contents of Sasol ash in the study conducted by Willis (1987) are much higher than that of Sasol ash analysed in this study. It is possible that the analysis of Sasol fly ash is similar to the result obtained by Willis (1987) as the values quoted in his study are calculated without L.O.I. results. If an L.O.I. as high as that reported in this study for Sasol fly ash (4.43%) was apparent when Willis performed his study, than his values are more similar to those obtained in this study once the L.O.I. has been taken into account. Even when taking the L.O.I. into account the SiO_2 content of Sasol fly ash in this study is slightly lower than that of Willis.

The results of the four fly ash samples are similar when compared to variances observed in studies of European and American ashes. There are, however, slight variations amongst the ashes that need to be considered. Matla has the lowest SiO_2 content (49.92 %) of the four fly ash samples, containing about 6% less SiO_2 than Kriel and Lethabo and 3% less than Sasol fly ash. The Al_2O_3 contents of the ashes are less variable with Kriel displaying a slightly lower Al_2O_3 content (27.21 %) with respect to the other samples. The Fe_2O_3 contents are all very similar. The three above-mentioned major phases, SiO_2 + Al_2O_3 + Fe_2O_3, are used by the American Society for Testing and Materials (ASTM) to classify fly ashes as to whether they will exhibit pozzolanic properties. The classification parameters for fly ash used by ASTM and the comparative results contained in this study are presented in Table 4.3.

Table 4. 2: Chemical composition (mass %) of fly ash from four South African coal burning power stations.

Major elements (%)	Present study					Willis (1987)[##]			Fourie *et al.* (1997)[+]
	Kriel	Lethabo	Matla	Sasol	RSD (%)	Kriel	Matla	Sasol	Lethabo
SiO_2	56.25 (0.5)[#]	56.29 (0.2)	49.92 (0.7)	52.98 (0.2)	5.8	55 – 61	38 – 50	61 – 67	50.22
TiO_2	1.72 (2.8)	1.62 (2.0)	1.58 (1.2)	1.69 (1.1)	3.7	1.5 – 1.7	1.4 – 1.7	1.2 – 1.4	1.73
Al_2O_3	27.21 (0.9)	31.52 (0.3)	30.45 (0.2)	28.45 (0.4)	6.6	26 – 29	25 – 32	23 – 27	32.36
Fe_2O_3	3.06 (0.8)	3.38 (0.3)	3.93 (0.3)	3.33 (1.4)	11	2.9 – 3.2	3.4 – 5.0	3.1 – 4.8	4.75
MnO	0.040 (4.9)	0.035 (0.5)	0.040 (6.1)	0.042 (1.4)	7.8	0.00 – 0.04	0.04 – 0.05	0.03	N/AV
MgO	1.46 (8.8)	1.08 (4.9)	2.24 (3.0)	1.35 (9.0)	33	1.9 – 2.8	2.0 – 3.5	1.4 – 1.7	1.66
CaO	7.66 (1.2)	4.23 (0.3)	8.57 (0.2)	6.40 (0.9)	28	7.9 – 12	8.7 – 15	6.1 – 7.1	5.75
Na_2O	0.2 (66)	0.1 (16)	0.4 (16)	0.4 (20)	48	0.30 – 0.49	0.55 – 1.0	0.76 – 1.3	N/AV
K_2O	0.759 (1.5)	0.525 (1.4)	0.939 (1.9)	0.460 (0.9)	33	0.56 – 1.0	0.79 – 1.0	0.31 – 0.48	N/AV
P_2O_5	0.827 (1.8)	0.312 (0.7)	0.974 (1.7)	0.255 (0.2)	61	0.74 – 1.9	0.63 – 2.9	0.22 – 0.51	0.9
SO_3	0.633	0.128	0.554	0.286	59	0.69 – 1.5	0.25 – 0.77	0.11 – 0.26	N/AV
L.O.I	0.384 (28)	0.803 (6.7)	0.626 (6.3)	4.43 (2.0)	123	N/AV	N/AV	N/AV	0.73

Numbers in brackets indicate the percent relative standard deviation between two replicate samples

XRFS analysis on fusion discs of replicate samples from Kriel (n = 7), Matla (n = 23), and Sasol (n = 2)

+ The average value of four replicate samples by XRFS (sample type not specified)

N/AV indicate values not available

Table 4.3: ASTM standards classification of Class F fly ash compared to fly ash from four South African coal burning power stations

Classification parameters	Class F	Kriel	Lethabo	Matla	Sasol
SiO_2 + Al_2O_3 + Fe_2O_3, min %	70.0	86.5	91.2	84.3	84.8
SO_3, max %	5.0	0.633	0.128	0.554	0.286
Moisture content, max %	3.0	0.062	0.016	0.057	0.158
LOI, max %	6.0	0.384	0.803	0.626	4.43
Available alkalis, as Na_2O, max %	1.5	0.65	0.41	0.95	0.67

In addition, ASTM also suggests that the L.O.I. and SO_3 content should be less than 6 % and 5 %, respectively. Both Matla and Kriel have twice as much SO_3 than Sasol and four times that of Lethabo. They are, however, still much lower than the ASTM guidelines. The additive used (if any) in the fly ash samples to aid in electrostatic precipitation is unknown. However, the sulphur in the ashes is most probably not derived from any addition to the ash of gaseous SO_3 at the power station, as it would only be added in very small quantities. Lethabo, Matla and Kriel all have similar L.O.I. contents, whereas that from Sasol is unusually high for a South African fly ash but still less than the value required by ASTM for an ash to possess pozzolanic properties. When all of the above mentioned components are taken into account all four fly ash samples can be classified as Class-F (ASTM, 1993); that is, they should possess pozzolanic activity.

In addition to the criteria for pozzolanic activity outlined by ASTM, Aitcin *et al.* (1985) stress that attention should be drawn to the SO_4 and lime present in the fly ash, since these two components enhance pozzolanic hardening. The CaO contents of the four ashes analysed is the most variable among the major elements. Matla possesses the highest CaO content at 8.57%, Lethabo the lowest at 4.23%, and Kriel and Sasol intermediate with CaO contents of 7.66% and 6.40%, respectively. The total CaO content detected by XRFS does not distinguish the free lime from that contained within the glass. The free calcium

oxide content may constitute as much as 3.5% of the mineral matter in fly ash (Wesche, 1991). The free CaO content is important because it will dissolve into solution at a faster rate than will the calcium contained within the glass matrix, which has implications for the pH of the pore water and hence hardening reactions.

Other oxides in Table 4.2 worth mentioning because of their variance include the P_2O_5 and MgO content. Both Matla and Kriel possess high P_2O_5 contents (0.974% and 0.827% respectively) while Sasol and Lethabo are almost four times lower. Bosch (1990) noted that both P_2O_5 and TiO_2 occur in much higher concentrations in South African ashes than in fly ashes from other coal burning nations, which is a result of higher contents in the parent coal. The MgO content is relatively similar in three of the ashes but Matla has twice as much (2.24%).

4.2.1.2 Fly ash mineralogy

The mineralogy of fly ash is directly related to the chemical and mineralogical composition of the parent coal. Due to the rapid cooling of molten ash in the power plant, fly ash consists primarily of noncrystalline particles, or glass, and a small amount of crystalline material. The three major mineralogical components of fly ash samples from Kriel, Lethabo, Matla and Sasol are quartz, mullite, and glass with smaller amounts of lime and hematite (Figures 4.2 and 4.3).

Although quantitative analyses of the fly ash samples were not performed, it would appear that, based on the relative intensity of the peaks, the quartz content is variable amongst the samples. This observation is confirmed by Willis (1987) who found that quartz not only is variable between samples of differing power stations, but also between fly ash from different precipitators at the same power station. Willis also found that the quartz contents for Kriel, Matla and Sasol fly ash ranged between 9 and 12 %, 3 and 8 %, and 8 and 16 %, respectively. Investigation of fly ash using SEM with a backscattered electron detector to reveal density differences identified that quartz occurs as single sharp angular grains. Lesch and Cornell (1987) also observed angular quartz grains and attributed their angular nature to the fact that quartz grains pass unmelted through the

combustion process. Matla appears to have much lower quartz content than Kriel, Lethabo and Sasol, which would follow from the XRFS results, which indicate Matla having the lowest Si content. This observation also confirms the results obtained by Lesch and Cornell (1987) who found that the Matla fly ash contained up to 15% less quartz than Kriel.

Mullite forms when kaolinite ($Al_2Si_2O_5(OH)_4$) is decomposed in the furnace through combustion of the parent coal. The kaolinite contents of coal used in the power stations appear to be present in similar quantities, as the relative mullite peak intensities of the resultant fly ash are not greatly variable. Willis (1987) found that the mullite contents of fly ash from Kriel, Matla and Sasol had little difference between the samples with typical values between 0.21 and 0.40% mullite.

The importance of the quantities of the mineral phases quartz and mullite is that they have been described by Wesche (1991) as being less reactive than the glass phase. Studies by Bosch (1990) and Lesch and Cornell (1987) on the mineralogy of South African fly ashes, including Kriel, Lethabo and Matla, found that the ash consists of a Si-Al-Ca-rich glassy phase containing 24 to 75 weight % of the bulk fly ash sample. Wesche (1991) indicates that the main components of fly ash contributing to its pozzolanic reactivity are its reactive silicates and aluminates that are contained within the glass. Hubbard *et al.* (1985) indicate that the clay minerals in the coal are the source of the pozzolanic components of PFA in that the clay minerals are responsible for the amount of glass cenospheres created.

The lime content is highest in Matla, Kriel and Sasol, while a very weak XRD lime peak is observed for Lethabo (Figure 4.3). Bosch (1987) found that when the CaO concentration of South African fly ashes, including Lethabo and Matla, is between 4 to 6%, the total measurable crystalline lime is zero. The bulk CaO content of Lethabo fly ash was found to be 4.23% and would thus be expected to have the lowest lime content.

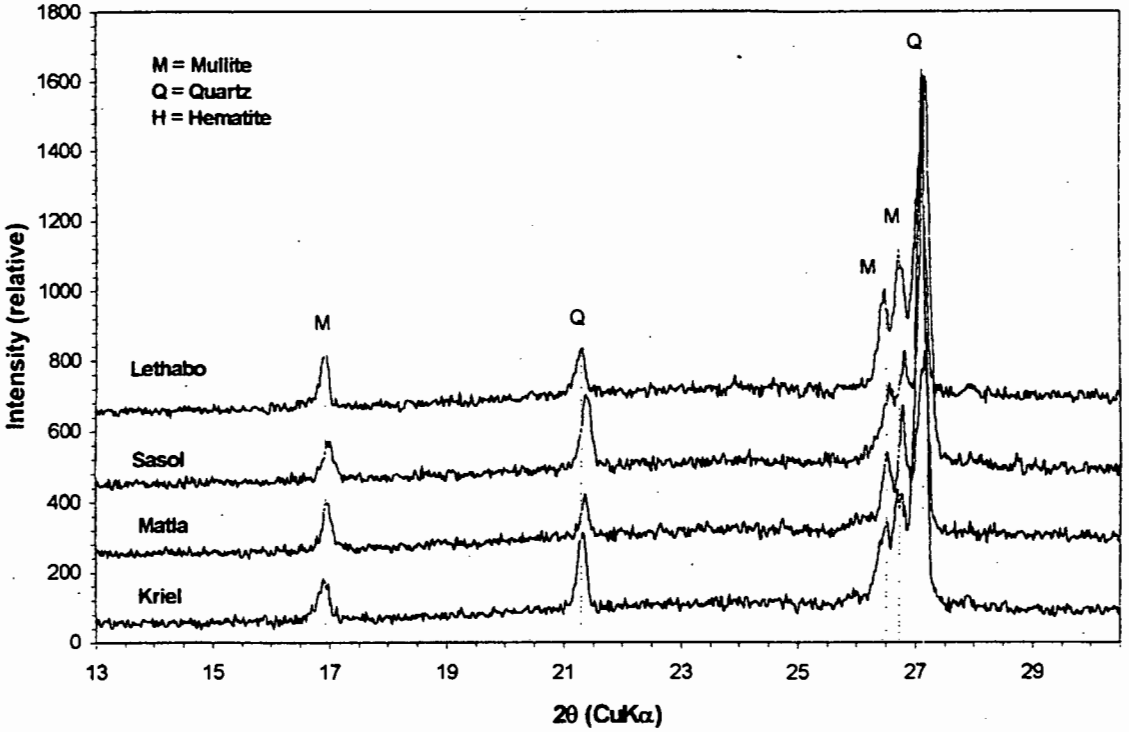

Figure 4.2: XRD patterns (5 – 30 degrees 2θ) on powder mounts using CuKα radiation on unweathered fly ashes from four South African coal-burning power stations.

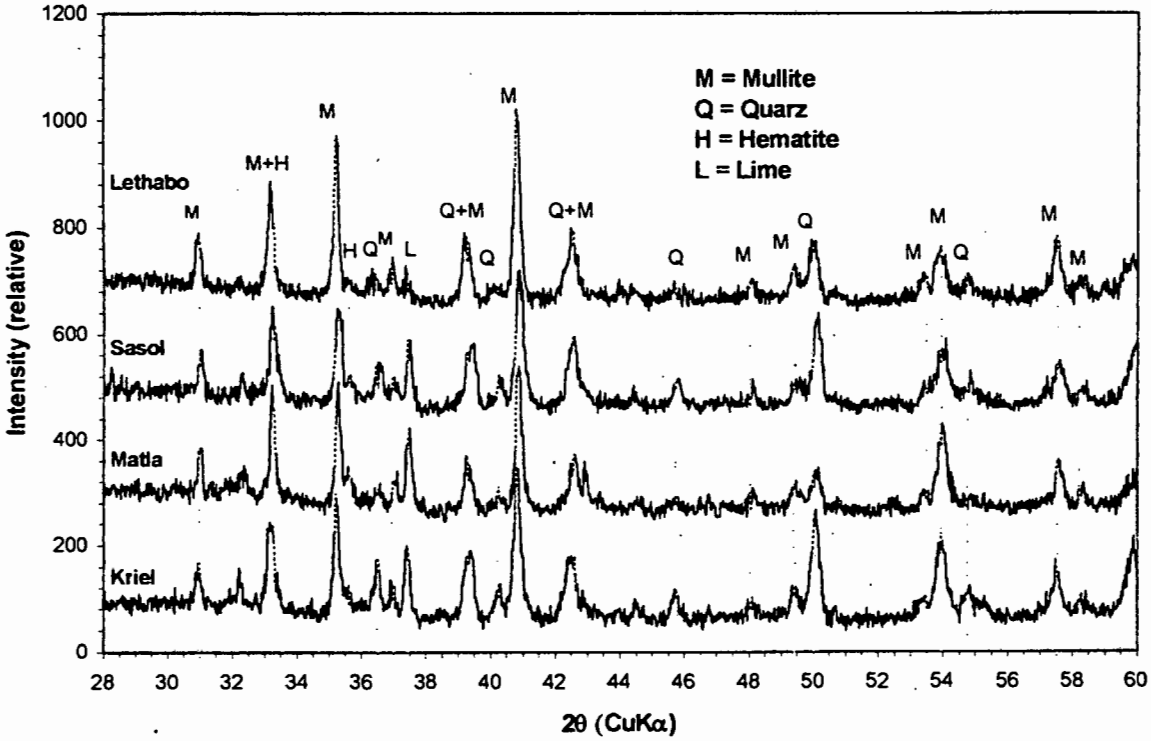

Figure 4.3: XRD patterns (28 – 60 degrees 2θ) on powder mounts using CuKα radiation on unweathered fly ashes from four South African coal-burning power stations.

Two magnetic phases have been previously identified in studies of South African fly ashes, namely maghemite (γ-Fe_2O_3) and hematite (α-Fe_2O_3) (Lesch and Cornell, 1987). Only hematite in the unweathered fly ash samples was detected by XRD analysis. It is possible that the boiler temperature during burning of coal was sufficient to convert most, if not all, of the maghemite to hematite or that it is present in such minute quantities that it is not detected.

4.2.1.3 Thermal analysis

The L.O.I. of each sample was analysed by DTA and TGA (Figure 4.4) to establish which component was responsible for the comparatively high L.O.I. of Sasol fly ash. All four samples show very similar humps spanning the whole DTA curve representing the same protracted, weakly exothermic reaction, but Sasol displays an added sharp exotherm at 600°C with a corresponding decrease in mass shown by the TGA curve. The Sasol L.O.I. (4.2% by mass of the fly ash) was found to be composed of 3.8% carbon, 0.10% adsorbed water, 0.15% water of hydration, and 0.13% sulphur. The large peak on the DTA curve at 600°C is most likely due to unburned coal. The broad hump occurring in all samples is unlikely water loss as it is an endothermic reaction or S loss which would be present at higher temperatures. Rather, the broad hump suggests a baseline drift associated with either inadequate heating rate control or differential thermal conductivity developing during heating between the sample and reference material surrounding the thermocouple. These suggestions are feasible because the equipment used was not modern and they would not have been as thoroughly designed to avoid this.

The quantity of unburned coal in the Sasol sample suggests that the efficiency of the power station at the time of sampling was poor. This might affect the fly ash due to inadequate boiler temperature causing incomplete melting of the mineral ash resulting in irregular shapes. The particle shape is important as it may affect particle motion in a fluid medium (Wesche, 1991). If this degree of inefficiency of the boiler is a regular feature, it may decrease the likelihood of hardening

reactions occurring due to the altered fluid mechanics of the fly ash paste (e.g. capillary suction). This may suggest a preliminary explanation as to why the ash at Sasol lacks hardening properties.

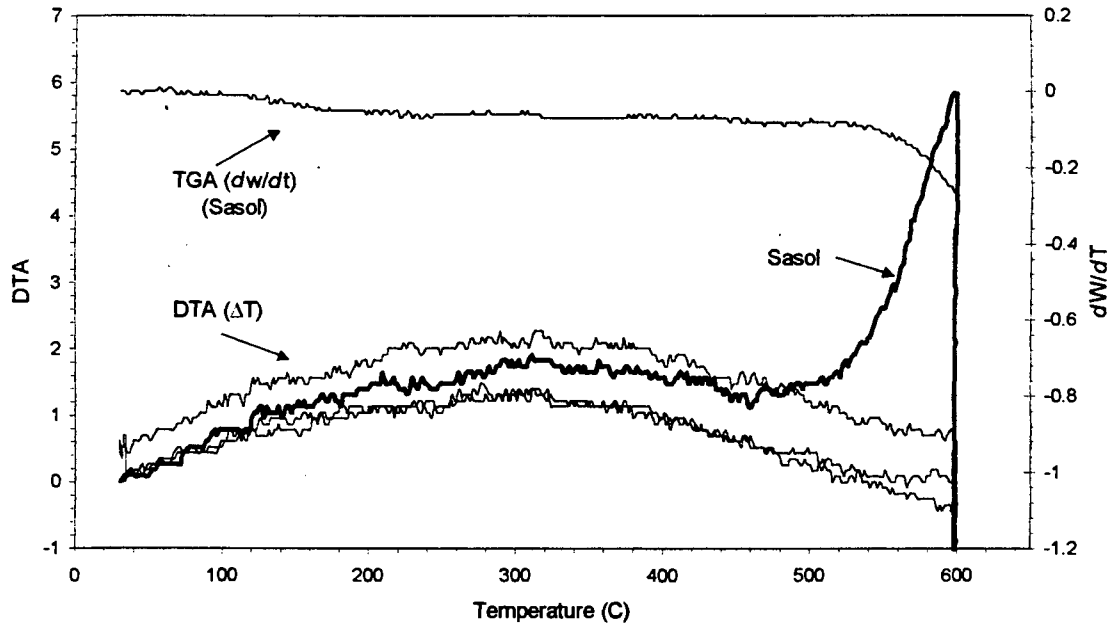

Figure 4.4: Thermal analysis showing the DTA and TGA curves for Sasol fly ash and the DTA curves for Kriel, Lethabo and Matla

4.2.2 Physical properties

4.2.2.1 Particle size distribution

The importance of establishing the fineness of fly ash stems from the fact that finer ash particles will dissolve and react faster once in the liquid phase of the hydrating system than will larger particles. Ultimately the fineness of the fly ash particle is related to how well the coal is ground prior to combustion. Jawed and Skalny (1991) indicate that the fineness of fly ash, and in particular the fineness of the glassy phase, is considered to be more important than its chemical composition in determining its reactivity. Two plots of the particle size distribution are presented in Figures 4.5 and 4.6. Figure 4.5 shows the range of particle sizes plotted on a logarithmic scale, which provides a better perspective of the fraction of smaller particles contained within the ash as well as the bimodal distribution of all four fly ash samples. Figure 4.6 provides information on the abundance of fly ash particles greater or less than a specific size.

All four samples show similar particle size distributions. The average particle size of the ashes does, however, show some variance. The particle size distribution displays a dominant mode at larger particle size and a smaller mode comprising the very fine particles. ASTM C618 considers the quantity of fly ash retained when wet-sieved on a 45 μm (No. 325) sieve an important factor as it is the smaller size fraction which is regarded as the more reactive fraction. Sasol shows the least amount of spheres below 45 μm at 48% less than the critical value, Matla at 58%, Lethabo at 59%, and Kriel the finest particle size of 63% below 45 micrometers.

The particle size distribution of all the fly ash samples is very broad with particle sizes ranging from < 1 to greater than 400 μm in diameter. The bimodal distribution is characteristic of all samples. The mode at small particle sizes occurs at similar values between 0.31 and 0.36 μm, whereas the mode at higher values is more variable. The large particle size mode follows a similar trend to that relating to the amount of fly ash particles below 45 micrometers. Kriel has the lowest mode at 66 μm and hence the finest particle size, Matla at 89 μm, Lethabo at 104 μm, and Sasol with the highest particle size mode at 120.7 μm.

The heterogeneity of fly ash would suggest that particles with smaller diameters might differ in composition from those with larger sizes. Mather (1984) found that most of the glass particles are spheres in the 1 to 20 μm size range. One of the observations during SEM analysis of fly the ash samples was that the carbon was very porous and appeared to be associated with the largest size fraction. Watt and Thorne (1965) performed extensive characterisation of fly ash particles based on bulk material analysis, magnetic properties, density, and microscopic examination. One of their findings was that particles with higher contents of iron are predominantly contained in the 5 to 30 μm size range. It is quite probable that the iron particles in the four South African fly ashes are concentrated in the smaller size fraction. Diamond (1983) has suggested that high-calcium fly ashes

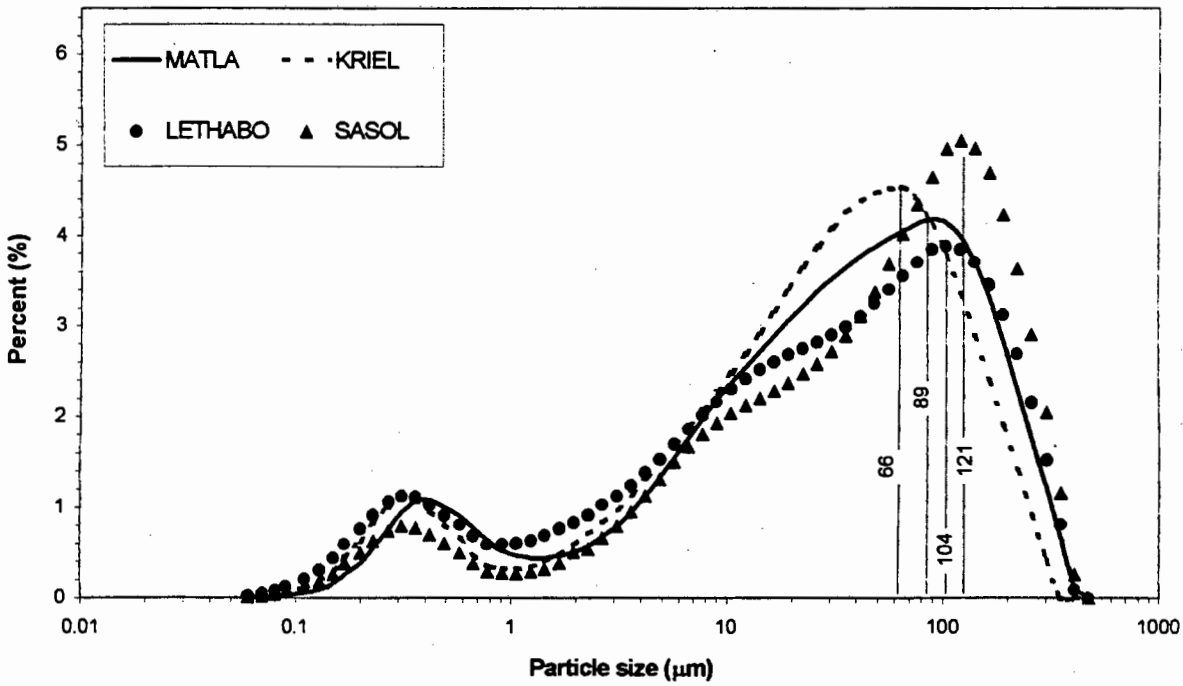

Figure 4.5: Particle-size distribution of fly ash from four South African coal-burning power stations showing the bimodal distribution and the particle size of the largest mode.

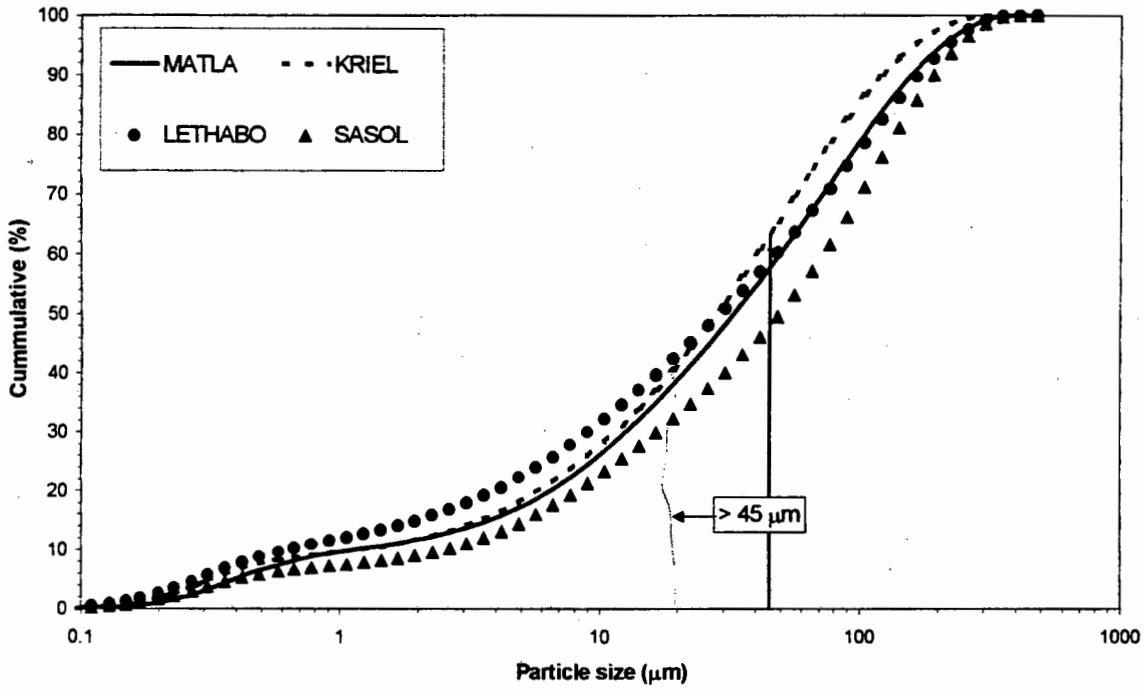

Figure 4.6: Particle-size distribution of fly ash from four South African coal-burning power stations showing the percentage of particles contained within a certain particle size range.

tend to have a finer particle size distribution (especially a larger Ca content within the very small spheres). Unweathered fly ash from Matla and Kriel have the highest calcium content of the unweathered fly ash, as well as the finest mean particle size distribution of 89 and 71 μm, respectively. Kriel has the largest proportion amount of particles less than 45 μm and the lowest mode of the coarse particle size fraction.

Assuming that the high L.O.I of Sasol ash has been correctly attributed by DTA-TGA analysis to unburned coal, the large average particle size (36 μm) of this ash is probably due to the relatively large coal particles. The large mean particle size of the Sasol ash may also be indicative of the boiler running at an inefficient level, since incomplete combustion of the coal in the boiler would lead to larger fly ash particles. Wesche (1991) indicates that if the combustion temperature is low, the coal ash fails to melt and the final shape of the resultant particle is irregular.

4.2.2.2 Liquid limit

The true complexity of fly ash can only start to be appreciated once the observation has been made of the state fly ash adopts, and the characteristics it assumes, as a saturated paste. The cementing reactions, by definition, only start to occur once the fly ash assumes a hydrated or moistened state. This 'complexity' occurs due to the thixotropic nature of the ash. Van Olphen (1977) indicates that "a complication often encountered in dispersed systems is that their flow diagram is dependent on the previous shear history of the system". When a finite shear force is applied to the saturated fly ash system, such as an attempt to mix the paste with a spatula, the result is a decrease in the viscosity of the system.

The determination of the liquid limit (i.e. the boundary between the liquid and plastic state) of the four unweathered fly ashes was complicated by their thixotropic nature. The rigid characteristic the pastes adopted when they were slightly undersaturated with respect to the aqueous phase hindered the determination, as did the liquid property fly ash paste would assume when slight supersaturation with respect to water was achieved. When preparing the paste

testing the liquid limit, one drop of water too much sent the system from a rigid paste to a liquid mass, while the converse applied when adding a small quantity of ash to the paste.

On the basis of their liquid limits the fly ashes of Kriel, Lethabo, Matla and Sasol can be separated into two groups. Kriel and Sasol fly ashes have high liquid limits of 37 and 32 % water by mass, respectively, whereas Lethabo and Matla have the same liquid limit of 19 % water by mass.

The amount of water necessary to obtain a paste at its liquid limit varies considerably in accordance with the carbon content (Alonso and Wesche, 1991). High carbon content is often associated with a high water requirement. In addition to the carbon content, the particle size and specific surface area also play a dominant role. The particle size of Sasol and Kriel bracket the other two ashes in this respect. This suggests that the liquid limit differences are not due to particle size alone and, besides the unburned coal aspect of Sasol ash, it is possible that particle shape an potential packing characteristics also play an important role in determining the liquid limit. Kriel has the greatest fine particle size fraction, which would increase the specific surface area and in turn increase the water requirement.

4.2.3 Interpretation in relation to hardening

Through the use of many analytical techniques and direct observation of the fly ash samples, coupled with information contained in the literature, it is possible to tentatively identify at this point some trends and anomalies that may relate to hardening of the ashes. The composition of the major elements contained in the four ash samples varied only over a narrow range with the exception of the CaO content. Some authors have suggested (Aitcin *et al.*, 1986) that the higher the calcium content in fly ash the better will be the pozzolanic reactivity. The amount of calcium is an important factor, but what is likely to be a more meaningful expression of the calcium content is the amount of free or available lime. The free lime content was not determined in this study because of the difficulties involved with the analysis, requiring quantitative XRD analysis to establish accurate

values. The soluble calcium in solution has been determined by IC of saturated paste extracts of fly ash and could be used as an index of the free lime content. This topic is investigated and discussed in Section 4.4.

Little mention in the literature on fly ash has been made about magnesium and to what extent it may participate in hardening reactions. The magnesium containing minerals found in South African coal, as described by Falcon (1978) and Falcon and Snyman (1986), include illite, montmorillonite, ankerite and dolomite. Padia *et al.* (1976) (cited in Fisher and Natusch, 1978) indicate that decomposition in the boiler of dolomite will form lime, MgO and CO_2. It is also probable that a large proportion of magnesium will also be contained in the glass of cenospheres, as it is illite that is responsible for cenosphere creation (Hubbard *et al.*, 1985). As mentioned previously the free CaO content of the fly ash is more likely to be the reactive phase of calcium, and it may follow that the free MgO will be the reactive magnesium phase.

Hodgson and Grobbelaar (1996) and Fourie *et al.* (1997) indicate that calcite is responsible, in part, for hardening properties exhibited in South African ash dams. What neither paper takes into consideration, is that the system is not an ideal calcite system and other ions in solution such as Mg^{2+} may alter the precipitation of calcite. In a study conducted by Bezuidenhout (1995) on the chemical and mineralogical changes associated with ash dam leachates equilibrium thermodynamic calculations indicated that the ash water was supersaturated with respect to magnesite ($MgCO_3$).

Magnesium is a divalent cation, much like calcium, and within a hydrated system it may precipitate as hydromagnesite ($Mg_4(OH)_2(CO_3)_3.H_2O$) or as magnesian calcite. If the calcium content plays as important a role as some authors have suggested, is it possible that the calcium and magnesium content combined is not a better index when discussing calcite formation and its effect on ash dam hardening? Taking the MgO content of the ash samples into consideration and relating the CaO+MgO content to the strength of the fly ash briquette measured in Section 4.1.2 does not affect the relative differences between the ashes.

Attempts to establish the relationship of pozzolanicity to fly ash fineness, specific surface area and chemistry abound in the literature (Frohnsdorff and Clifton, 1981: Hubbard *et al.*, 1985: Hubbard and Dhir, 1984: Watt and Thorne, 1966: Ravina, 1980: Raask and Bhaskar, 1975). Many indices, such as the pozzolanic potential index (PPI) and the pozzolanic activity index (PAI), do not correlate with each other although they are often established to achieve the same purpose. By definition the pozzolanic reaction is a chemical reaction of fly ash with Ca^{2+}, which suggests that fineness and specific surface area, although important, play a secondary role. Hubbard *et al.* (1985) recognised the need to develop a classification of pozzolanicity (the PPI) in terms of the potential for the material to act as a pozzolan, given appropriate environmental conditions and time, rather than the early surface activity of the fly ash (the PAI).

The PPI is based on the parameter K/A (molar K_2O/Al_2O_3) to predict the proportion of pozzolanic material in the ash. This value, K/A*10, was plotted by Hubbard *et al.* (1985) against the total amorphous phase and a good correlation was found to exist ($r = 0.81$). To test the PPI for SA ashes, data were taken from a previous study on the mineralogy of SA ash (Bosch, 1990) and plotted following Hubbard *et al.* (1985). Data were taken from Bosch (1990) and not from this study because quantitative XRD analysis was conducted in the Bosch study and on the same power stations. There was no evidence to suggest that the PPI could be useful for evaluating pozzolanic activity among SA fly ashes.

At this stage some provisional conclusions can be put forward:

1. For 3 of the 4 unweathered ashes investigated, there is a very strong linear relationship between total Ca content and modulus of rupture of fly ash briquettes cured for a short period of time.
2. The fourth ash, from Kriel, deviates from this relationship which indicates that other physical factors such as particle size and shape and chemical factors such as the proportion of total Ca which exists as free lime (as opposed to that incorporated in the glass fraction) and, possibly, the content of other alkaline constituents such as MgO, are probably important as well.
3. It is also known that short and long-term hardening properties of fly ash are not necessarily correlated and different results may therefore have been

obtained if hardening experiments were done over a longer reaction period. Therefore, a simple explanation for ash hardening properties will probably remain elusive.

4.3 Leaching tests

Saturated paste extracts of unweathered fly ash from Sasol, Kriel and Matla were prepared in an effort to establish the ions in solution that may relate to the differences observed in fly ash hardening. A series of extracts was collected over the same length of time that the fly ash briquettes were cured, at intervals of 5, 10, 30, 60, 360, 720 and 1440 minutes. The data collected, which include pH, EC and major ions by IC, are presented in Table 4.4. Alkalinity determination of the saturated paste extracts was not performed as precipitation within the sample containers was observed before analysis could be performed.

The lack of carbonate/bicarbonate data provides complications in trying to establish the ionic strength of the solution. Rather than calculating the activity coefficients from the electrical conductivity following the relationship obtained by Griffin and Jurinak, 1973):

$$\mu = 0.013\ EC$$

where μ is the ionic strength in moles/L and EC is the electrical conductivity in mS/cm, the alkalinity was approximated using the anion imbalance.

Approximations of ionic strength using the EC of the solution can be applied to dilute solutions rather than the highly concentrated saturated paste extracts used in this study. By calculating the alkalinity of each solution allowed for speciation determination by input into the model MINTEQA2 (Allison *et al.*, 1991).

Preparations of the Sasol fly ash saturated paste extracts revealed a strong smell of NH_3 almost immediately following hydration of the ash, whereas the presence of NH_3 in the other samples was not detectable by the sense of smell. Concentrations of NH_4^+ in Sasol ash extracts exceeded those in Kriel and Matla extracts by at least an order of magnitude and in some cases twenty times

greater. The source of NH_4^+ in Sasol ash compared to the other South African ashes is unknown. It may, however, be derived from soluble NH_4^+ salts (ex. NH_4Cl) created from higher nitrogen content in the parent coal. NH_4 shows a decreasing trend, with the exception of a couple of anomalous points for Kriel, over time for all samples. The decrease in concentration can be attributed to the declining abundance of NH_4-salts over time resulting in less abundant dissolution.

Sodium and chloride normally behave conservatively (i.e. a complete and relatively constant solution concentration), but both show a marked decline in concentration during the equilibration period. It is possible that the ions are either being incorporated into new, secondary mineral precipitates (e.g. zeolite-like framework structures) and/or are being adsorbed on these new surfaces. Therefore, these surfaces must be characterised by the presence of both positively and negatively charged sites (M.V. Fey, pers. comm.)

High Mg levels initially, such as Sasol and especially Matla, show a sharp decline. The much higher values found in the early Matla solutions seem to correspond with much higher sulphate concentrations initially found in the Matla extracts compared with those of the other ashes. This suggests a $MgSO_4$-rich phase in the fresh Matla ash.

One of the most striking changes observed in the extracts collected over the sampling period is the pH (Figure 4.7). The pH of Matla rises slowly from 7.9 to a final value of 12.9 whereas Sasol establishes a pH of 12.7 after five minutes and remains constant over the curing period. Kriel is intermediate in terms of initial pH (11.9) as well as the moderate increase in pH over the sampling time. The pH of the solutions changed little after about 60 minutes of equilibration with the fly ash.

The slow rise in pH of the Matla sample may be related to the high SO_4^{2-} content in solution (Figure 4.8). The sulphate curves reflect similar results to the pH in Figure 4.7 in that the decrease in SO_4^{2-} of Matla and Kriel follow the increase in pH. Matla initially displays high concentration in solution and decreases to a steady state after 60 to 360 minutes of hydration to a point one third of the original value. The relative decrease in Kriel SO_4^{2-} levels is similar to that of Matla

Table 4.4: pH, EC and major ions (mg/L)) by IC for fly ash saturated paste extracts collected over a period of 24 hours.

Sample	Time (min)	pH	EC (mS/cm)	Na	NH_4	K	Mg	Ca	Sr	F	Cl	SO_4	CO_3^{2-} *
Sasol	5	12.7	9.7	229	89	24	20	2181	15	2	105	1521	2181
	10	12.8	10.0	223	87	22	17	2279	17	2	108	1490	2847
	30	12.7	8.2	225	81	20	16	2117	21	2	120	1374	2692
	60	12.7	9.7	249	61	4	14	2060	22	2	129	1473	2516
	360	12.8	9.1	101	71	21	4	2028	36	1	26	1122	2578
	720	12.8	9.4	99	49	20	2	1634	94	1	38	1143	1926
	1440	12.9	9.6	105	57	24	2	1648	N/AV#	< 0.01	20	1134	1992
Matla	5	7.9	6.2	151	6	51	547	1703	16	< 0.01	33	3450	1961
	10	8.6	6.1	145	4	37	446	1771	33	1	22	3421	2741
	30	12.4	6.6	112	10	29	15	1763	17	< 0.01	20	2794	1082
	60	12.6	8.0	117	5	33	5	2085	28	< 0.01	97	2136	1895
	360	12.7	8.3	113	6	36	3	1748	56	< 0.01	38	1280	1958
	720	12.8	9.5	129	4	47	39	1876	139	< 0.01	16	1266	2401
	1440	12.9	10.6	124	2	51	2	1907	< 0.01	< 0.01	15	1341	2205
Kriel	5	11.9	4.1	68	12	28	2	1355	15	2	34	2720	420
	10	12.4	4.8	62	4	22	1	1152	34	2	19	1584	840
	30	12.8	9.7	73	6	32	3	2096	32	1	30	1258	2468
	60	12.8	9.1	78	5	31	4	1940	36	< 0.01	34	1157	2303
	360	12.8	10.5	58	9	33	3	2152	67	< 0.01	20	1163	2626
	720	12.8	10.8	44	2	28	< 0.01	1633	151	< 0.01	35	1144	1883
	1440	10.8	12.9	40	13	28	13	1648	< 0.01	< 0.01	9	720	2083

N/AV = not available

* alkalinity was not analysed quantitatively and the figures reported represent the charge imbalance (cation excess) of the solution recorded as CO_3^{2-}. The theoretical alkalinity value was used to determine the saturation index for gypsum.

suggesting that they may be following a similar reaction pathway. Sasol, much like the pH curve, exhibits only slight changes in SO_4^{2-} concentrations. Sasol drops by 400 mg/L over the experimental range, whereas Matla and Kriel drop by approximately 2000 mg/L.

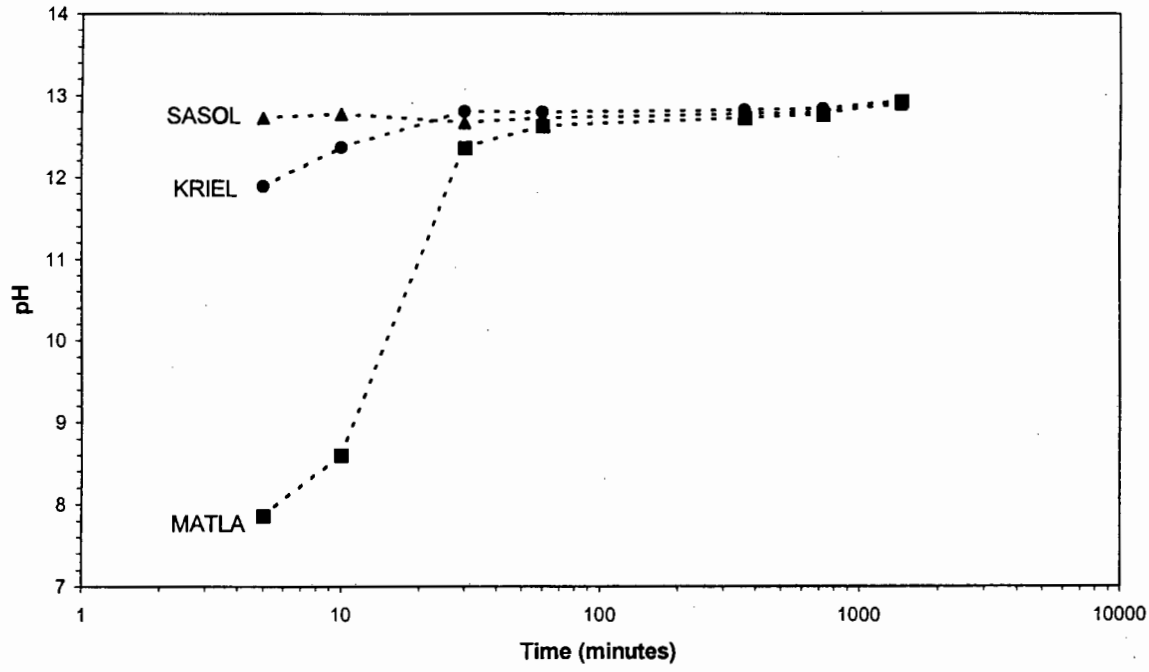

Figure 4.7: Change in the pH of the saturated paste extract over the setting time of fly ash briquettes

The relatively constant value of sulphate in the Sasol solutions indicates that the rapid increase in SO_4^{2-} concentration, or a decrease from a higher value, to the initial reading has done so before the first sampling time of 5 minutes. If Sasol follows the same trend observed for Kriel and Matla, the rapid decrease in the first 5 minutes of sulphate in solution may be attributed to secondary mineral formation. The rapid formation of secondary sulphate minerals has occurred too quickly to enable development of distinct crystal structures resulting in very small or amorphous structures. The much slower decrease in SO_4^{2-} of Kriel and especially Matla suggest that secondary crystal growth is occurring at a much slower rate, which would allow growth to form from a nucleated site resulting in much larger and better defined crystal structure. The slower formation would allow for bridges to form between fly ash particles and creation of a well-established crystal matrix.

In Sasol ash, Ca is already highest after 5- 10 minutes (Table 4.5 confirms that the increase is sharp within the first 5 minutes), whereas in Kriel and Matla, Ca continues to increase in concentration, peaking only after about one hour, and then declining. This trend seems to correspond with the fact the pH starts lower and increases in the early Kriel and Matla equilibration solutions, whereas in Sasol it is high to start with.

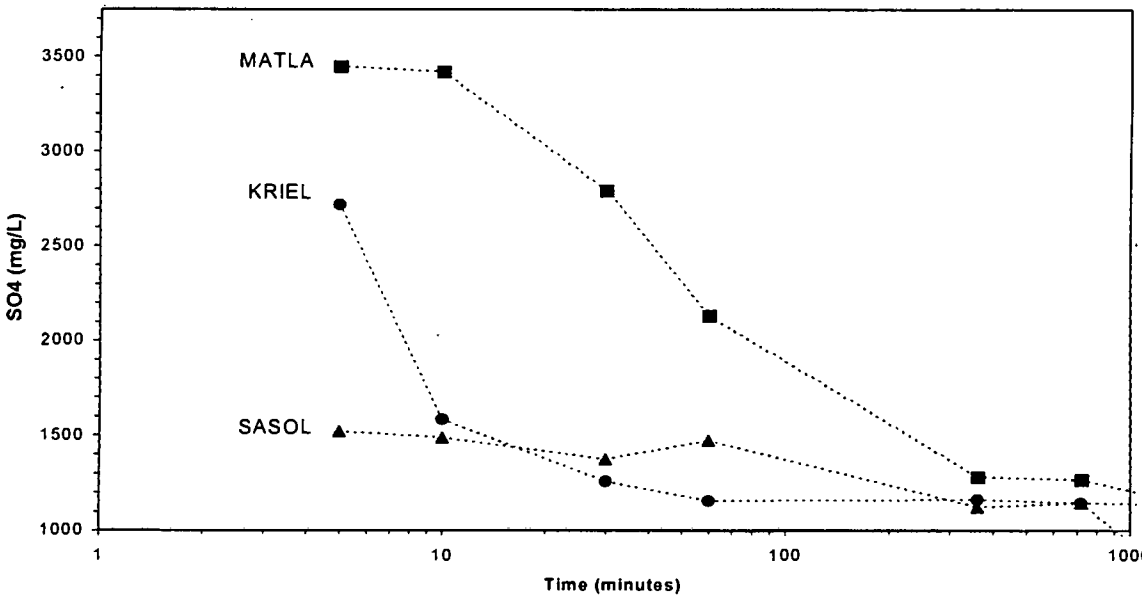

Figure 4.8: Change in SO_4^{2-} of the saturated paste extract over the setting time of fly ash briquettes

The EC of a sample is related to the sum of the soluble anions and cations in the sample solution. The trend in the EC of the saturated paste extracts does not appear at first to follow its basic relation of anion/cation balance. In most cases it is the anions which decrease while the EC remains virtually constant, which can be attributed to the increasing concentrations of HCO_3^-/CO_3^{2-} at such high pH values. Identification of ettringite formation indicates the presence of Al species in solution, which at such a high alkaline value is expected along with silica. The presence of Al and Si was not analysed for and these constituents could well contribute to the overall charge imbalance.

Further investigation into the early stages of hydration are provided in the curves displayed in Figure 4.9 for the set of dilute aqueous extracts obtained from fly ash sampled at intervals of 0.5, 1, 2, 3, 5, 7.5, 10 and 15 minutes. The pH values in

Figure 4.9 are not directly related to Figure 4.7 because they are dilute fly ash/water mixtures and thus the content of fly ash reacting with the aqueous phase is much less than is available for a saturated paste. The results do, however, show the same relative trend with respect to pH and ions in solution at early stages of hydration. Major ions were analysed by IC for the Sasol and Matla samples taken at intervals of 0.5 and 5 minutes and are presented in Table 4.5.

All of the ashes have assumed a steady state with respect to the dilute aqueous extract pH after 5 minutes of equilibration. The initial pH of Matla fly ash solutions is low compared to all of the other samples and it is characteristic of high sulphate levels. Matla fly ash also displays high magnesium concentration, which was observed in the saturated paste extracts as well. Sasol fly ash has almost reached a constant state after only 1 minute and displays low levels of sulphate in solution. The rise in SO_4^{2-} content of Sasol is very rapid and has reached a constant level after 30 seconds. The rate of pH rise in Matla mimics the saturated paste extracts in that the rise is very gradual, even with fly ash at a higher water content.

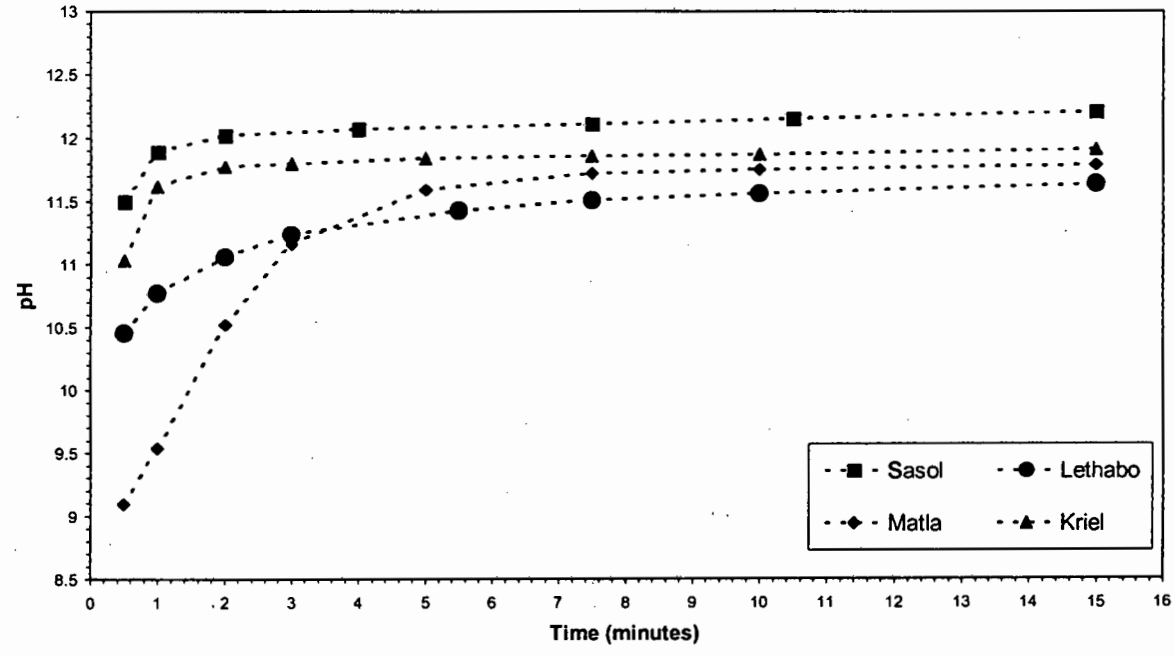

Figure 4.9: The pH of dilute aqueous extracts from four South African fly ashes

Table 4.5: Dilute aqueous extract data (0.5 and 5 minutes) for four South Africa fly ashes

	Lethabo (min.)		Sasol (min.)		Kriel (min.)		Matla (min.)	
	0.5	5	0.5	5	0.5	5	0.5	5
pH	9.7	11.4	11.9	12.2	10.3	12.0	8.9	11.8
EC (mS/cm)	0.3	0.8	2.4	4.2	0.9	2.6	1	2.1
Na (mg/L)	7	2	6	8	5	6	6	6
NH_4	<0.01	1	6	6	<0.01	<0.01	<0.01	<0.01
K	3	2	5	8	5	6.25	6	4
Mg	4	1	1	7	16	1	41	2
Ca	69	197	424	730	238	570	273	444
F	7	7	<0.01	1	2	1	1	1
Cl	3	2	38	12	3	5	2	4
SO_4	123	109	166	180	486	386	713	690

The decrease in Ca^{2+} and SO_4^{2-} can be explained by plotting the saturation index (SI) for gypsum obtained from MINTEQA2 speciation modelling. The SI curve for gypsum (Figure 4.10) follows the trend observed in Figure 4.8 for the decrease in SO_4^{2-} concentration over time. After 360 minutes all of the saturated paste extracts (with the exception of Kriel) are undersaturated with respect to gypsum. This is the same stage at which the SO_4^{2-} concentration becomes constant (Figure 4.8).

The decrease in SO_4^{2-} over time can be explained by gypsum precipitation up until the point that the concentration and SI become constant. The fact that no gypsum was detected by XRD adds to the complexity, but the SI values are provisional and if alkalinity had been analysed quantitatively rather than estimated by difference it is possible that the SI may have reflected an undersaturated state over the full experimental period. It is also possible, given the only slight saturation with respect to gypsum, that the amount of gypsum precipitation is below the XRD detection limit.

Thus, the decrease in sulphate concentration (Figure 4.8) can be explained simply in terms of gypsum formation. This does not negate any possibility of an

ettringitic phase, but as a simple explanation for some of the trends, its possibility cannot be ignored.

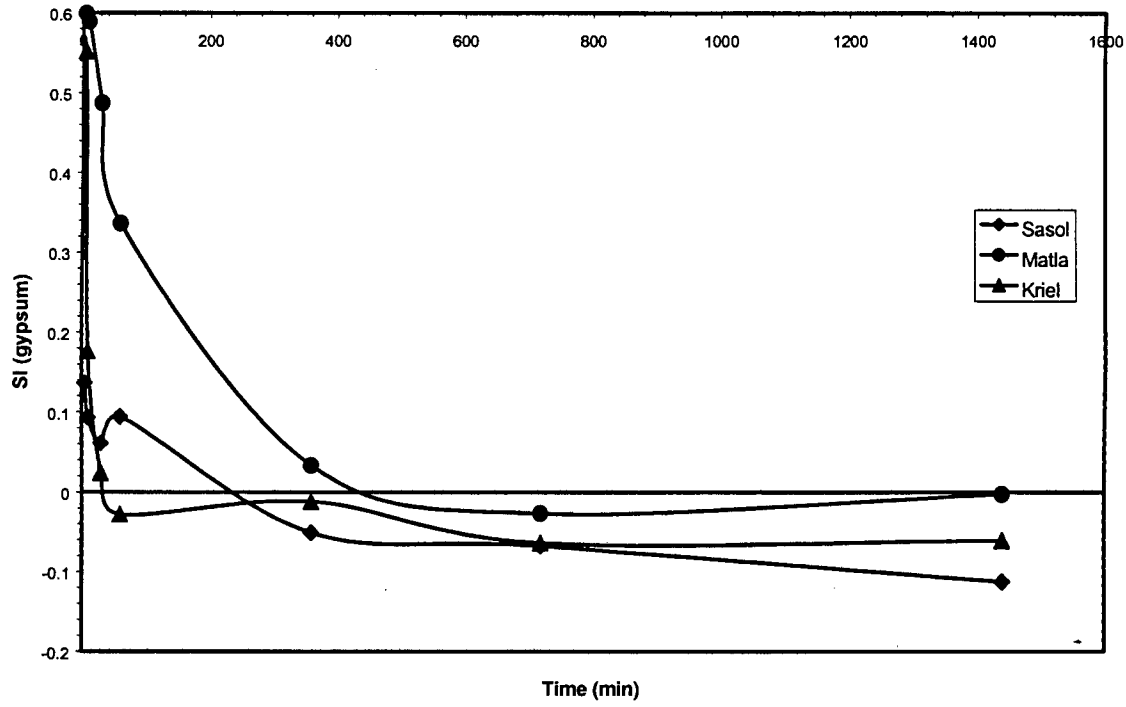

Figure 4.10: Saturation index (SI) for gypsum of fly ash saturated paste extracts from Kriel, Matla and Sasol over a twenty-four hour sampling period.

When taken together, these data suggest that a secondary precipitate is forming which incorporates mainly Ca, Mg (only significant in Matla) and SO_4, plus a small amount of Cl and some Na. The ions which obviously are not accounted for by these analyses are CO_3^{2-}, OH^-, $Al(OH)_4^-$ and $H_3SiO_4^-$. We simply do not know what form the precipitate would take and further study should take this into account.

If we assume that ettringite, thaumasite, gehlenite and/or calcite are the kind of secondary phases which form then we could offer a tentative explanation for the trends observed in solution composition. Alternatively, solubility product data for these minerals would be needed in order to calculate SI values to see with respect to which of these minerals the equilibrium solution is saturated or supersaturated (a plot of SI vs. reaction time for each mineral would help considerably in the interpretation). At this stage, the data are highly instructive in highlighting:

- the fact that secondary precipitates can form quickly (within a matter of hours);
- the precipitates probably have a complex composition, consisting of a "cocktail" of metals and ligands, and are therefore probably poorly crystalline, if at all;
- the dissolution-reprecipitation process is slower with Matla and Kriel ashes compared to Sasol, for which the initial sulphate concentrations are also significantly higher than in Sasol.

In evaluating relative hardening, care in comparing field observations with laboratory data (modulus of rupture) must be exercised because of the uncertainties about sulphate addition to the ash in ion exchange regeneration solutions, which boost both Na and SO_4 concentration. The Na and SO_4 in the saturated paste extracts obviously emanate from the ash itself.

4.4 Characteristics of weathered ash

In the previous sections on the physical and chemical variations of the unweathered fly ash samples, coupled with the literature review, it was concluded that Matla has the potential to show the greatest strength based on bulk CaO content alone. Kriel fly ash, with the finest particle size distribution, should show the highest strength based on this criterion alone. Sasol and especially Lethabo fly ashes have physical and chemical characteristics that show the potential for the lowest hardening strength. These predictions are strengthened based on the degree of hardness observed in the ash dams.

One of the major questions posed in the introduction to this dissertation was that relating to which of the secondary minerals were responsible for the hardening of ash dams and why these differences are observed between ash dams. The following sections will aim to establish whether secondary minerals of differing composition or abundance are observed amongst the samples and whether they may have contributed to the varying degrees of hardening. Much of the focus lies on the weathered fly ash samples and the secondary minerals associated with

hardening. SEM, coupled with XRD, has been applied extensively to the weathered samples to assess the secondary minerals and to attempt to relate them to the fly ash chemistry.

To be able to associate the reactions, reaction products and the secondary minerals formed as a result of hardening to the chemistry of fly ashes, the chemical composition of the weathered and unweathered samples was determined. XRFS data for the weathered and unweathered fly ash samples are presented in Table 4.6 for Kriel, Matla and Sasol. The weathered fly ash samples for Lethabo were not analysed due to time constraints. Changes in the oxide contents of Kriel and Sasol fly ash as weathering progresses are displayed in Figure 4.11. Matla fly ash has not been graphically represented as only two samples were analysed.

Comparisons between the weathered and unweathered fly ash samples can be drawn accurately only if the composition of the ash from a given power station has remained relatively constant over the length of time that the ash samples from the dam were taken. Willis (1987) found that the ash from Matla power station changed little over a two year sampling period. Comparison of the unweathered samples in this study with those of Willis (1987), Fourie *et al.* (1997) and Bosch (1990) in Chapter 4 showed that the composition of the fly ashes has changed little over a ten year time period. Based on these findings, the assumption can be made that the fly ash in the dumps at varying locations and present at differing stages of weathering were derived from fresh ash samples of similar composition.

4.4.1 Kriel fly ash

In terms of fly ash weathering the sample labelled Kriel is the youngest (fresh fly ash from the hopper) with sample KrielStp being the most weathered of the samples. Two intermediate samples include sample KrielCbt from the conveyor belt of the power station and sample KrielTop. Data for sample KrielCbt are not presented as this constitutes essentially fresh ash that has been slightly moistened.

Table 4.6: XRFS data for weathered and unweathered fly ash samples from three South African coal-burning power stations

Major elements (%)	Kriel	KrielTop	KrielStp	Sasol	SasolTop	SasolBot	Matla	MatlaDam
SiO_2	56.25 (0.29)#	52.36 (0.77)	49.79 (0.09)	52.98 (0.10)	53.16 (0.18)	52.16 (0.16)	49.92 (0.35)	49.13 (0.76)
TiO_2	1.72 (0.05)	1.59 (0.04)	1.53 (0.07)	1.69 (0.02)	1.51 (0.02)	1.26 (0.03)	1.58 (0.02)	1.38 (0.08)
Al_2O_3	27.21 (0.26)	25.11 (1.16)	23.92 (1.23)	28.45 (0.11)	27.21 (0.06)	22.22 (0.03)	30.45 (0.06)	27.77 (1.95)
Fe_2O_3	3.06 (0.02)	3.76 (0.32)	3.61 (0.85)	3.33 (0.05)	2.87 (0.05)	4.49 (0.01)	3.93 (0.01)	4.42 (0.57)
MnO	0.040 (0.002)	0.050 (0.005)	0.050 (0.006)	0.042 (0.001)	0.030 (0.003)	0.040 (0.002)	0.040 (0.002)	0.050 (0.000)
MgO	1.46 (0.13)	2.02 (0.22)	2.05 (0.13)	1.35 (0.12)	1.65 (0.08)	1.97 (0.13)	2.24 (0.07)	2.20 (0.01)
CaO	7.66 (0.09)	10.19 (0.74)	10.78 (1.51)	6.40 (0.06)	7.05 (0.06)	10.17 (0.15)	8.57 (0.02)	7.61 (1.24)
Na_2O	0.2 (0.1)	0.3 (0.1)	0.6 (0.1)	0.4 (0.1)	0.9 (0.0)	1.0 (0.0)	0.4 (0.1)	0.4 (0.1)
K_2O	0.759 (0.011)	0.740 (0.013)	1.14 (0.123)	0.460 (0.004)	0.390 (0.006)	0.440 (0.002)	0.939 (0.018)	1.14 (0.017)
P_2O_5	0.827 (0.015)	0.880 (0.030)	0.890 (0.043)	0.255 (0.001)	0.170 (0.004)	0.690 (0.021)	0.974 (0.016)	0.890 (0.074)
SO_3	0.633##	0.550	0.300	0.286	0.130	0.290	0.554	0.610
L.O.I	0.384 (0.11)	2.17 (0.30)	5.56 (0.22)	4.43 (0.09)	5.04 (0.09)	5.44 (0.00)	0.626 (0.04)	3.95 (0.30)

Numbers in brackets indicate the standard deviation between the two replicate samples

Value based on one analysis

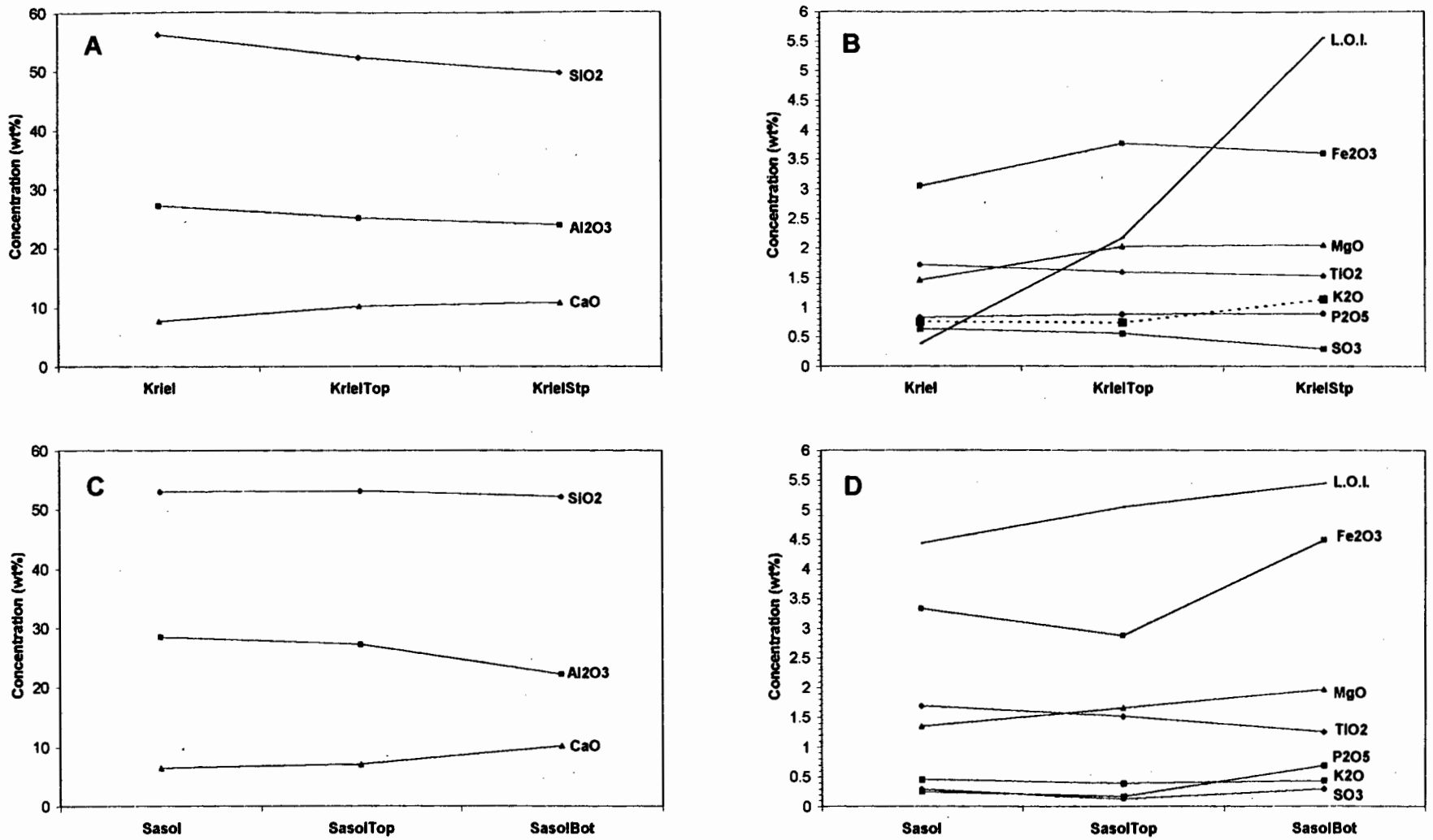

Figure 4.11: Changes in oxide content as weathering increases of fly ash samples from Kriel (a and b) and Sasol (c and d).

4.4.1.1 Morphology

The objective of looking at the series of weathered fly ash samples with SEM was to develop an appreciation of the order and form of hardening within the samples. In addition, the identification and characterisation of any secondary minerals present, especially secondary minerals that are associated with the hardening, were sought through the SEM studies. Two Kriel samples, KrielTop and KrielStp, were studied using SEM back-scattered and secondary electron imaging. Imaging was performed directly on weathered fly ash as well as polished thin sections of the same sample location. The images of Kriel fly ash are presented in Figures 4.12 and 4.13 while the images of the thin sections are presented in Figure 4.14.

The images from the weathered fly ash samples KrielStp and KrielTop reveal a plethora of information meriting discussion. To begin with, it would appear that there are at least two types of crystals present when comparing the two fly ash images, or the same type of crystal at different stages of formation. Sample KrielStp (Figure 4.12a and b) shows an extensive network of interlocking crystals that are some cases from bridges between fly ash spheres. The growth would appear to be a protective coating around the particle. The large fly ash sphere displayed in Figure 4.12b suggests that the skin is exfoliating from the surface, as there is spacing between the coating and the reacted fly ash particle. Under the exfoliating layer there would appear to be another layer visible between the fly ash sphere and the crystal coating (best seen in Figure 12b) on the large sphere where a fragment is separated from the bulk of the coating). The spacing between the sphere and the skin could be due to increased dissolution of the sphere through diffusion-controlled kinetics of the protective covering rather than a reaction-controlled mechanism (Joshi and Rosauer, 1973).

The sample KrielStp is very hard and has attained, in the ash dam, a state of very strong cementation. This is reflected in the SEM image for the sample portraying a very rigid state of interlocking crystals and matrices between the fly

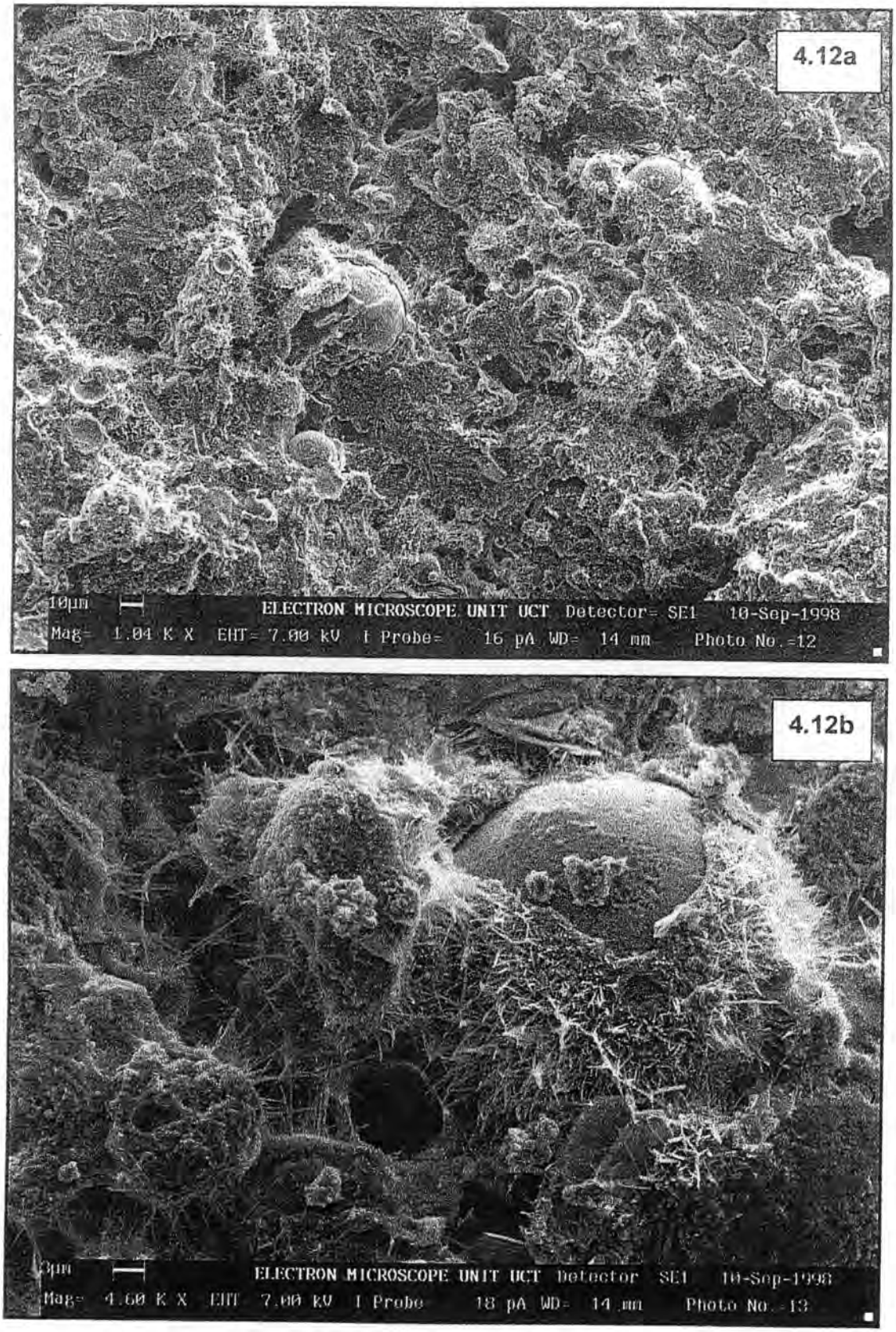

Figure 4.12: SEM images of sample KrielStp at a) 1000x magnification, and b) 4600x magnification. The images show an extensive network of crystal growth which gives the weathered fly ash the appearance of being well cemented.

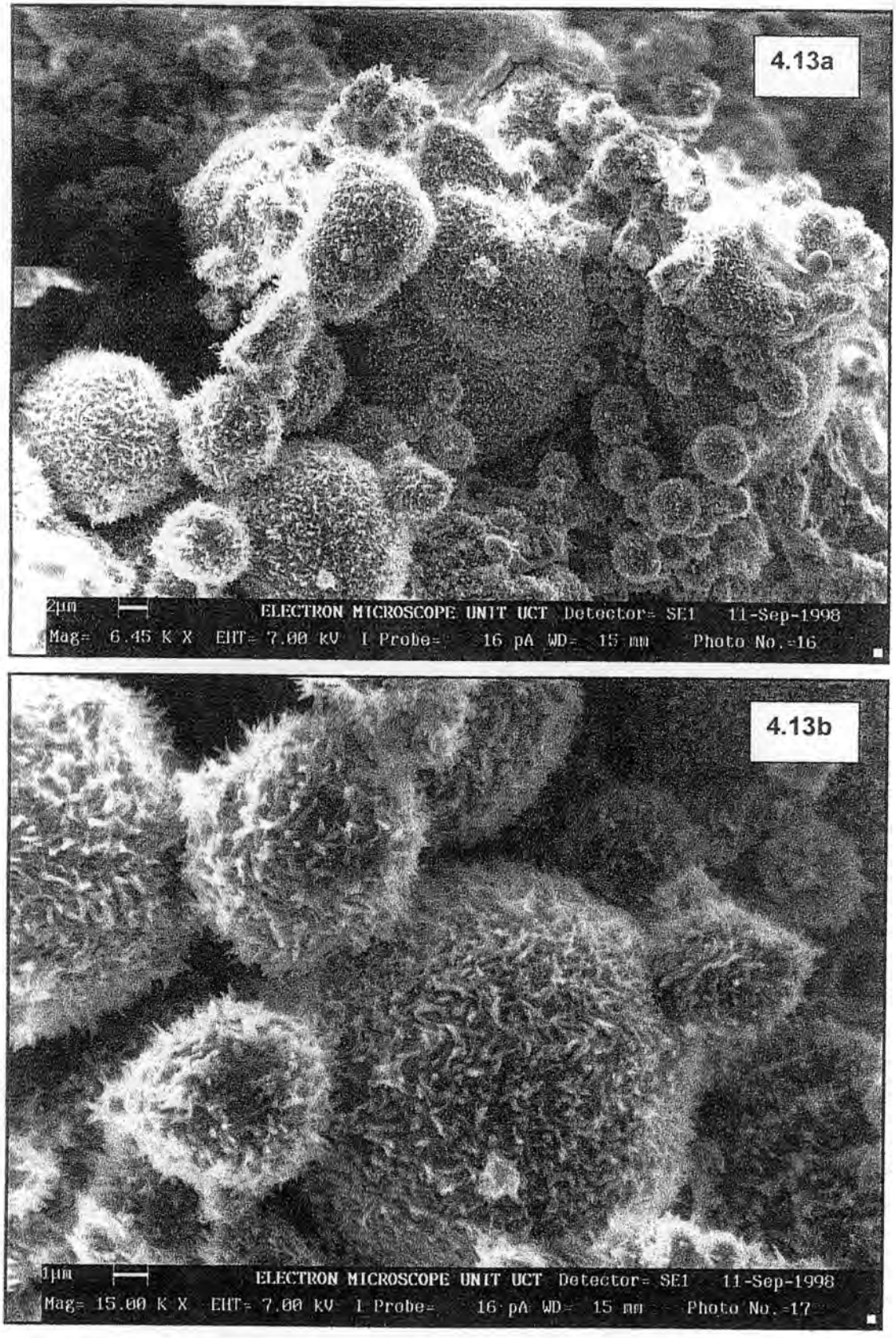

Figure 4.13: SEM images of sample KrielTop at a) 6450x magnification, and b) 15000x magnification. The images show an extensive covering of small crystals giving the fly ash spheres a fuzzy look to them. It would appear that the fuzzy coating is binding the spheres together.

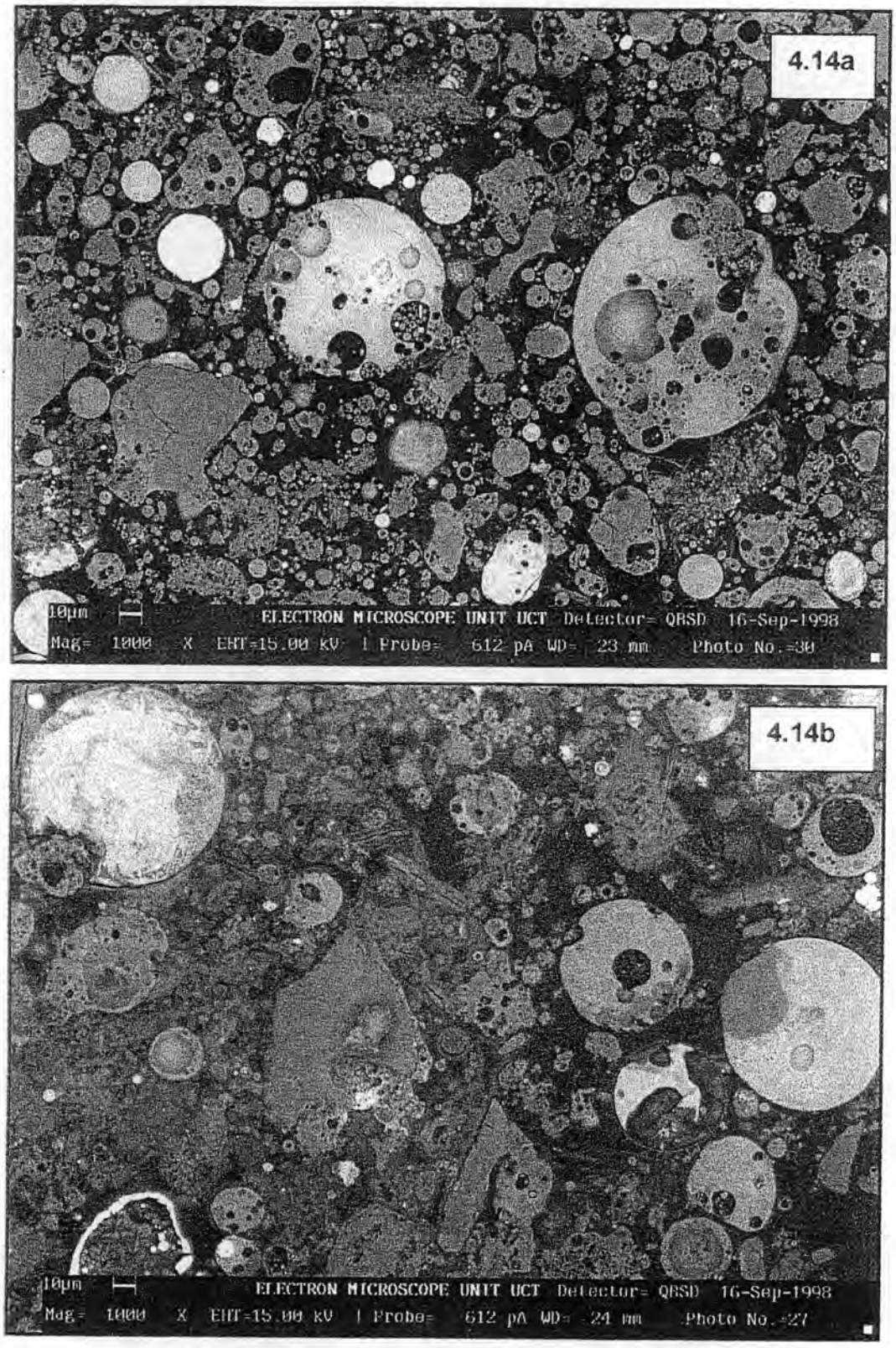

Figure 4.14: SEM images of thin sections from sample a) KrielTop and b) KrielStp. The presence of a matrix is noticeable in between the fly ash spheres of the more weathered sample KrielStp. No crystals are observed on the fly ash spheres using this type of sample preparation and magnification.

ash particles. The matrix (Figure 4.12a) masks the distinct spherical nature of the fly ash spheres and only few spherical particles are recognisable.

Sample KrielTop (Figure 4.13) has a distinctly different crystal form from the more weathered KrielStp sample, although they may be reacting by the same mechanism but currently are at different stages. The fly ash spheres in the KrielTop sample are covered completely by small crystals less than 1μm long giving the fly ash spheres a fuzzy appearance. The crystals seem to be growing on the surfaces of the fly ash spheres forming a skin around the particle but have not established a complex bridging matrix similar to that seen in sample KrielStp. However, the presence of the crystals does appear to be linking the fly ash particles together via an interlocking 'Velcro' type bonding. The small crystals on the spheres have the same appearance as tricalcium silicate after 12 and 24 hours of hydration, observed under SEM by Valenti *et al.* (1978). The polished thin sections (Figure 4.14) of the weathered Kriel samples were analysed with a backscattered detector, enabling detection of compositional data based on the contrast in intensity of the sample. The two samples both show similar distributions of particle size ranging from very small fly ash spheres to large spheres and angular particles. Sample KrielStp displays a matrix between the fly ash spheres which is not present in the KrielTop sample. The matrix of the thin section is most likely the extensive interlocking crystals observed in Figure 4.12. The presence of the smallest particle size fraction in the thin section of sample KrielStp is not as evident as in sample KrielTop because the interlocking matrix is masking the small fraction. It would appear that the smallest spheres have been incorporated into and are being obscured by the matrix.

4.4.1.2 Bulk chemistry and mineralogy

The data for weathered and unweathered samples were presented earlier in Table 4.4 with representations of the changes being plotted in Figure 4.11. The SiO_2 and the Al_2O_3 contents of the ash samples KrielTop and KrielStp decrease with increased weathering. However, the ratio SiO_2/Al_2O_3 (2.1) remains the same as weathering proceeds. This would suggest that the SiO_2 and Al_2O_3 contents

are decreasing relative to the bulk sample due to a dilution effect of increasing L.O.I. and CaO content.

The CaO and the L.O.I. of the samples are most probably related. The constituents contributing to L.O.I. of fly ash samples can typically vary, but the most common of phases associated with weight loss include carbonates, combined water, and combustion of free carbon (Wesche, 1991). The L.O.I. of the Kriel samples is unlikely to be due to the combustion of free carbon as the L.O.I. of unweathered fly ash did not show the same DTA peak at 600°C (Figure 4.4) as the Sasol sample, which was attributed to unburned coal. There are two ways that the L.O.I. of the Kriel samples could increase without any contribution from unburned coal, namely water of hydration and carbonates. Both may be associated with the calcium content of the ash.

Possible calcium containing minerals that can be attributed to the increased L.O.I. of the Kriel samples include calcite and ettringite, and to a lesser extent gypsum as it is less hydrated. Assuming that the increase in L.O.I. from the unweathered Kriel fly ash to the sample KrielTop is entirely due to calcite formation, then the molar increase of CaO should be equivalent to the molar increase of CO_2 from the L.O.I. of the sample. The molar CaO content, calculated to be 2.16 ± 0.71 moles, and the CO_2 content, 1.79 ± 0.41 moles, occur in relatively similar abundance. The assumption does not agree for the sample KrielStp as the increase in L.O.I. is much greater than the corresponding increase in CaO content. This suggests that the L.O.I. relationship for calcite formation is not a linear trend and thus there must be contributions apart from CO_2 within the L.O.I. of the sample. Alternatively, to assume that the weight loss is due to water of hydration from ettringite, or an ettringitic type mineral, between the unweathered fly ash and sample KrielTop can be justified only if the hydration of the ettringite molecule is $18H_2O$, whereas it should be $32H_2O$. It would appear that the combination of calcite and another hydrated mineral component would best account for the increased L.O.I. of the samples. In both cases, however, it would appear that it is a calcium-rich phase which is involved.

The presence of calcite ($CaCO_3$) and ettringite ($Ca_6Al_3(SO_4)_2.32H_2O$) within the fly ash matrix is supported by X-ray diffractograms of the samples. Figures 4.15a and 4.15b show the diffraction pattern series of the Kriel fly ash samples. Ettringite is present in all weathered samples and shows an increase in peak intensity corresponding to an increase in the weathering of samples. The unweathered sample, labelled Kriel, shows neither ettringite nor calcite, which was expected due to the fact that the sample has yet to come into contact with an aqueous phase to begin hydration and carbonation reactions.

The presence of other phases within the binding matrix of sample KrielStp or KrielTop is not ruled out. Some phases may be in such small quantity that they either are masked by peak overlap from some of the primary minerals seen within fly ash, or are present as an amorphous phase. Odler (1998) indicates that the C-S-H phase ($CaO_x.SiO_2.H_2O_y$) is a nearly amorphous material and its structure cannot be studied by X-ray diffraction.

The presence of increased CaO content in the weathered samples is either due to leaching of ions other than calcium from the sample or addition of calcium to the sample. Bezuidenhout (1995) found that the CaO concentrations increased with depth within an ash dam at Kriel Power Station, which was attributed to leaching of calcium through the dam and precipitation of Ca-containing secondary solids. This is contrary to what seems to be occurring in the present materials since it has been found that the greatest concentration of CaO occurs at the top of the ash dam (KrielTop, Table 4.6).

It is possible that some form of capillary rise of water occurs within the ash dam. Ash water would be drawn upwards in continuous pores, until the suction gradient acting upwards is balanced by the gravitational head gradient (White, 1997). Evaporative concentration at the atmosphere-ash dam boundary will accumulate salts at the surface and most probably react with CO_2 at that boundary and precipitate calcite. The longer exposure of the sample KrielStp to CO_2 at the surface than sample KrielTop may provide an explanation for the differing strengths observed between the two samples. The precipitation of

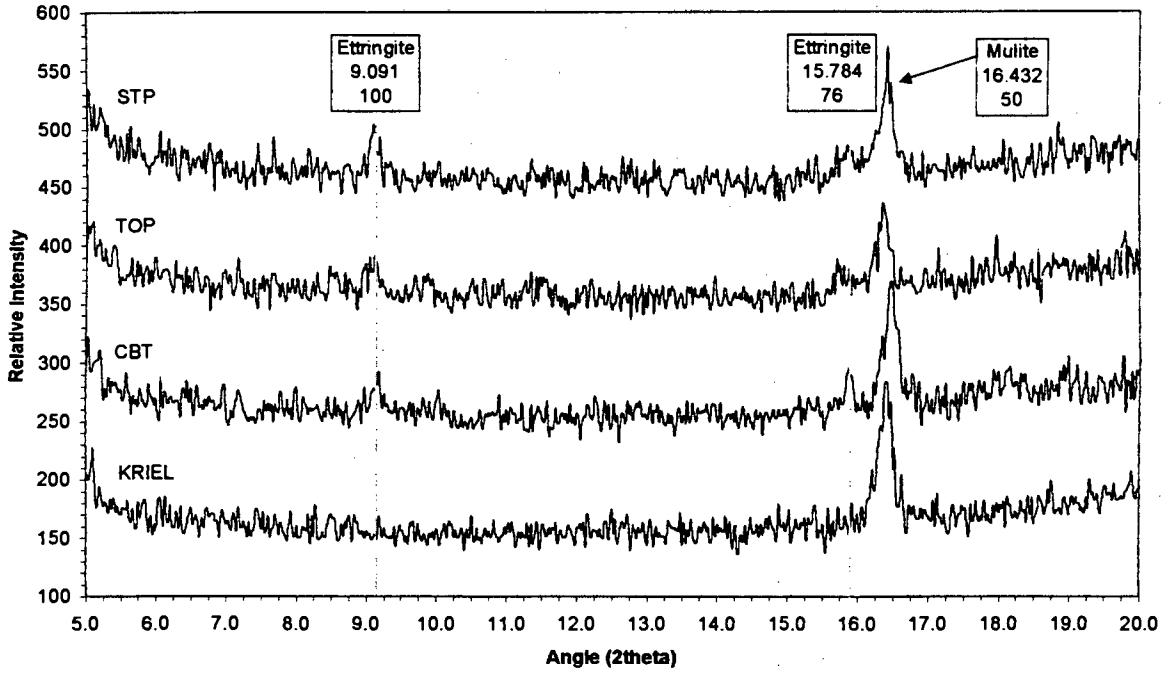

Figure 4.15a

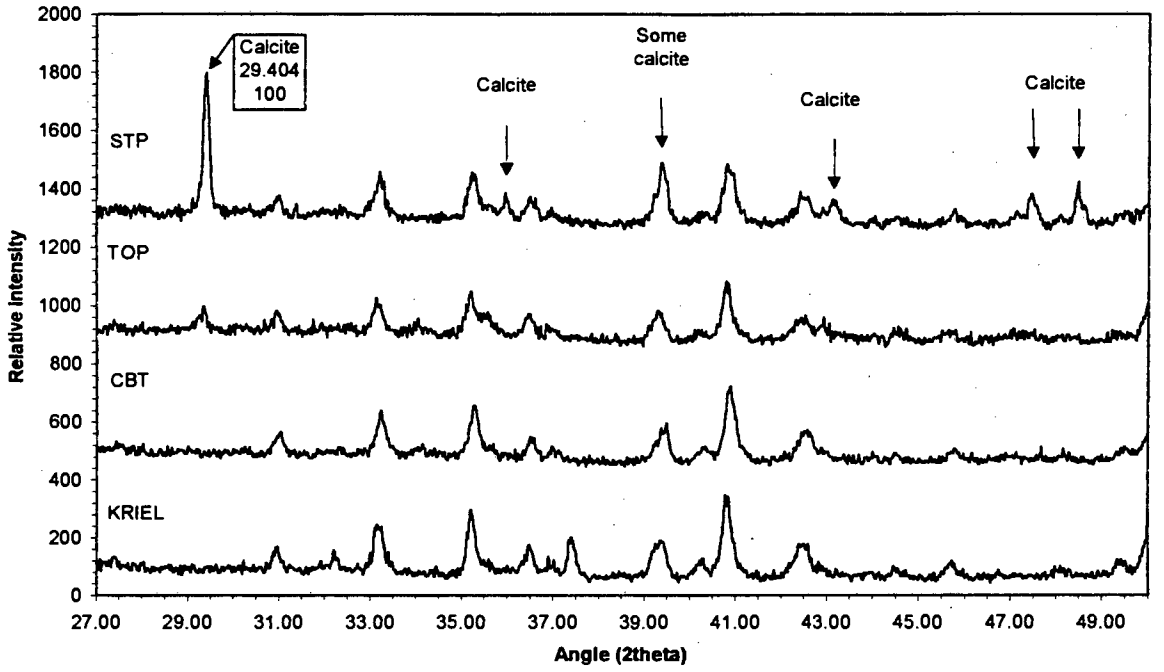

Figure 4.15b

Figure 4.15: The presence of a) ettringite and b) calcite in weathered samples of Kriel fly ash. The XRD patterns from bottom to top within each Figure are a progression in weathering of the sample series.

calcite is dependent, however, on Ca^{2+} being the dominant cation in the pore water of the ash dam. This was confirmed by Bezuidenhout (1995) who found that calcium in Kriel ash dam leachate was the dominant cation, with sulphate and carbonate/bicarbonate as the dominant anions in solution. The dominant ions in solution have the potential to precipitate calcite and gypsum as the dominant secondary solid phases at the atmosphere-ash dam boundary. However, no gypsum was identified in the XRD patterns of any of the weathered fly ash samples from Kriel.

4.4.1.3 Semi-quantitative SEM EDXRF analysis

The composition of the dense covering of crystals and interlocking matrix of the weathered fly ash spheres was, at this stage of the study, unknown. XRD patterns of weathered ash from this study indicated the presence of calcite and ettringite, but no gypsum or secondary silicate minerals were detected. Secondary silicate minerals, such as calcium silicate hydrate, have been reported to be non-detectable by XRD analysis (Odler, 1998). In addition, other silicate mineral phases such as gehlenite ($Ca_2Al_2SiO_7$), tricalcium silicate (Ca_3SiO_5) and calcium silicate ($CaSiO_3$) are common in reactions involving Portland cement. It is probable that some of these phases exist in weathered fly ash but their XRD pattern is obscured by those of primary minerals already contained within the fly ash matrix. In addition, some of the secondary minerals may be present in such small quantity that they are below detection limits. The main peak in the gehlenite diffractogram (JCPDS card 35-0755) will be partially obscured by mullite peaks, (JCPDS card 15-0776).

SEM-EDXRF analysis was performed on the regions outlined in Figures 4.16 for sample KrielStp, and Figure 4.17 for sample KrielStp and KrielTop, to try to identify the presence and composition of secondary minerals and their contribution to fly ash hardening. The SEM-EDXRF results from the spot analyses of sample KrielStp and KrielTop are presented in Table 4.7 in addition to the bulk chemical analysis of weathered Kriel fly ash. The images for the KrielStp samples suggest the presence of a hard shell that has encased the fly ash sphere and

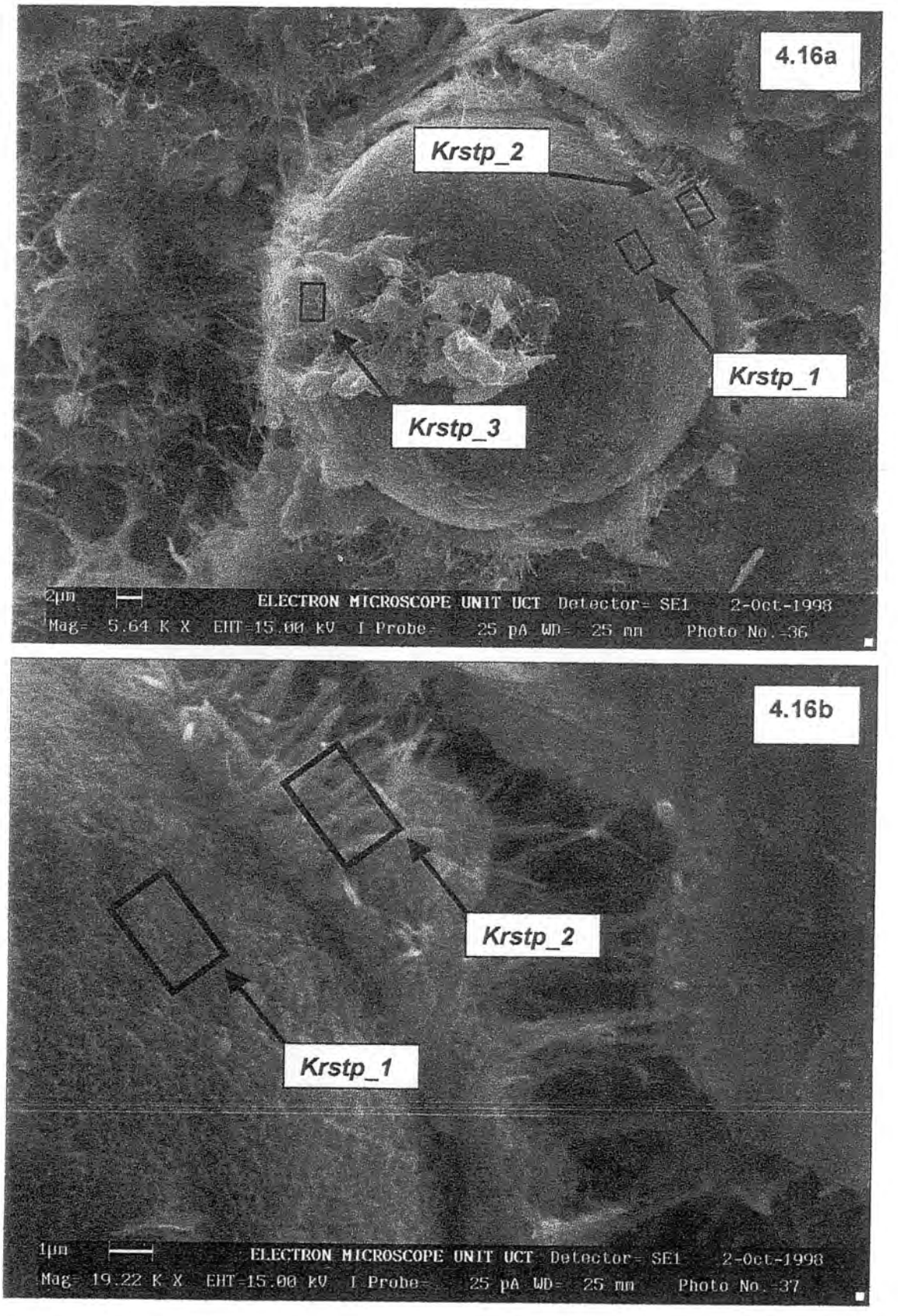

Figure 4.16: SEM images of the weathered KrielStp fly ash at different magnifications and showing the locations of the spot analyses taken for EDXRF data required for secondary mineral identification.

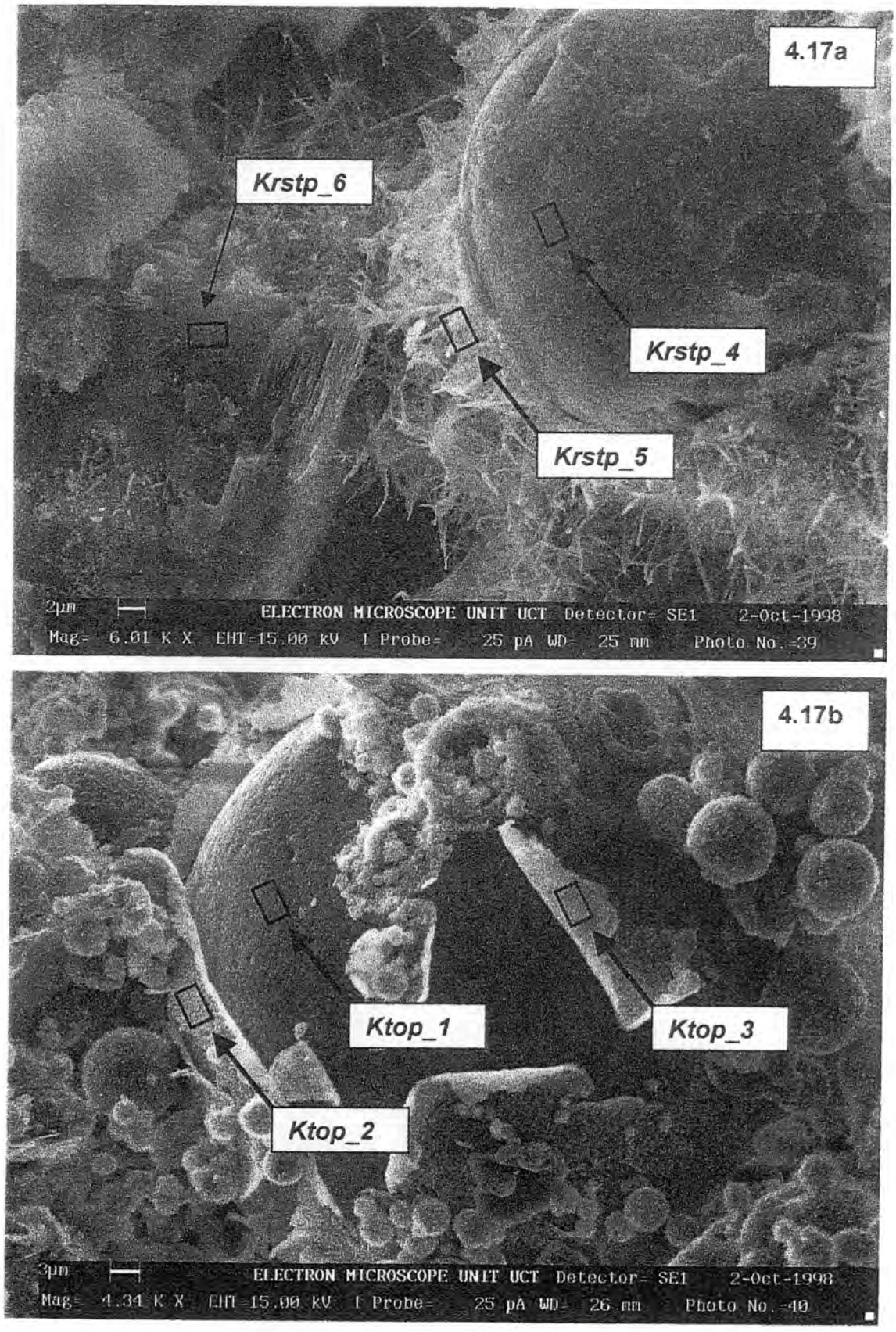

Figure 4.17: SEM images of weathered a) KrielStp and b) KrielTop fly ash and the locations of the spot analyses taken for EDXRF data required for secondary mineral identification.

Table 4.7: SEM EDXRF data (weight %) for spot analyses on Kriel fly ash of the images present in Figures 4.16 and 4.17

Element	KrielStp (ash)	Krstp_1 (sphere)	Krstp_4 (sphere)	Krstp_2 (crystal)	Krstp_3 (crystal)	Krstp_5 (crystal)	Krstp_6 (matrix)	KrielTop (ash)	Ktop_1 (sphere)	Ktop_2 (crystal)	Ktop_3 (crystal)
O	46.9	46.7	33.0	46.2	47.3	38.4	38.3	47.5	47.9	46.7	50.6
Na	0.5	0.4	0.6	2.0	0.7	0.6	0.8	0.2	0.5	0.6	0.5
Mg	1.31	3.15	1.52	0.77	1.47	1.03	0.35	1.25	2.38	1.73	0.70
Al	13.4	8.49	17.7	8.72	9.44	11.4	4.97	13.6	12.1	13.1	18.7
Si	24.6	17.0	24.8	14.6	12.1	11.6	15.3	25.1	15.7	23.2	22.6
P	0.41	0.43	0.39	0.24	0.22	0.46	1.15	0.39	0.67	0.43	0.55
S	0.13	0.34	0.21	3.84	3.46	5.02	2.25	0.22	0.29	1.41	0.64
Cl	NA*	0.11	0.21	0.56	0.39	0.52	0.69	NA	0.12	0.00	0.09
K	1.0	0.39	0.75	2.63	1.46	1.58	1.58	0.63	0.30	0.90	0.67
Ca	8.14	21.0	16.6	18.8	21.5	26.6	32.0	7.47	18.5	9.14	3.79
Ti	0.97	1.34	3.58	0.79	1.06	1.46	0.21	0.98	0.45	1.17	0.36
Fe	2.67	0.61	0.69	0.80	0.96	1.38	2.39	2.63	1.08	1.59	0.74

* NA = element not analysed

appears to have separated from the inner sphere. Revealed layering is probably due to a physical breaking apart to expose a fresh analytical surface during sample preparation. In addition to the crystalline skin surrounding the spheres, there is also a weathered matrix giving the appearance of an angular crystalline or amorphous phase. The surface of the sphere in Figures 4.16a and 4.17a has been weathered quite deeply as there is evidence of a series of exfoliating layers which are not dominant in the sphere observed in Figure 4.17b.

It was suggested that the coating observed in Figure 4.13 was a layer of secondary minerals causing the fuzzy appearance of the spheres. The SEM images provide confirmation of the assumption, taking into consideration the peeling layer of secondary minerals observed in Figure 4.16b. It is possible that the layer was a continuous wrapping around the fly ash sphere and may be starting to peel due to shrinking of the layer resulting from dehydration of the secondary minerals. Massazza (1998) indicates that if crystals of ettringite are dehydrated, lattice shrinkage occurs and when under vacuum gross morphological changes are easily effected in the electron microscope.

4.4.1.3.1 Uncertainties of SEM-EDXRF analysis

It has been suggested that calcite and ettringite may be present (XRD supports this in the matrix of fly ash), and may contribute to ash dam hardening. However, their detection will depend on crystal size. The crystals observed by SEM are very small, at most 5μm long by 1μm thick with the majority less than 2μm long and < 0.5μm thick. Although some of the images show vast masses of interlocking crystals and a dense covering on the fly ash spheres, various problems are encountered in quantitatively analysing the crystal composition. Because of the uncertainty involved with analysing the crystals, the results can only be considered semi-quantitative.

The first problem encountered involves the volume that the SEM-EDXRF system analyses. The analysing volume is of the order of 2 μm^3 while the thickness of even the largest crystal observed is 2 μm long and fractions of a micrometer thick. Frequently the analysing volume is larger than even the smallest crystals, which,

when analysed, will include contributions from underlying and surrounding matrices. This leads to the second problem encountered, which is the magnitude of the contribution to the crystal data and what contribution to the data obtained can be attributed to the surrounding and underlying matrix. This can be corrected for by analysing the surrounding matrix or phase if it is present without covering or interference of crystals. Subtraction of the two spectra, e.g. Krstp_2 minus Krstp_1/3 (Figure 4.16b), coupled with data manipulation, provides corrected data for the crystals themselves. The corrected data can only be achieved by assuming that one of the analysed elements is solely from either of the matrices. Thus, the resultant spectrum is biased towards the element which is selected as being absent from the crystal matrix.

For the reasons outlined above, the extensive use of SEM EDXRF for detection and characterisation of new secondary minerals has not been applied. The data are used rather to identify and establish trends and characteristics between the fly ash spheres and the crystals present, and in so doing potentially to identify a secondary mineral phase which is known to be present within the fly ash sample.

4.4.1.3.2 Kriel steps

The two series of samples Krstp_1,2,3 and Krstp_4,5,6 differ other and will be discussed briefly in turn. The sphere from which analyses Krstp_1, 2 and 3 were derived shows at least four different layers. It is probable that spot sample Krstp_1 represents the perimeter of the fly ash sphere and can be used to compare compositional differences between the fly ash particle, the secondary minerals and the bulk chemical analysis. The first exfoliation layer, which was not analysed, can be seen approximately 2 μm below the spot sample Krstp_1. The second exfoliation layer (Krstp_2 and Krstp_3) was analysed and can best be observed under the high magnification image of Figure 4.16. The fourth layer consists of a series of circular rings found on the bottom of the fly ash sphere in the image 4.16a.

Differences between Krstp_1 and the bulk chemical analysis for Kriel fly ash include substantial increases in Ca and Mg coupled with decreases in Al, Si, Fe,

and K. The ratio of Si:Al for both the bulk chemical analysis KrielStp fly ash and sample Krstp_1 has remained the same, suggesting that the decrease in Si and Al is due to a dilution of Ca and Mg. The compositional characteristic of Krstp_1 is suggestive of a high Ca-Mg "glass". The decrease in Fe content of the fly ash sphere is, not surprisingly, lower as Fe occurs frequently as a single phase and does not incorporate itself within the glass of the fly ash sphere (Watt and Thorne, 1965).

The analyses of Krstp_2 and Krstp_3 are of the second exfoliation layer observed in Figure 4.16 and they indicate a very similar composition to that of sample Krstp_1. Potassium is concentrated in the secondary minerals compared to the bulk chemical analysis. Sulphur content is an order of magnitude higher in the secondary minerals than that of the adjacent exposed sphere. The ratios of the crystal matrices have decreased considerably to 1.67 and 1.28 for samples Krstp_2 and Krstp_3, respectively, with respect to the same ratio for Krstp_1. The changing ratio is not due to an increase in Al, as this remains constant over the sampled series, but rather due to a considerable decrease in Si content within the crystal matrix. The Ca content remains essentially constant throughout the series of samples.

The increase in sulphur and aluminium, and especially aluminium relative to silicon, and the consistently high Ca content of the secondary minerals, suggest a Ca-Al-SO_4 type structure. Ettringite has been previously identified by XRD and provides a possible structure to match the EDXRF data.

The second series of data include samples Krstp_4, 5 and 6. The fly ash sphere analysed in Figure 4.17a displays three altered stages. The first observable layer is the "purest" glass, which was not analysed. The first altered or exfoliating layer analysed (Krstp_4) lies on top of the glass and below the second altered layer (Krstp_5) displaying vast quantities of long needle-like crystals. Another phase was analysed to the left of the exfoliating sphere, which may be indicative of the inter-particle matrix observable in Figures 4.12 and 4.14b.

Sample Krspt_4 is distinctive because of the low O content. This may suggest that the silicate and aluminate bonds have decreased due to substitution or exchange within the glass matrix. It is improbable that the decrease in O content is due to loss of hydration because the bulk analysis for sample KrielStp, which has an O content of 47%, was dried at 900°C and, if anything, would be less hydrated than the data derived from SEM EDXRF. The fly ash sphere in sample Krstp_4 also has a high Ti content, perhaps suggesting a higher rutile content within the parent coal, as substitution and exchange reactions with titanium are unlikely to produce a titanium concentration of 3.6%. Calcium and, to a lesser extent, aluminium are high with respect to the bulk fly ash sample KrielStp, while the Si content is equivalent to the bulk sample, which results in a lower Si:Al ratio.

The crystals analysed in sample Krstp_5 show a decrease in magnesium, silicon, aluminium and titanium concentrations relative to the adjacent exfoliating layer and bulk chemical analysis of the fly ash. These decreases are due to large increases in the Ca and S content of the crystals. The Si:Al ratio has increased to 0.98 which indicates a relative increase in Al content with respect to the Si content of the crystals. The most marked change of the matrix analysed in sample Krstp_6 involves the Si:Al of the sample. The Al is extremely low while the Si has decreased to a lesser extent, which results in a very small Si:Al ratio of 0.32. The Ca content is very high and may be attributed to the dilution effect of the other elements with respect to the sample Krstp_4 and 5. The sulphur content is higher than the first exfoliating layer but much less than the second layer. The high content of calcium in the matrix coupled with decreases in aluminium suggest that the matrix could be calcite.

The general trends between the bulk chemical analysis for weathered KrielStp fly ash and the secondary crystal matrices include elevated levels of Ca, S and K. The ratio of Si:Al is decreasing, except for sample Krstp_6, indicating relatively less Si and more Al present.

Bezuidenhout (1995) and Mattigod *et al.* (1990) suggest that ettringite may be forming in ash dams, while Fourie *et al.* (1997) and Hodgson and Grobbelaar

(1996) associated calcite and gypsum with ash dam hardening. Based on these three studies, and the positive identification of calcite and ettringite by XRD in this study, coupled with the trends observed from the SEM EDXRF data, it can be concluded that the crystal matrices displayed in Figure 4.16 may include calcite, gypsum and ettringite. The presence of gypsum has not been confirmed by XRD, which leads to the strong possibility that the high S contents in the crystal phases are due to sulphate in the ettringite structure.

4.4.1.3.3 Kriel top

The data series for KrielTop is very different from the highly weathered KrielStp sample. Sample Krtop_1 shows the same trends with respect to its chemical signature compared to the bulk chemical analysis KrielTop. The changes in the chemical signature of the secondary minerals on the surface of the sphere, however, do not mirror those seen for the KrielStp samples. The thin coating on spheres has a much lower Ca content and higher Si and Al content. This pattern of results is very similar to Krstp_4 which, from the images, is not unexpected as they are both "initial" layers. The Si:Al ratio compared to that of Ktop_1 (1.30) has increased for Ktop_2 (1.77) and in sample Ktop_3 has decreased (1.21) suggesting that either the thickness of the secondary mineral coating varies, or that, due to the different angle of the incident beam to the X-ray signal, the underlying glass phase is contributing either more (Ktop_3) or less (Ktop_2). The increase in S and K content in the secondary minerals has more than tripled for sample Ktop_2 and doubled for Ktop_3. The magnitude of the elements is much less, however, than observed for KrielStp samples.

Although the presence of ettringite and calcite has been detected for the sample KrielTop (Figure 4.15), the chemical signature of the secondary minerals of the samples would not seem to match the XRD pattern. The dramatic decrease in the Ca content and the weak increase in the S content, coupled with the increase in the Si and Al content, suggests that the secondary minerals observed in Figure 4.17b are neither calcite nor ettringite, but rather an alumino silicate phase. It is highly probable that the exfoliating layer observed in 4.17b is the beginning of the layering observed for the KrielStp samples.

4.4.2 Matla

The order of weathering for the series of Matla fly ash samples proceeds from sample Matla, which is the fresh fly ash sample from the hopper at the power station, towards samples Matla4dy and MatlaDam. The sample MatlaFlr has an unknown degree of weathering because of its isolation from all other ash dam samples. Judging from the degree of hardening that the sample had established it would seem to be close in degree of weathering to sample MatlaDam.

4.4.2.1 Morphology

The morphology of weathered Matla fly ash was studied by looking at samples MatlaDam and MatlaFlr by SEM analysis. The images taken (Figures 4.18 and 4.19) of weathered Matla fly ash show differences amongst the secondary minerals present within each image as well as between images of different samples. Sample MatlaFlr (Figure 4.18a and b) portrays an ash sample that is cemented together as a result of the presence of inter-sphere bonding through a well-established crystal matrix. The low magnification image of MatlaFlr (Figure 4.18a) lacks the typically smooth nature often encountered in fly ash spheres and instead appears to have a coating around the spheres to which a large amount of very fine particles adheres. The sample is well packed with respect to the amount of spheres in a given volume. The spacing between large spheres appears to be taken up by smaller fly ash particles and a secondary matrix, which limits the pore space of the system.

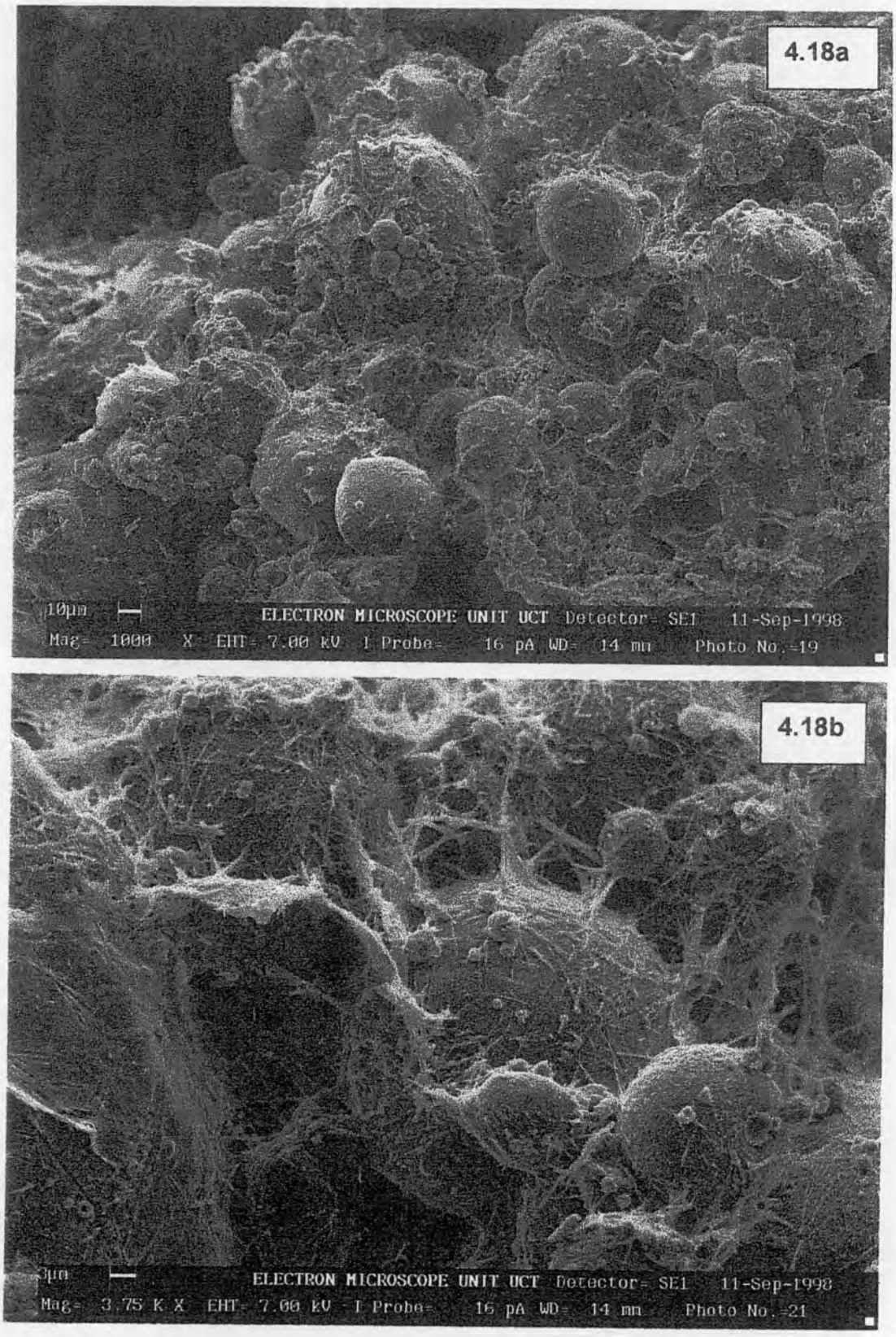

Figure 4.18: SEM images of sample MatlaFIr at a) low magnification, 1000x, and b) high magnification, 3750x. The images reveal an inter-sphere crystal matrix appearing to be responsible for the hardening of ash associated with the ash dam.

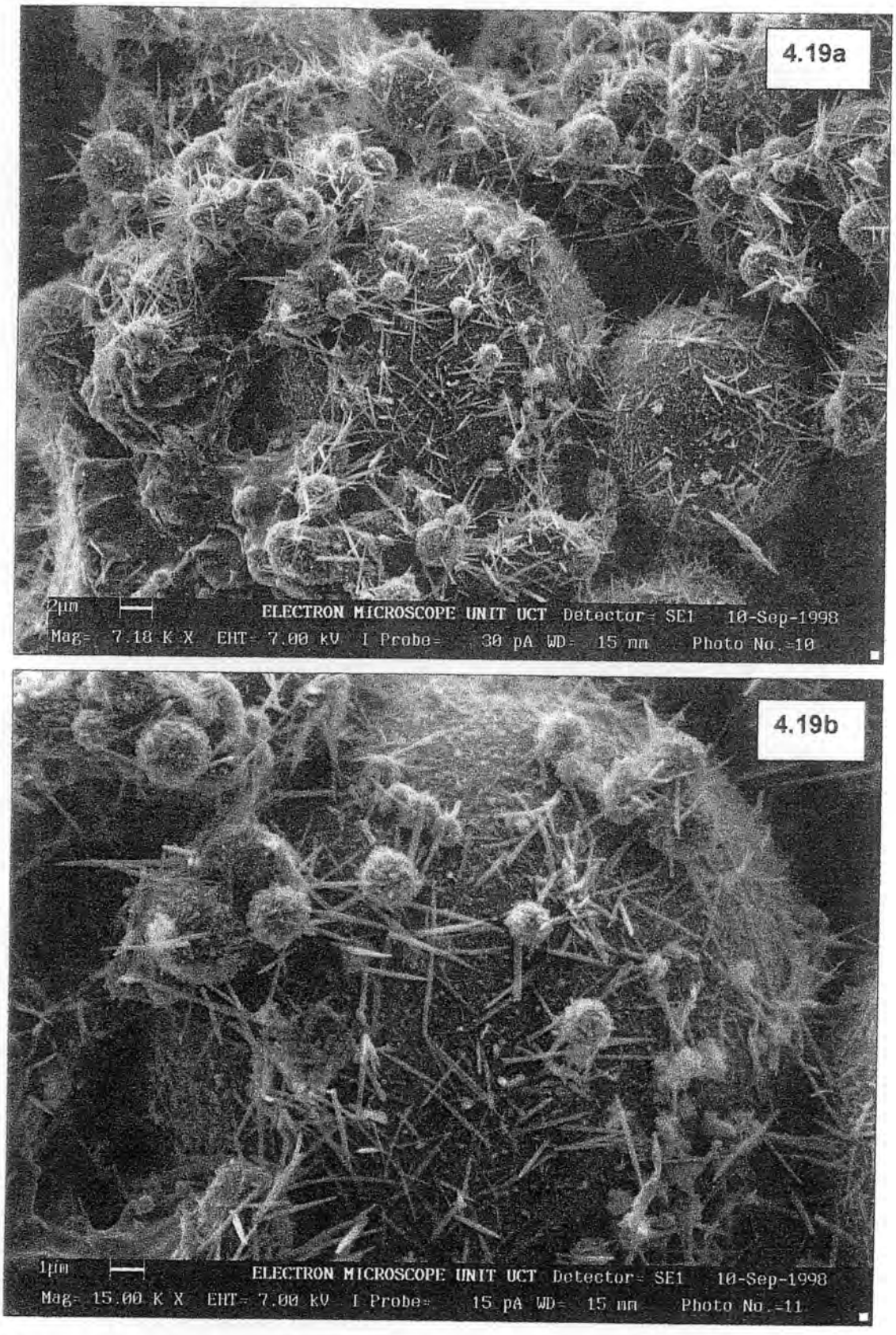

Figure 4.19: SEM images of sample MatlaDam at a) 7180x magnification and b) 15000x magnification. Substantial inter-sphere crystal matrix is lacking but the abundance of at least three types of secondary growth is evident.

Figure 4.18b reveals a sphere bound to a series of fly ash particles through a complex system of bridging crystals. The left-centre of the image reveals where a sphere has been removed most probably during cleaving the sample during sample preparation. The crystal matrix exoskeleton has remained intact around the space from which the sphere was removed, providing evidence that the formation of a coating around the sphere is contributing to fly ash hardening. In addition, many of the spheres display grooves and markings on the surface, most probably as a result of removal of a sphere during sample preparation which was bonded to the observed surface via a secondary mineral framework. The grooves are thus due to the ripping off of a linking crystal attached to another fly ash sphere from the surface.

The fly ash sample MatlaDam is very different to that of sample MatlaFlr in terms of the inter-sphere matrix as well as the type and abundance of secondary minerals observed. Either the secondary minerals are different, or if they are the same, then at a different stage of formation. The images from sample MatlaDam (Figure 4.19a and b) show the presence of at least three different matrices. The first is the long needle-like minerals displaying random orientation on the surface of the fly ash particles They do not appear to have developed an extensive bridging network between spheres. The second mineral phase can best be seen in Figure 4.19b, especially on the smaller particles contained within the image. The smaller spheres, to a larger extent than the larger fly ash particles, display a covering of small crystals that impart an appearance to the spheres of being fuzzy, a coating similar to that observed in Figure 4.13b for the fly ash sample KrielTop. The third phase can be seen on Figure 4.19a on the bottom left hand corner of the image, present as a thin continuous coating over the spheres with no apparent crystal matrix incorporated in the coating. It is possible that this phase is amorphous.

It would appear as though the same needle-like crystals predominantly observed in Figure 4.19 are also present in the MatlaFlr sample displayed in Figure 4.18. It seems as though the needle-like crystals are the same types that may have caused the markings on the fly ash spheres in Figure 4.18. The crystals observed

in both of the Matla samples possess the same geometry and have the same appearance, although the development in Figure 4.18 is far more advanced than that in Figure 4.19.

4.4.2.2 Bulk chemistry and mineralogy

Sample MatlaDam as well as the unweathered fly ash Matla were analysed by XRFS (Table 4.6). However, the sample MatlaFlr was not analysed. The analysis of sample MatlaDam compared to the unweathered fly ash is almost identical in terms of its bulk chemical composition. The slight exception is a narrow decrease in the Ca content (8.57 to 7.61) coupled with a decrease in the Al_2O_3 content (30.45 to 27.77), which is matched by a large increase in the L.O.I. content of the ash (0.63 to 3.95). The combined decrease in CaO and Al_2O_3 content is 3.65% which closely matches the increase observed for L.O.I. at 3.33%.

Thermal analysis of Matla fly ash (Figure 4.4) showed a broad hump across the analysing temperature range, but no peak at 600°C was observed, as in the Sasol sample, which was attributed to unburned coal. It is reasonable to suggest therefore that the high L.O.I. of the MatlaDam sample is not attributed to unburned coal but rather to a calcareous or hydrated phase similar to that suggested for the Kriel fly ash samples. The secondary minerals observed in Figure 4.19 can most likely be attributed to the L.O.I. of the weathered ash.

Mineralogical analyses of the weathered samples provide a means of identifying secondary minerals associated with the hardening of the ash dam. X-ray diffractograms for the series of Matla fly ash samples are presented in Figure 4.20. Two secondary minerals are identifiable within the diffractograms, namely ettringite and calcite. Both are calcium containing minerals and have been previously identified in weathered Kriel fly ash samples.

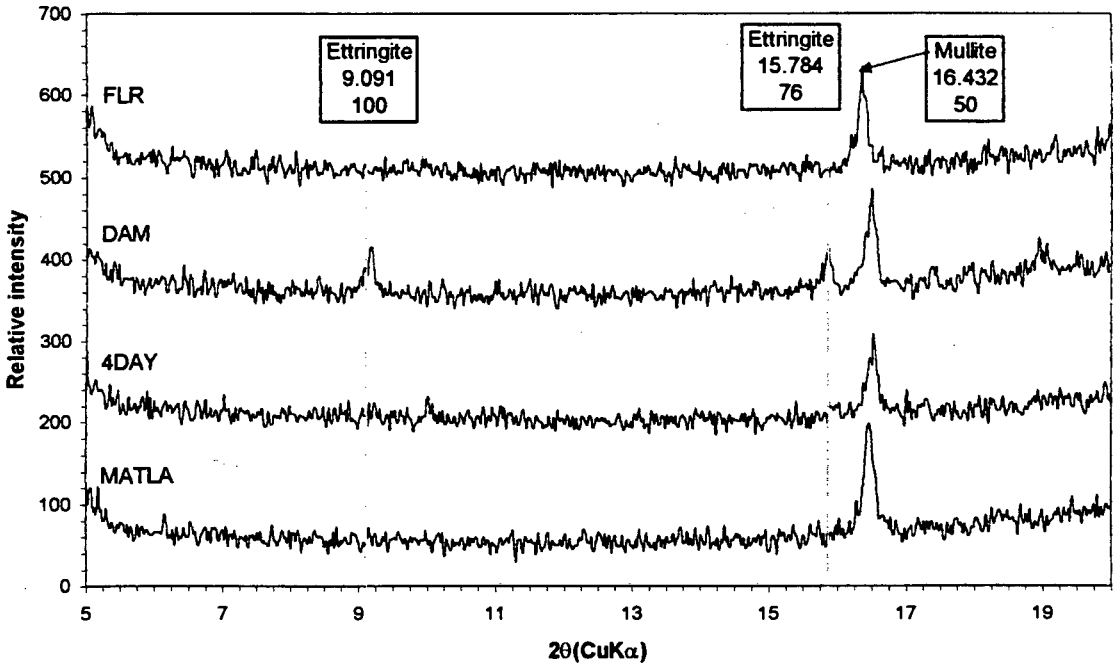

Figure 4.20a

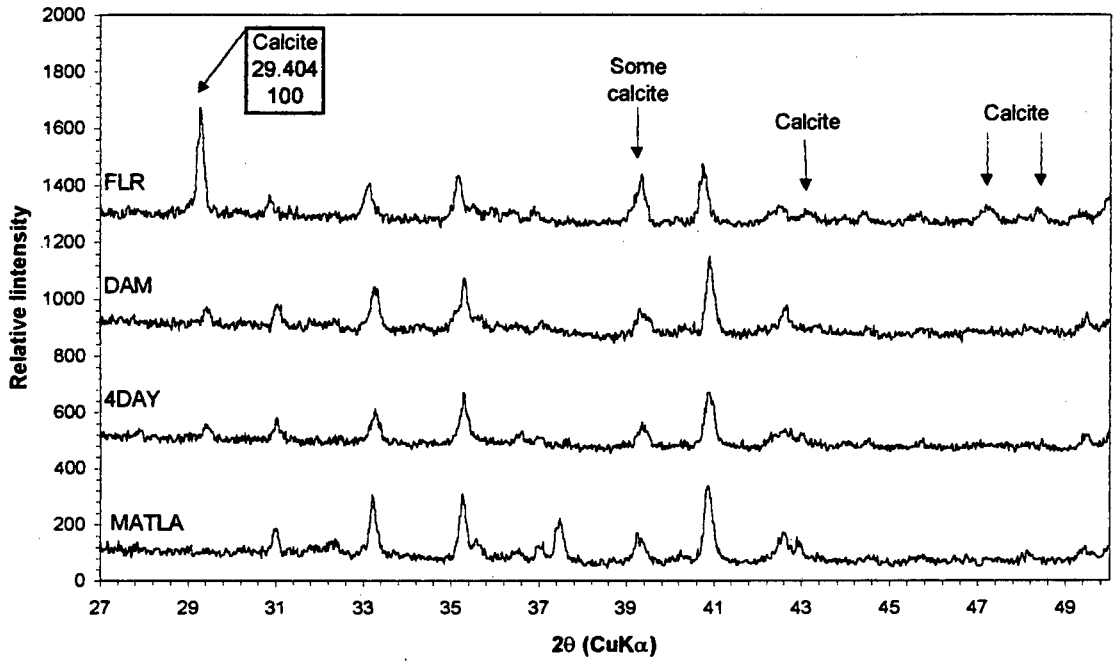

Figure 4.20b

Figure 4.20: The presence of a) ettringite and b) calcite in weathered samples of Matla fly ash. The XRD patterns from bottom to top are a progression in weathering of the samples.

Ettringite is only detected in the sample MatlaFlr, which under SEM was found to contain an extensive matrix of interlocking secondary minerals. Calcite is also present in the sample MatlaDam, although the intensity of the peaks is not very strong. It is probable that the secondary mineral observed in Figure 4.18 is ettringite and/or calcite. Sample MatlaDam shows the presence of no ettringitic phase but does show strong intensity peaks for calcite. It would appear that the dominant crystalline phase observed in Figure 4.19 is calcite. The youngest weathered sample shows only small amounts of calcite and no ettringite present. However, the reactions involved in ettringite production may be kinetically slower than that of calcite, especially considering the presence of CO_2 which would quickly react with calcium.

The fact that no gypsum was detected in any of the samples can be explained in part by the results obtained in the leaching experiments (Section 4.3). The saturated paste extracts were undersaturated (after 360 min) with respect to gypsum and any gypsum that had precipitated prior to the point at which saturation occurred may be below detection limits. In addition, the fresh unweathered fly ash may be a slightly different composition to the weathered samples. Alternatively, the environmental conditions present in-situ may have been significantly different as to alter the SI of gypsum compared to the 'ideal' conditions encountered within the lab.

4.4.2.3 Semi-quantitative SEM EDXRF analysis

One of the problems associated when analysing crystals similar to those observed in Figure 4.19b is to assess whether they are indeed secondary minerals responsible for the hardening observed in the ash dam or whether they are a manifestation of the drying process. There is little doubt that the extensive inter-sphere network of crystals observed in Figure 4.18a is not a result of mineral precipitation brought about by drying the sample during storage and sample preparation and analysis. The crystalline phases observed in Figure 4.19 may be an artefact of sample preparation. If this is the case, however, the presence of the secondary minerals alone suggests that the sample possesses potential hardening characteristics through secondary mineral growth.

Many of the difficulties associated with SEM EDXRF analysis have been outlined in section 4.3.1.4.1. One of the biggest problems associated with analysing sample MatlaDam is the abundance and size of the secondary minerals observed on the surface, which are possibly associated with the hardening of the sample. The nature of the sample for MatlaDam can only provide a visual account of the secondary minerals since the SEM EDXRF data obtained from preliminary analyses is semi-quantitative at best. SEM EDXRF data for sample MatlaFlr on the other hand has wielded a wealth of information worth discussing.

Two series of data from MatlaFlr have been derived from the images in Figures 4.21 and 4.22. Figure 4.21 shows an abundance of secondary minerals that provide a good opportunity for a substantial contribution of signal from the crystals and little from the underlying and surrounding matrix. Figure 4.22a reveals several features of interest. The first is the continuous coating that can be seen around the spheres in the upper left side of the image with varying degrees of roughness and scarring from what is most likely to have been the removal of crystal growths. The second feature can best be seen in Figure 4.22b, which is the presence of a cobweb-type crystal structure composed of long, thick secondary minerals radially emanating from the same focal point.

The EDXRF data obtained for the spot analyses are presented in Table 4.8. The first series from MatFlr_1 to 3 contains a spot from the large patch of secondary minerals in the upper right hand corner of Figure 4.21 as well as two spot analyses from fly ash spheres that are present without the presence or abundance of crystals. The two spot analyses of fly ash spheres in Figure 4.21 are very similar to the chemical signature obtained for MatlaDam fly ash. Sample MatFlr_2 has a much higher Mg content than does the bulk chemical analysis coupled with a low Fe content. The decreased Fe content was expected because of the nature of Fe in fly ash associating itself frequently as a single grained phase. The Ca content is a little higher in the sample Matflr_2 while the Al and Si are much the same as in the bulk reference sample MatlaDam. The general chemical signature of the spot analysis MatFlr_2 is characteristic of the glass content of fly ash and is not indicative of a secondary mineral phase. The same

can be said of MatFlr_1 as the decrease in Ca is due in part to an increase in Al. The data are still characteristic, however, of the glass of a fly ash sphere.

The data obtained for MatFlr_3 are much different from those of the preceding spot samples, but are similar to some of the data obtained for secondary minerals analysed in sample KrielStp. The matrix of secondary minerals in sample Matflr_3 is richer in Ca, Mg, S and Al, and much depleted with respect to Si, which may have originated being detected from the underlying matrix. The fly ash sample MatlaFlr is the only weathered Matla sample that was identified as having ettringite within the sample. Thus, based on the EDXRF data, coupled with the increase in Ca, Al and S content, but no gypsum pattern observed by XRD, it is probable some of the secondary mineral matrix analysed in sample MatFlr_3 is attributed to ettringite.

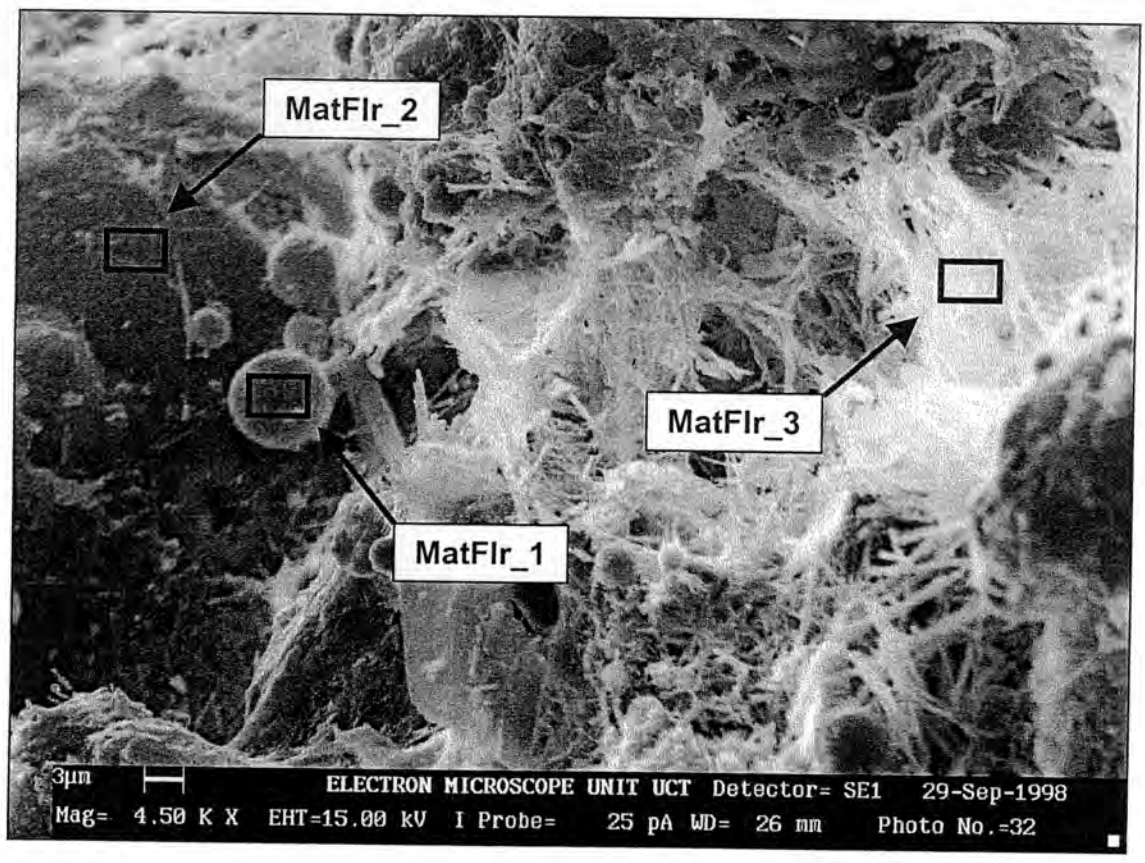

Figure 4. 21: SEM image of weathered Matla fly ash showing the locations of the spot analyses taken for secondary mineral identification.

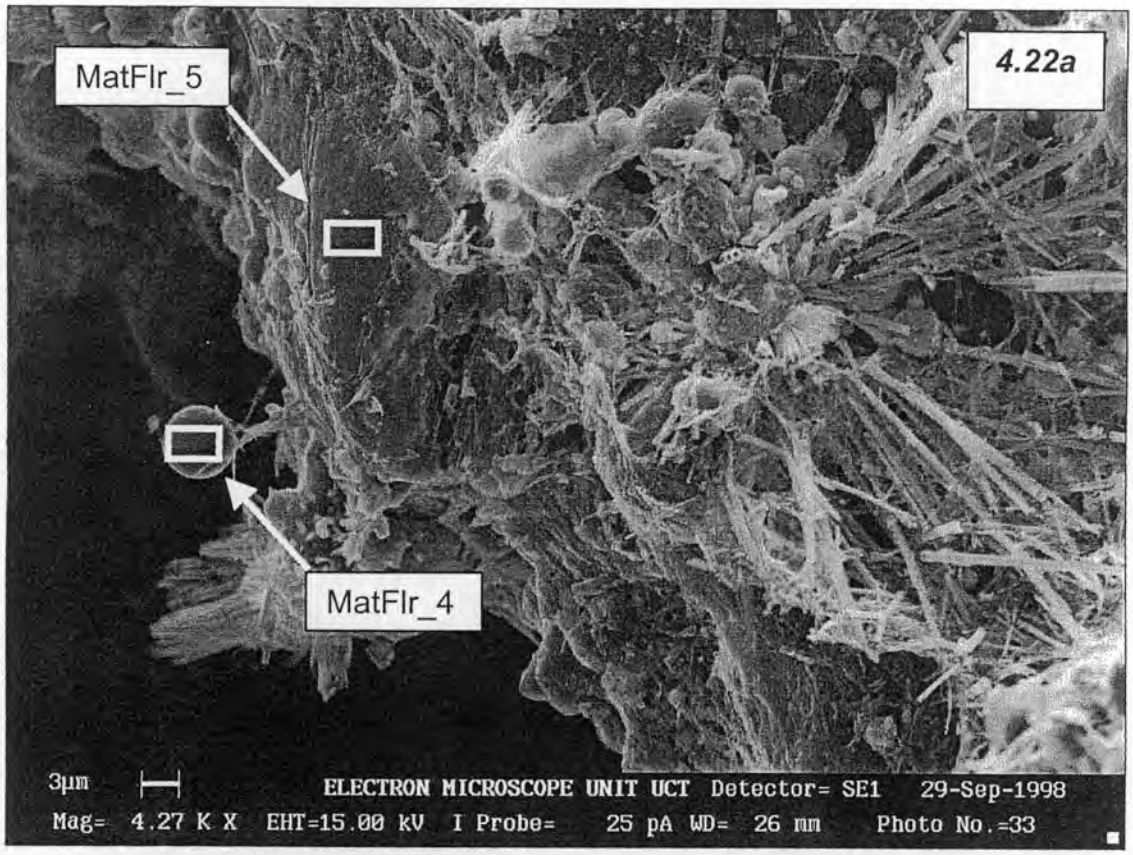

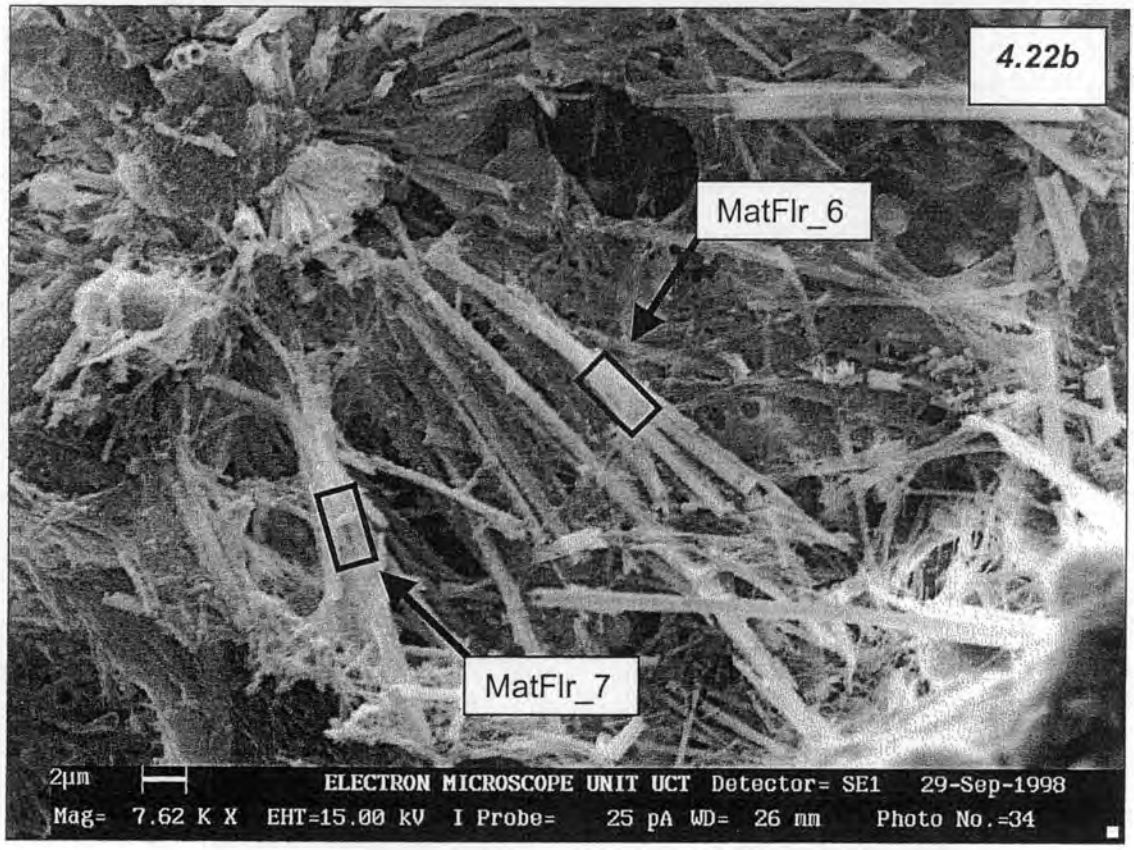

Figure 4.22: a) low magnification and b) high magnification of MatlaFlr fly ash showing the location of spot analyses used for secondary mineral identification.

Table 4.8: SEM EDXRF data (weight %) for spot analyses of Matla fly ash of the images present in Figure 4.21 and Figure 4.22.

Element	Matla (ash)	MatlaDam (ash)	MatFlr_1 (sphere)	MatFlr_2 (sphere)	MatFlr_3 (crystal)	MatFlr_4 (sphere)	MatFlr_5 (matrix)	MatFlr_6 (crystal)	Matflr_7 (crystal)
O	47.39	45.23	46.21	45.43	48.50	53.72	54.23	42.39	49.04
Na	0.3	0.3	0.85	1.26	1.45	0.32	0.51	1.01	0.77
Mg	1.36	1.33	1.51	4.36	3.79	0.47	0.62	2.05	1.59
Al	16.18	14.70	19.68	13.68	10.86	2.71	6.37	13.85	11.59
Si	23.43	22.97	25.98	22.63	8.35	37.56	2.36	11.08	8.59
P	0.427	0.389	NA	NA	NA	0.16	0.13	0.33	0.09
S	0.223	0.224	0.68	0.80	5.50	0.49	8.93	6.80	5.88
Cl	NA*	NA	0.23	0.71	1.65	0.33	0.44	1.12	1.13
K	0.783	0.947	1.17	0.57	0.65	0.68	0.20	0.49	0.46
Ca	6.15	5.44	2.52	8.56	17.28	2.21	25.32	19.36	18.89
Ti	0.95	0.83	0.26	1.11	0.51	0.28	0.17	0.61	0.95
Fe	2.76	3.09	0.92	0.90	1.46	1.08	0.71	0.90	1.03

* NA = element not analysed

The second series of EDXRF data, MatFlr_4 to 7, were derived from Figure 4.22a and b and their corresponding data are presented in Table 4.8. The small spherical particle analysed under spot MatFlr_4 is of a composition not yet found for any of the spot samples. The major elements within the phase are Si and O with very small contributions from calcium and aluminium. The composition strongly suggests that it is a quartz grain. Willis (1987), however, indicates that quartz grains will not be melted in the furnace and as a result should not be spherical. Above 1630°C silica volatilises, however the temperature within the furnace, typically 1500°C, is not generally sufficient to vaporise the quartz grain. It is probable, however, that small impurities such as Ca and Al in the parent material will lower the melting temperature of quartz to one that will undergo melting within the furnace, thus producing a spherical Si-oxide particle.

Samples MatFlr_5, 6 and 7 are more indicative of secondary minerals that have been analysed in previous samples. The characteristically high calcium, sulphur and aluminium concentration coupled with decreases in Si and Fe point toward a secondary mineral composition. The abundance of Si and Al has changed dramatically compared to the bulk chemical analysis and with respect to each of the samples in the series. The Si content in sample MatFlr_5 is very low and is close to three times less concentrated than the Si content. The sample has a very high calcium level and may suggest a calcite phase, however, the elevated Al as well as the sulphur levels does not correspond to the suggested calcite phase. It is possible that the phase is calcareous and that the signal from other elements is from the underlying matrix, which can only be quantified with further study. Samples MatFlr_6 and 7 have chemical characteristics very similar to previous samples in which the elevated S, Ca and Al concentrations were attributed to ettringite.

4.4.3 Sasol fly ash

The fly ash dump at Sasol displays limited hardening. The chemical composition of unweathered fly ash, discussed in section 4.2, revealed that Sasol fly ash differed from the other ashes in terms of the high L.O.I. as well as slightly lower calcium concentrations than the Kriel and Matla ashes. To assess whether these factors may effect the unhardened state that the Sasol ash adopts, the chemical composition and the morphology of the weathered fly ash particles need to be considered. The order of

fly ash weathering for Sasol ash increases from the fresh fly ash, Sasol, to SasolTop and then SasolBot.

4.4.3.1 Morphology

The morphology of Sasol fly ash was investigated in the sample displaying the highest degree of weathering, SasolBot. The SEM images taken during the investigation are presented in Figure 4.23. The most conspicuous feature of the ash is the lack of any secondary minerals present on the spheres or within the pore spaces between the fly ash particles. The fly ash spheres have a smooth appearance and do not exhibit evidence of having undergone dissolution of the surface to produce exfoliating layers similar to those observed for the Kriel fly ash samples (Figure 4.17a). The magnification of Figure 4.23b is 8000 times, which is higher than that of many of the images taken for Kriel and Matla where secondary minerals were observed.

The polished thin section for sample SasolBot is displayed in Figure 4.24. The image shows the abundance of what appear to be unburned coal particles, identifiable from the nature of the porosity of the particle. It is probable that the particles are unburned coal, as it was found in previous sections on the analysis of unweathered Sasol fly ash that the sample contained a large amount of unburned coal. In addition to the porous unburned coal particles, the presence of a large amount of angular particles is also evident. The large angular particles have similar brightness and contrast to the fly ash spheres, suggesting that they are of similar composition (Si, Al, Ca) and could be minerals that have survived the combustion process, possibly due to the lower combustion temperature as indicated by the presence of unburned coal. The large blocky particles seem to occur as single phases rather than in-filling between the fly ash particles, suggesting that they may not be secondary minerals but rather primary.

Although there is no evidence of secondary minerals within the fly ash sample, there is no doubt some bonding occurring between the particles that is responsible for the slight hardening that the fly ash exhibits. Physical adsorption or retention via van der Waals forces, although they are weak they are additive, may be sufficient to bind the particles into a mass that exhibits some order of strength.

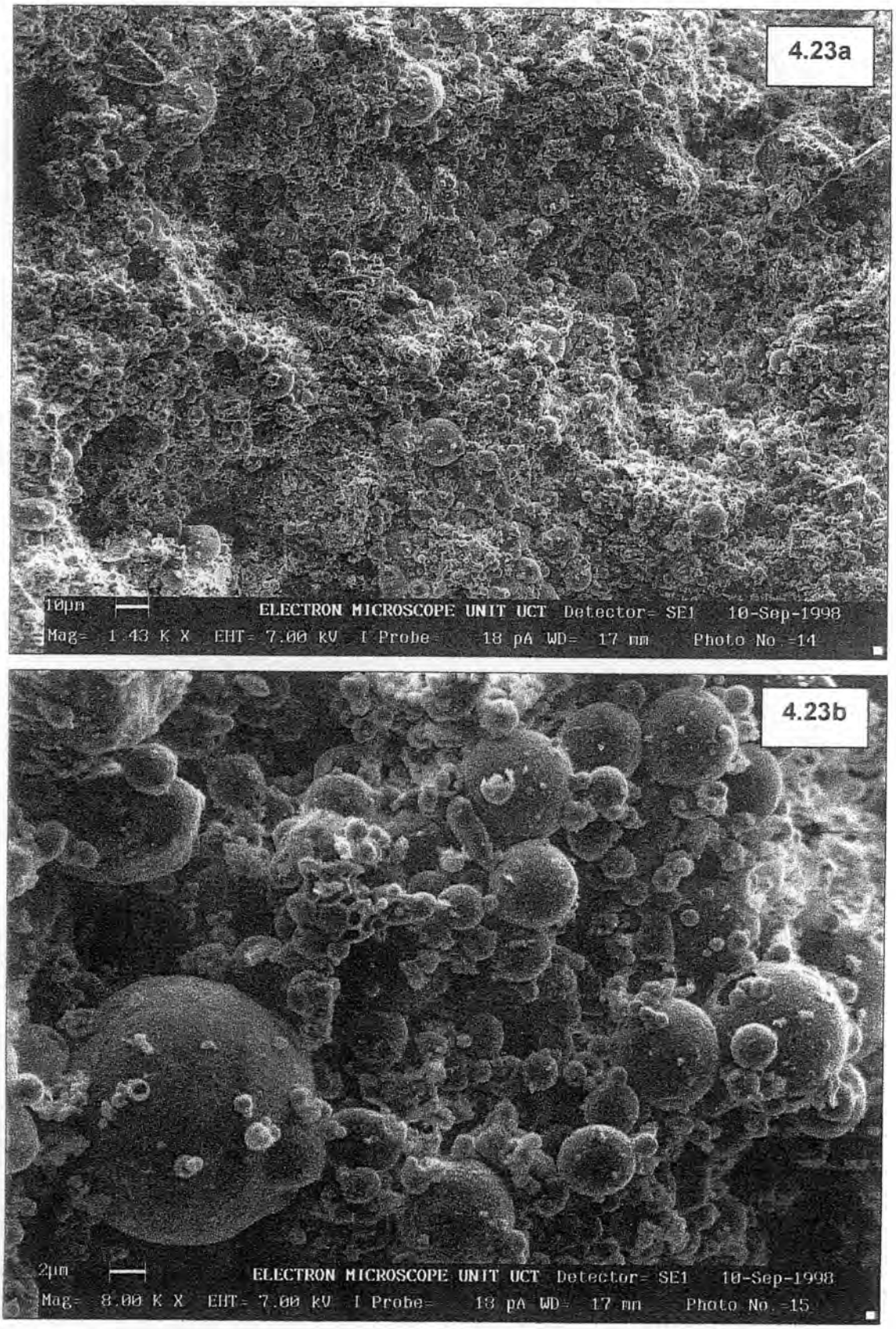

Figure 4.23: a) low magnification and b) high magnification image of weathered fly ash displaying the loose nature of the ash and the lack of any secondary minerals.

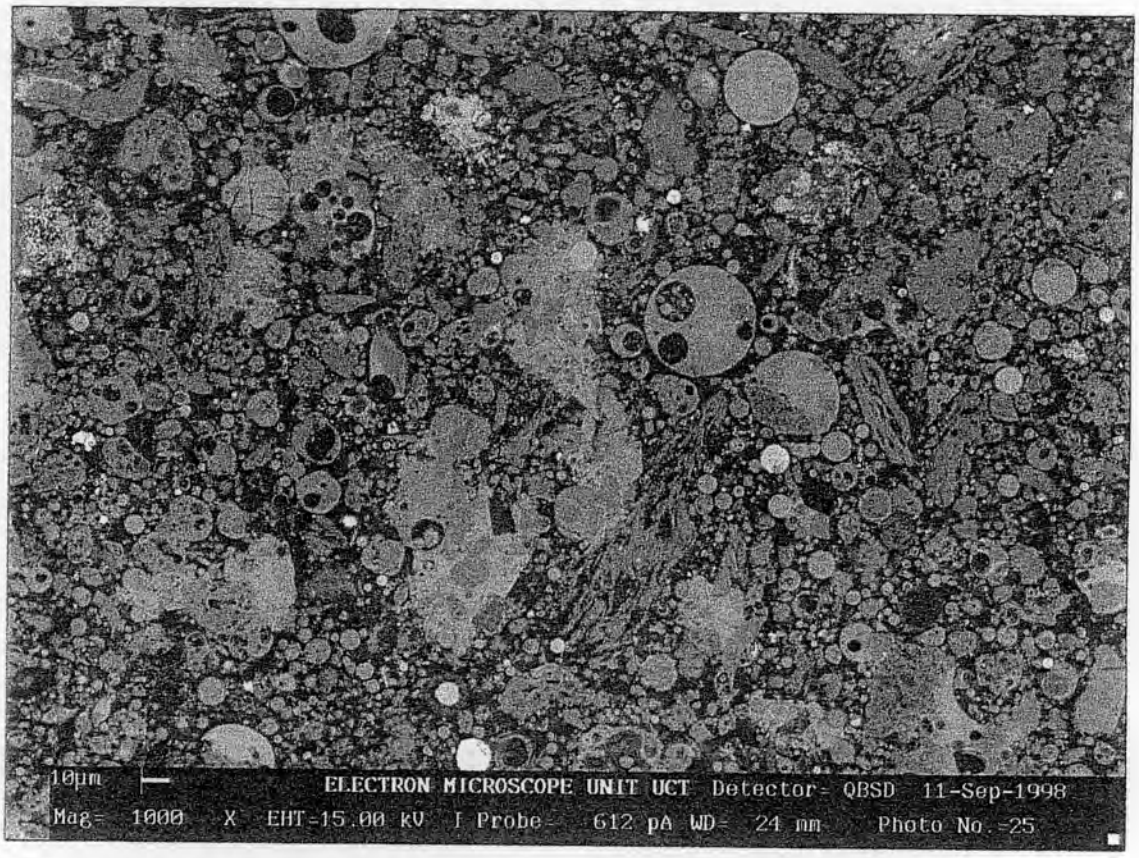

Figure 4.24: Polished thin section of SasolBot fly ash displaying the abundance of angular particles and large porous particles dispersed amongst fly ash spheres.

It is most likely that the major binding force between the Sasol fly ash particles results from suction processes. The fly ash is disposed of in the wet state and upon drying within the ash dam the macropores will empty of water and bring the spheres into close contact with one another. As the particles get closer together, as a result of capillary suction through dehydration, van der Waals attractive forces increase proportionally to the seventh power of the distance between the particles (van Olphen, 1977).

4.4.3.2 Bulk chemistry and mineralogy

To ascertain whether there are any secondary minerals contained within the weathered Sasol fly ash sample, the chemistry and mineralogy of the ash must be considered. The XRFS analysis for the Sasol fly ash series are presented in Table 4.4 and at first glance may appear somewhat similar. There are subtle differences between the samples that merit discussion.

The most striking features of the XRFS data include the increase in calcium and Mg content and L.O.I as weathering proceeds. Aluminium has decreased through the weathering range while the Si content has remained constant. The Fe content is variable throughout the samples.

The high L.O.I. of the samples may be related to unburned coal as was determined for the unweathered fly ash sample, although there is a slight increase in L.O.I. of the sample as the degree of weathering increases. There is also an increase in Ca and Mg content of the ash, which may suggest the presence of a calcareous fraction contained in the weathered sample. Figure 4.25 displays the XRD patterns of the series of Sasol fly ash samples. The only secondary mineral detected using this method is calcite. It would appear that the increase in L.O.I. is associated with CO_2 from carbonates, which is associated with calcite as determined by XRD. The higher concentration of fly ash in the samples SasolBot and SasolTop is not likely to be attributable to the changing composition of fly ash, as it was determined previously that the fly ash composition has remained effectively constant over at least the age of the ash samples taken. The increase in Ca at the surface of the ash dam cannot be through concentrative downward leaching since it is a surface sample. It is possible that the water used for dust suppression and vegetation of the ash dam is high in calcium, and thus calcium could be concentrated at the surface. However, what seems more reasonable is that a form of capillary rise is occurring in the ash dam, which is concentrating calcium in solution at the surface through evaporation which then reacts with CO_2 to form calcite.

The presence of calcite in the weathered ash, as detected by XRD, is surprising given that no secondary mineral phase of any type was observed under SEM. Further study and investigation of Sasol samples is therefore warranted. A preliminary explanation might be that the detection of calcite depends on sample preparation. Samples for SEM are required to be relatively large because cleaving of the sample is required to produce a fresh surface for analysis. If secondary

calcite accumulation is distributed heterogeneously within the ash sample, a cleaved surface may well be devoid of significant calcite as observed under SEM.

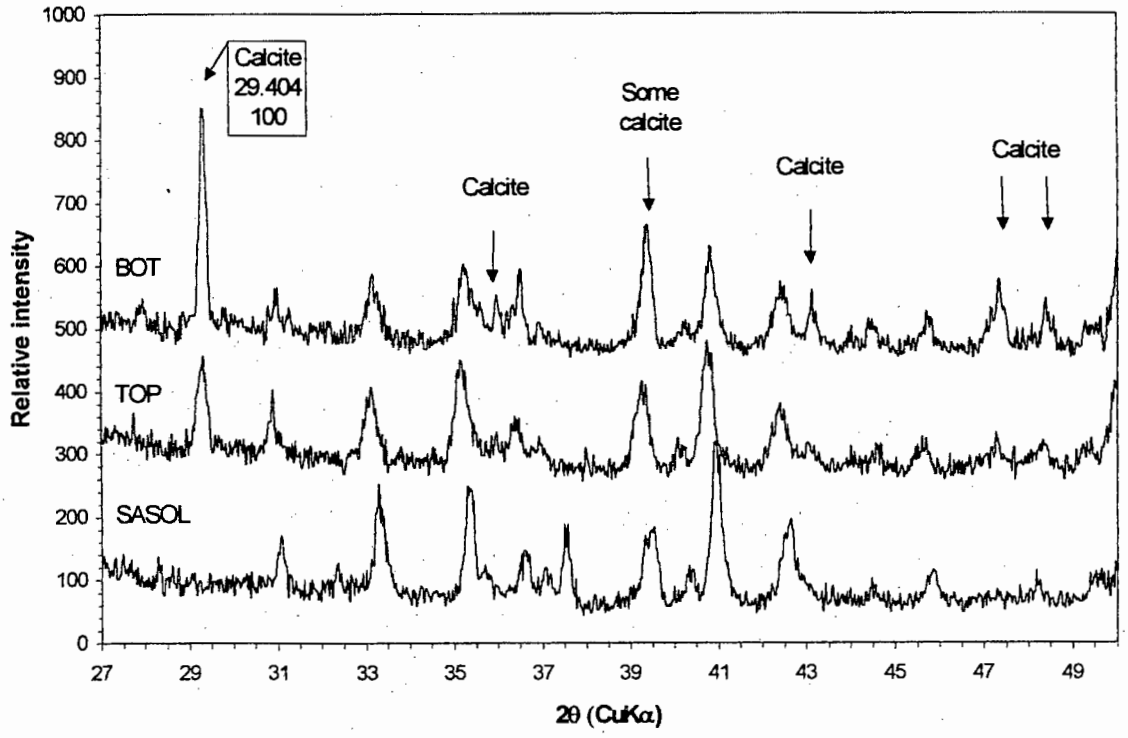

Figure 4.25: The presence of calcite in weathered samples of Sasol fly ash.

4.4.4 General discussion

When comparing the SEM images for all three fly ash series, Sasol, Kriel and Matla, the most striking feature is the lack of secondary mineral growth observed in the Sasol samples. From the secondary minerals observed under SEM and analysis with EDXRF, a common theme of the data arises. All of the crystals analysed, excluding the matrix analysed under spot sample Krstp_6, show increases with respect to the bulk phase and surrounding spheres in S and Ca content, as well as an increased aluminium concentration relative to silicon. These three elements point strongly to Ca-Al-SO_4 containing secondary minerals, yet only calcite and ettringite were detected by XRD. Massazza (1998) indicates that the reaction products resulting from the hydration of pozzolanic cements include ettringite, tetracalcium aluminate hydrate (often carbonated), monosulphoaluminate, $Ca_2Al_2SiO_7.8H_2O$, $CaSiO_3.H_2O$, $Ca(OH)_2$ and $CaCO_3$.

Although the system being dealt with is not a cement in the common meaning of the term, the fact that ettringite was formed in the hardened fly ash suggests that other reaction products are possible and failure to detect these by XRD may simply be attributed to their very low concentration.

Crammond (1985) synthesised pure ettringite from a solution of $Al_2(SO_4)_3$ and $Ca(OH)_2$, both of which reactants are likely to occur in the fly ash paste. In a mortar or paste in which sulphate ions are present, Taylor (1997) indicates that the sulphate minerals which may form include ettringite, thaumasite ($Ca_3Si(OH)_6[CO_3][SO_4].12H_2O$) and gypsum. Thaumasite has a structure similar to that of ettringite, with Si^{4+} replacing Al^{3+} and SO_4^{2-} and CO_3^{2-} groups in the channel sites (Taylor, 1997). Their XRD patterns are often confused since the main diffraction peak occurs at 9.214 2θ (JCPDS card 46-1360) for thaumasite and 9.091 2θ (JCPDS card 41-1451) for ettringite. Taylor (1997) indicates that the ideal conditions for thaumasite formation include high relative humidity, adequate supplies of SO_4^{2-} and CO_3^{2-} ions, the presence of Al and a temperature of 5 to 10°C, while Crammond (1985) found that it does not form above 25°C. These conditions would have been met in the weathering ash, and suggest that thaumasite could be present in addition to ettringite. Interestingly, for thaumasite precipitation to occur, prior formation of ettringite is needed for nucleation (Taylor, 1997). However, the XRD spacing (9.100-9.125 °2θ) is more characteristic of ettringite and in addition, the increase in Al with respect to Si in the weathered ash relative to the unweathered ash would suggest an aluminous rather than a siliceous secondary mineral.

Ettringite is not the only secondary mineral detected by XRD in weathered fly ashes. Calcite formation at the ash dam-atmosphere boundary may be crucially important in ash dam hardening. In the case of Kriel and Sasol, movement of ash dam pore water towards the surface could possibly account for the elevated concentration of calcium at the surface of the dam. The pore water, acting under capillary suction, transports calcium-rich solution to the surface of the ash dam allowing for reaction with CO_2 and formation of calcite. The formation of a layer of calcite at the surface of the ash dam may be of critical importance with respect to

ash dam hardening in providing a capping on the surface. The hard crust would limit moisture loss and allow the hydration reactions involved with phases such as ettringite to proceed unhindered.

Distinguishing between secondary minerals in the fly ash that have formed in situ and secondary minerals as a result of evaporation due to sample drying is difficult. To investigate this aspect further, the 24-hour saturated paste extract from Matla was evaporated on the surface of a glass slide. The glass slide was analysed by XRD and the resultant diffractogram is presented in Figure 4.26. Matla has gypsum present with very small contributions from calcite. The high background values can be attributed to the glass phase present in the glass slide. Gypsum is the only sulphate containing mineral present, which suggests that any ettringite formed has done so by reactions other than direct evaporation of the pore water, since no ettringite was found upon evaporation of the saturated paste extract.

In all the ashes there is a rise in the L.O.I. of the weathered sample relative to that of the unweathered fly ash sample. The L.O.I. has been attributed to the calcareous phase in the weathered fly ash, but may also be indicative of hydrated phases within the crystal matrix. Identification of these crystal matrices through using SEM EDXRF, while fruitful in the sense of gaining an appreciation of the extent of the secondary minerals occurring and predicting trends, is not a viable method for quantifying the composition of secondary minerals. Further investigation into the types of secondary minerals by the use of other methods, such as TGA and DTA, is required.

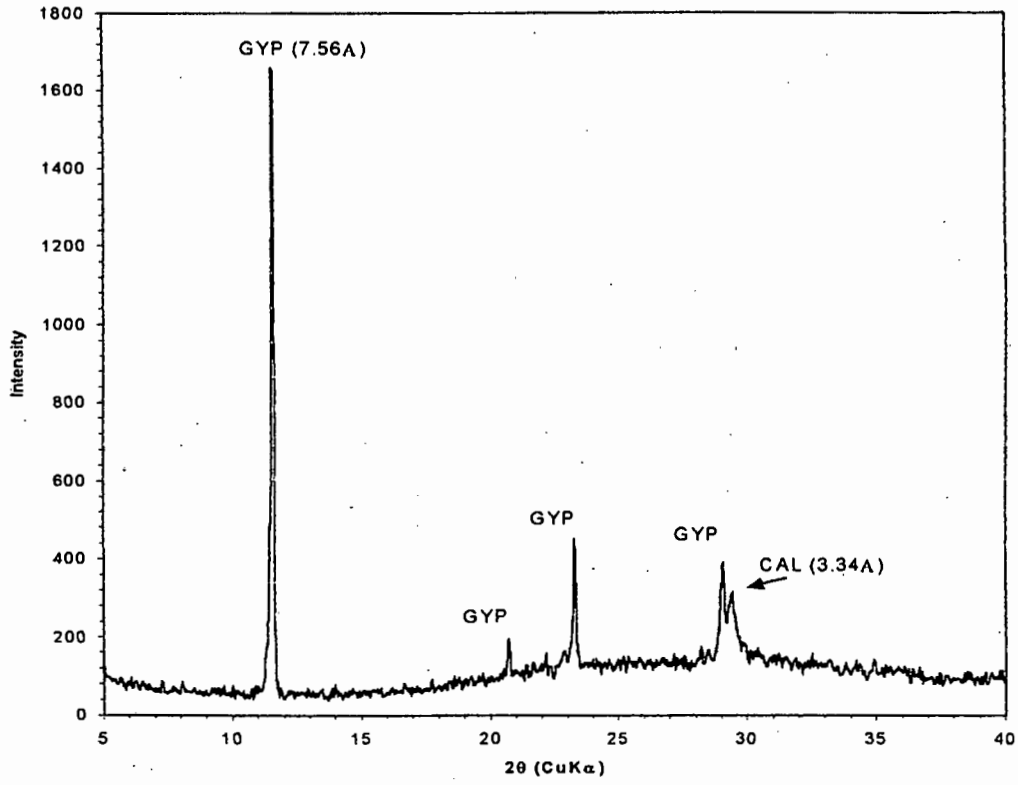

Figure 4.26: Diffractogram of the glass slide prepared by evaporation of the saturated paste extract of Matla fly ash (CAL = calcite, GYP = gypsum).

4.5 Treated fly ash

Both calcite and ettringite have been positively identified by XRD and both are calcium containing secondary minerals. Calcium has been identified by Aitcin *et al.* (1986) to be important when considering the reactivity of fly ash. The glass content is suggested by Hubbard *et al.* (1985) to be the most reactive phase, which differs in composition and structure in high-calcium compared to low-calcium fly ashes (Diamond, 1983). Based on the presence of Ca-containing secondary minerals detected and suggestions in the literature concerning the importance of calcium in fly ash, a plot of the modulus of rupture against the bulk chemical Ca content was performed (Figure 4.1). It was found from this plot that the Kriel fly ash falls off a very strong linear correlation line for the other three fly ash samples.

Massazza (1998) showed for 8 pozzolans that the compressive strength increases as the amount of combined lime increases, however, there was no general relationship between the two parameters, only within each pozzolana. Based on the findings by Massazza, the addition of $Ca(OH)_2$ to Sasol fly ash to enhance the strength of the ash was performed. Data for the modulus of rupture required to break replicate fly ash briquettes made from the addition of $Ca(OH)_2$ to unweathered ash cured for 24-hours is presented in Table 4.9. The Data is plotted in Figure 4.27 as the equivalent addition of CaO to Sasol fly ash.

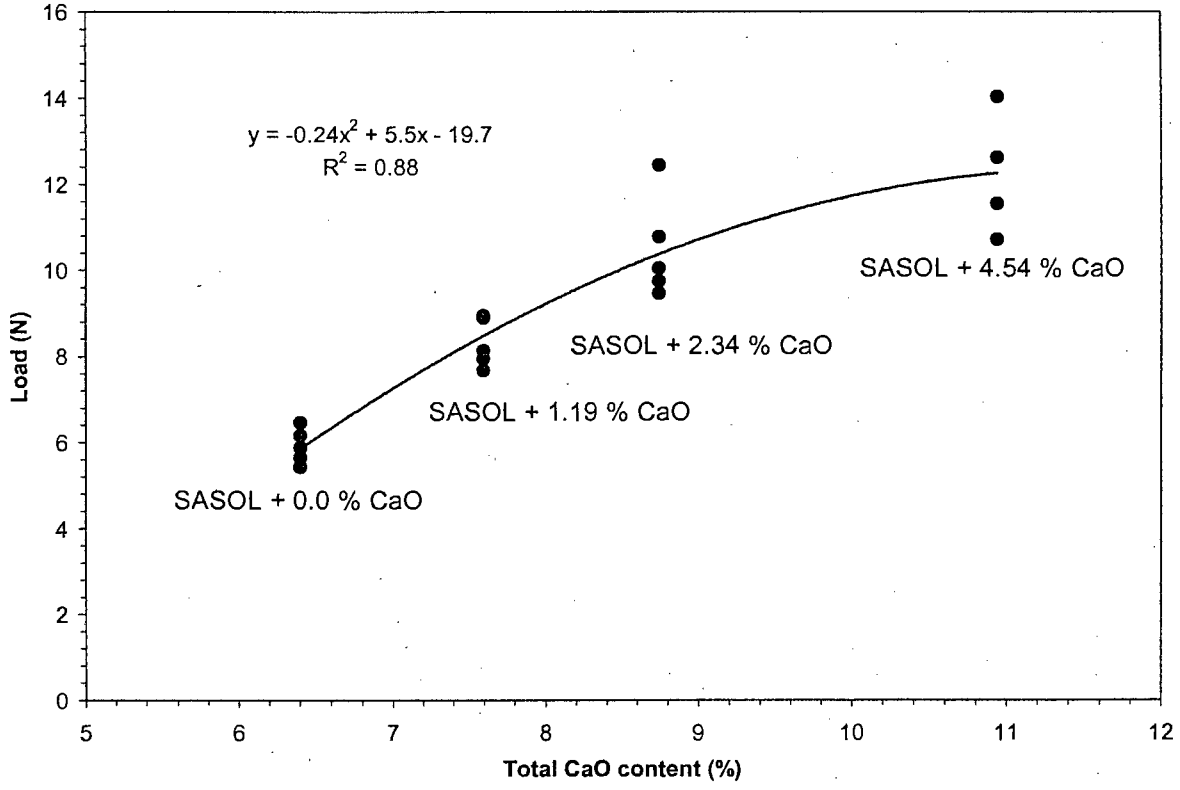

Figure 4. 27: Modulus of rupture (s) of fly ash briquettes made from the addition of $Ca(OH)_2$ to unweathered Sasol fly ash plotted against CaO content.

Massazza (1977: cited in Massazza, 1998) has indicated that there is little consistency in the behaviour of pozzolans, which most probably is the result of differing chemical and physical properties. The ashes in this study, however, are very similar with respect to both bulk chemical analysis and their physical properties. Taking this into account, the modulus of rupture of replicate samples

to which varying amounts of $Ca(OH)_2$ had been added to Sasol fly ash and the modulus of rupture of the other three ashes have been plotted together against CaO content in Figure 4.28. It is noteworthy that the enrichment of the CaO content of Sasol fly ash results in a modulus of rupture which adheres to the original relationship defining Sasol, Matla and Lethabo (but not Kriel) ashes.

Table 4.9: Modulus of rupture data for Sasol fly ash briquettes at varying CaO content (%) cured for one day (the levels of CaO above 6.40 were achieved by admixture of $Ca(OH)_2$).

CaO	Modulus of Rupture (N/cm^2)					
(%)	N	Mean	S.D.	Min	Max	Median
6.40	*5*	*5.87*	*0.34*	*5.43*	*6.23*	*5.88*
7.59	*5*	*8.31*	*0.57*	*7.67*	*8.95*	*8.14*
8.74	*5*	*10.49*	*1.19*	*9.46*	*12.44*	*10.05*
10.94	*4*	*12.23*	*1.43*	*10.71*	*14.03*	*12.09*

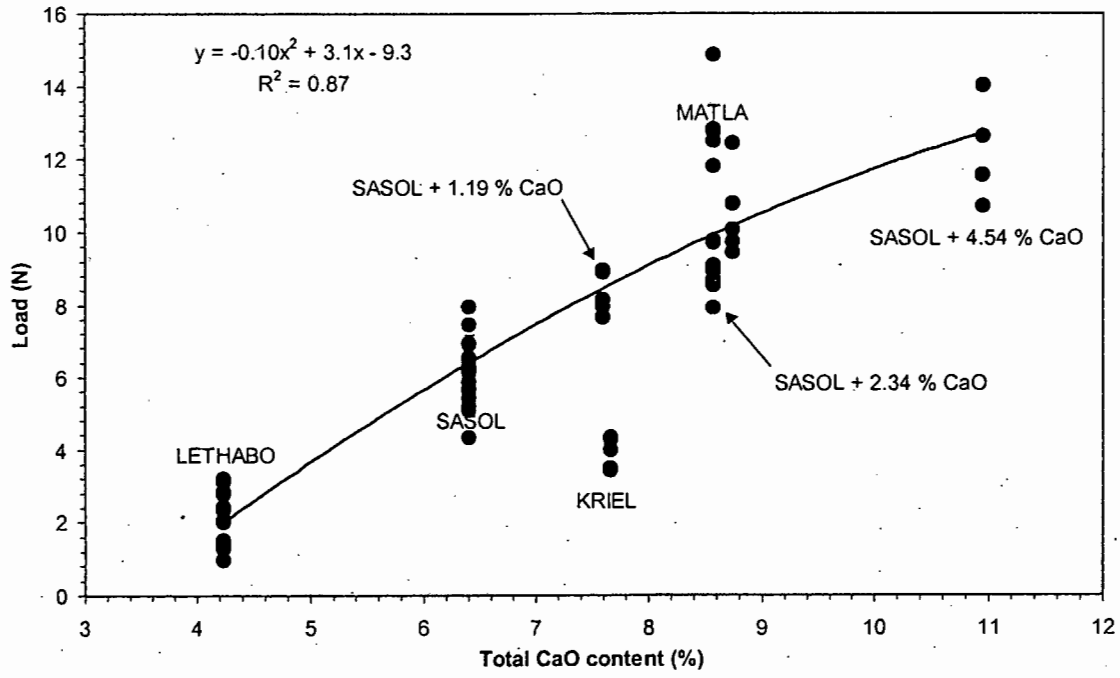

Figure 4.18: Modulus of rupture (s) of fly sash briquettes made from the addition of $Ca(OH)_2$ to unweathered Sasol fly ash plotted against CaO content.

A possible interpretation of the result is that the hardening behaviour of Lethabo, Sasol, and Matla ashes can largely be ascribed to their free lime content. Whereas in Kriel a portion of the CaO content is present as a less labile (possible glass) form resulting in a lower modulus of rupture than that predicted by the relationship for the other ashes, including the free lime-enriched Sasol ash.

4.5.1 Mineralogy of treated ash

The XRD patterns for the $Ca(OH)_2$-treated Sasol samples are presented in Figure 4.29. The only secondary mineral phase detected in the ash briquettes was calcite, which is present in all samples but only in trace amounts in the untreated Sasol fly ash and Sasol+1.19% samples. In addition to the calcite peaks, there are contributions from portlandite, which indicates that complete dissolution of the added $Ca(OH)_2$ had not occurred.

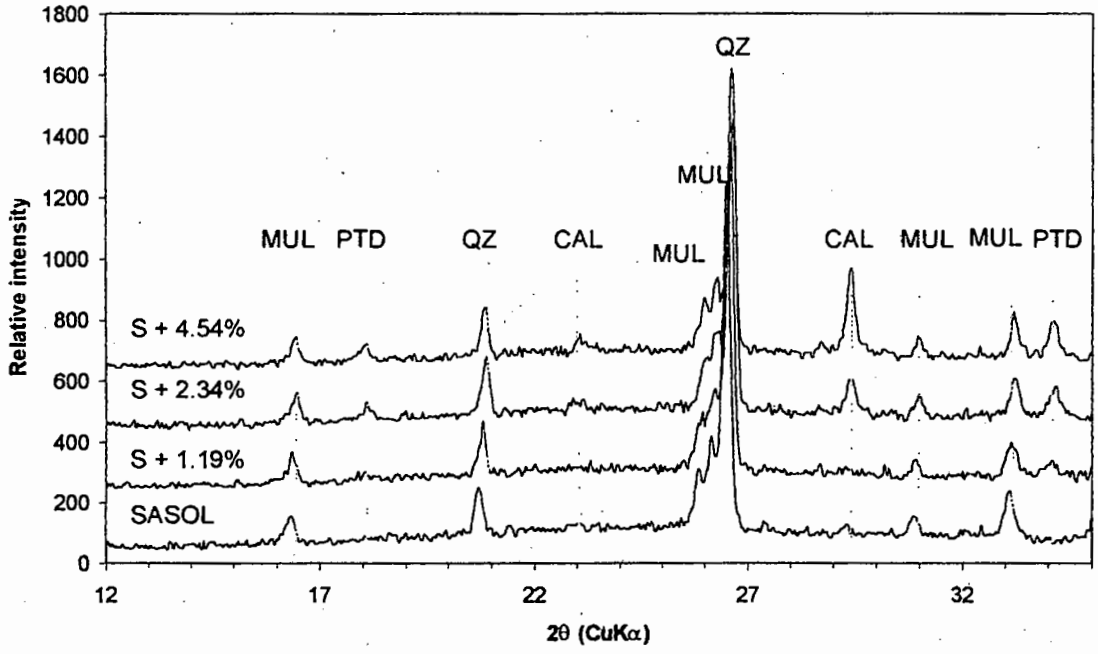

Figure 4.29: Mineral composition of $Ca(OH)_2$ treated Sasol fly ash (MUL = mullite, QZ = quartz, CAL = calcite, PTD = portlandite).

Diffractograms shown earlier (Figures 4.15, 4.20 and 4.25) of the Kriel, Matla and Lethabo fly ash briquette samples revealed only the presence of calcite and no ettringite. Both Matla and Kriel ashes displayed ettringite peaks, however, only in weathered samples from the ash dams. The lack of any secondary minerals,

apart from calcite, suggests that the conditions during curing of the 24-hour briquettes were not conducive to ettringite formation. The temperature, drying rate and size of the briquette may have been contributing factors to the lack of ettringite formation. Joshi and Rosauer (1973) identified ettringite in fly ash mortars after one week of hydration and is quite possible that ettringite will not form over the shorter (1 day) curing time used in the present study.

4.5.2 Morphology of fly ash briquettes

The strength of the fly ash briquettes would seem to be associated with calcite formation, since no ettringite or other secondary minerals were detected by XRD. It is quite possible that calcite is the first secondary mineral to form and that subsequent reactions produce other phases. Analysis of the morphology of fly ash briquettes may provide some insight into the type of secondary minerals formed over a short curing period and whether the same type of crystal growth is observed as in the weathered fly ash samples that have been forming in some cases for years. The SEM images for Matla, Kriel are presented in Figure 4.30a and 4.30b, respectively, and the $Ca(OH)_2$-treated Sasol briquettes are presented in Figure 4.31 for Sasol + 1.19g and Sasol + 5.45g.

The morphology of the briquettes from Matla and Kriel show some evidence of secondary mineral growth, although the extent of the minerals is not nearly as great as in the earlier images for the weathered fly ash samples. It would appear from the Kriel and Matla samples (Figure 4.30) that the early formation of secondary minerals in fly ash is sphere specific, as in both images there are fly ash spheres devoid of any growth while others are covered with a secondary mineral coating. This may possibly relate to the calcium content in the fly ash sphere. Matla (4.30a) appears to have a coating around the particles, linking the particles together with what looks like glue between spheres. The coating is less apparent in samples from Kriel. The fly ash particles in the Kriel sample (4.30b) have taken on a globular look to them as opposed to the smooth spheroidal appearance that fresh ash spheres often exhibit.

The lack of extensive crystal matrices observed in the samples from Kriel and Matla suggest that the curing time for the samples was too short to allow for abundant crystal growth. It is quite probable that the rate of evaporation in the sample, due to the small size, did not allow for development of definite crystal structures but rather amorphous coatings on the fly ash spheres. In addition, the size of many of the secondary minerals observed in Figure 4.30, and the abundance observed, would most likely not be detectable by XRD analysis. Calcite is the dominant secondary mineral as detected by XRD, but differing types of crystals in small quantities observed in Figure 4.30 suggest that calcite is not the only secondary mineral present. The addition of $Ca(OH)_2$ to Sasol fly ash briquettes produced an increase in strength but no observable amount of secondary minerals (Figure 4.31). The fly ash spheres again appear to be coated with an amorphous or poorly crystalline phase, which from the XRD analysis is most likely calcite. The lack of any bridging matrix or well established crystal phases suggest that the addition of $Ca(OH)_2$ increases the strength over the short curing time solely as a result of calcite formation. The long-term strength, which is known to differ from the short-term strength (ASTM, 1993), may be attributed to the formation of other secondary minerals other than calcite. This suggests that briquette-hardening experiments of the kind performed in the present study need to be repeated with much longer curing times before any conclusions an be drawn concerning the relationship between hardening and the formation of secondary minerals.

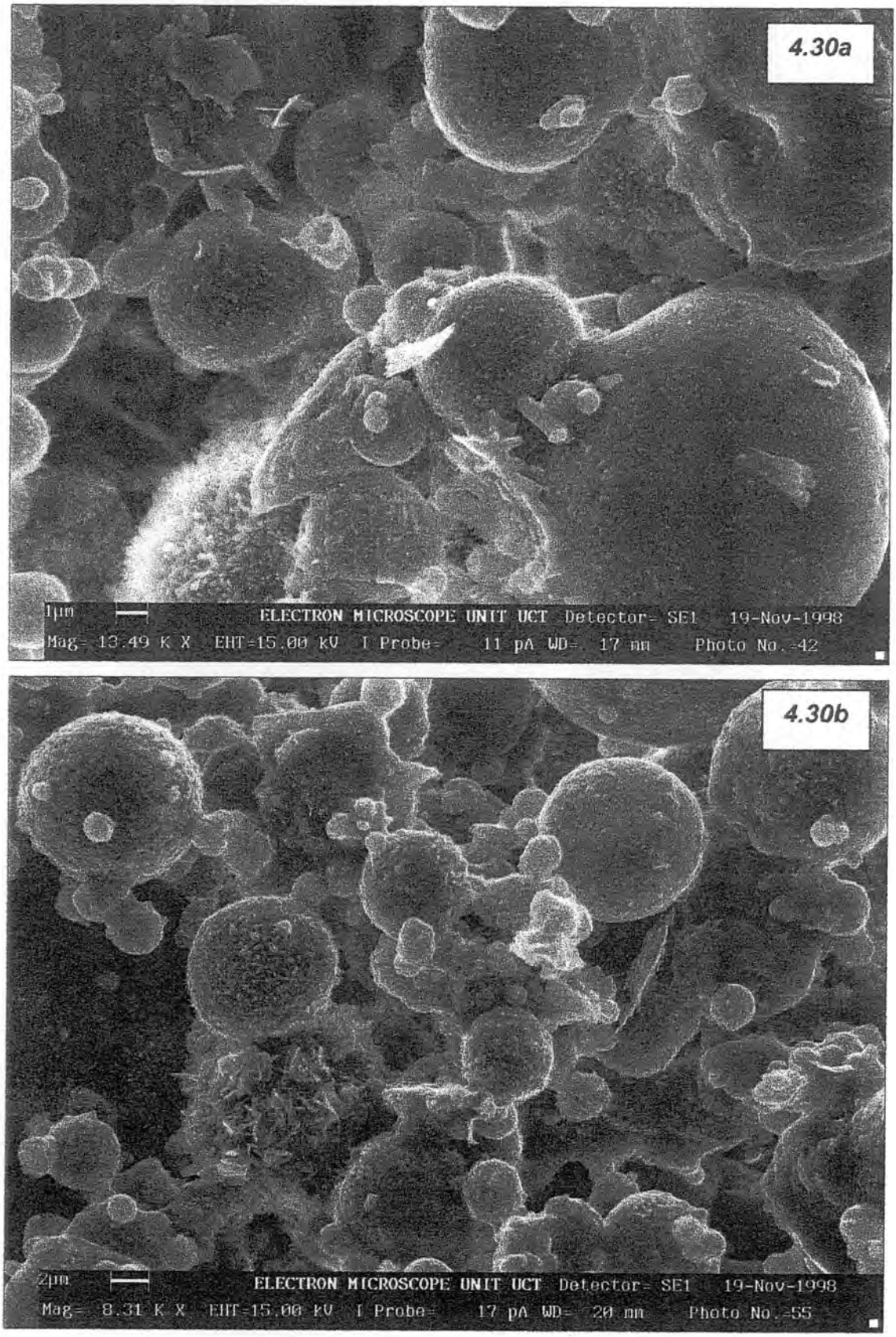

Figure 4.30: Morphology of a) Matla and b) Kriel fly ash briquettes cured for 24 hours

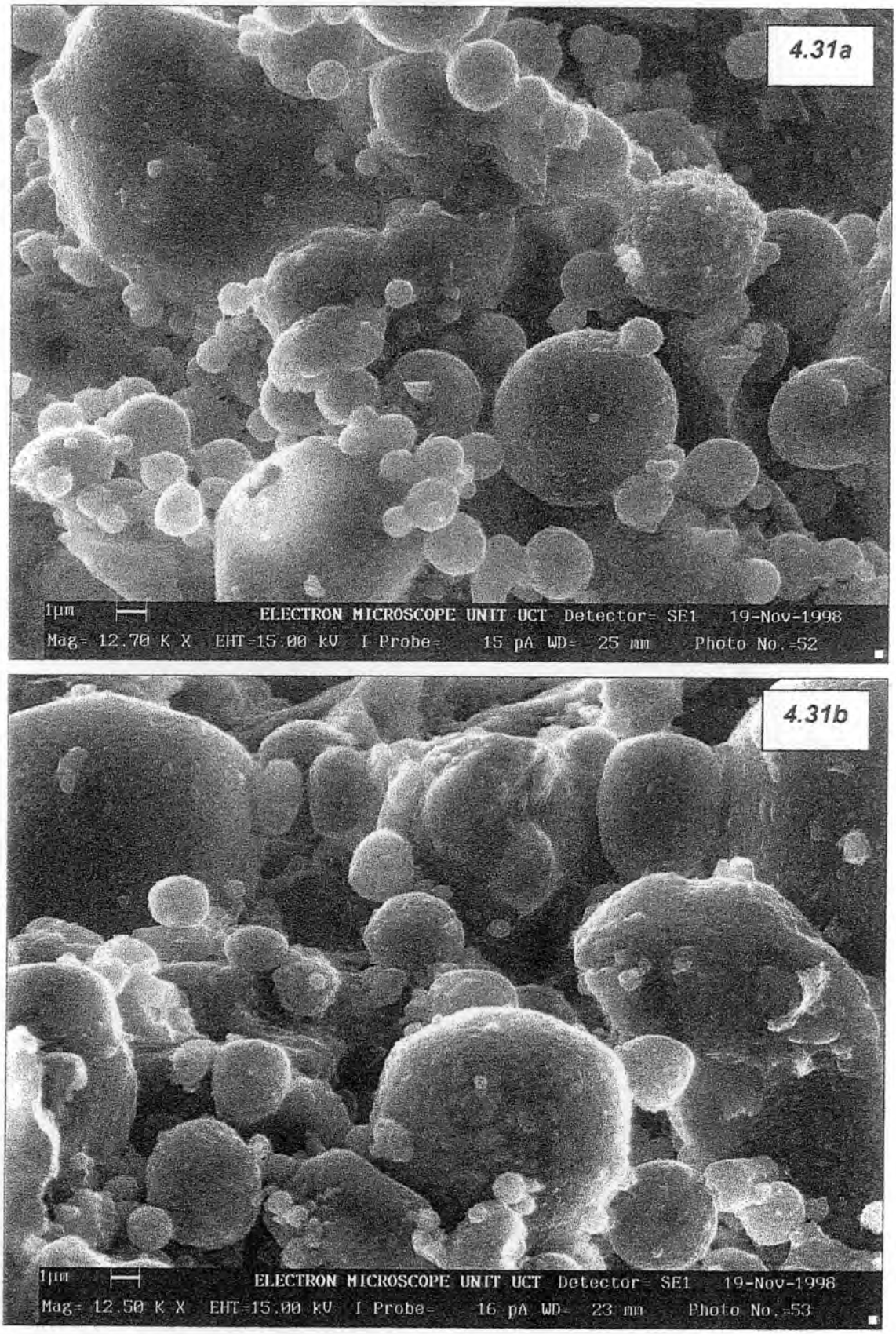

Figure 4.31: Morphology of Sasol fly ash briquettes to which a) 1.19% CaO and b) 4.54% CaO were added as $Ca(OH)_2$ and cured for 24 hours.

Chapter 5: Conclusions

It was the objective of this study to investigate four main aspects of the hardening of fly ash. The extent to which new light has been shed on each of these subjects will now be discussed.

5.1 The extent of hardening exhibited by selected South African fly ashes.

Modulus of rupture experiments conducted on unweathered fly ash briquettes cured for 24 hours indicated that the short-term strength is greatest for Matla fly ash, intermediate for Sasol and Kriel and lowest for Lethabo. For three of these four unweathered ashes, there is a strong linear relationship between total CaO content and modulus of rupture. The Kriel ash deviates from the relationship exhibiting a lower strength than would be predicted based on CaO content. This indicates that other physical factors such as particle size and shape and chemical factors such as the proportion of Ca existing as free lime may also be important.

Field observations do not fully agree with the results of these short-term experimental hardening trials. Although Matla exhibits high strength in the field while Lethabo and Sasol do not, Kriel fly ash on the ash dam develops a degree of hardening superior to all the other ashes. Comparing qualitative field observations with the results from modulus of rupture experiments must be done with caution, however, because of such uncertainties as the co-disposal of other wastes, such as ion exchange regeneration solutions which boost both Na^+ and SO_4^{2-} concentrations, and also the extent to which hardening may have been influenced by evaporative concentration of solutes in the surface layers of the ash dam.

5.2 The secondary minerals formed during hardening

Investigating the solution chemistry of wetted ashes appears to be one of the most promising lines of study for better understanding of hardening reactions. Aqueous extracts from saturated pastes and more dilute suspensions of ash

suggested that secondary precipitates form quickly, within a matter of hours. The precipitates most likely have a complex composition, but the simplest explanation for the decrease in sulphate over a 24-hour equilibration time is the precipitation of gypsum. The ion activity product (IAP) of Ca^{2+} and SO_4^{2-} at each sampling stage was greater than the K_{sp} for gypsum, indicating supersaturation of the extracts with respect to gypsum. The dissolution-reprecipitation process is slower in Matla and Kriel ashes compared with that of Sasol, while in Matla and Kriel the initial sulphate concentrations are also significantly higher.

The morphology of secondary precipitates viewed under SEM reveals their cementing function. The weathered samples from Kriel and Matla show varying degrees of secondary mineral formation and well-developed matrices binding the fly ash spheres together. Sasol was found to contain no visible evidence of secondary mineral formation in weathered samples.

The EDXRFS data for secondary crystals in weathered Matla and Kriel ashes, while semi-quantitative at best, indicate a greater concentration of S, Ca and Al compared to the surrounding or underlying phase. Two secondary minerals, calcite and ettringite, were positively identified by XRD. Calcite appears to form rapidly as a secondary product. Ettringite was detected only in samples from Kriel and Matla, whereas calcite was detected in all samples. The presence of thaumasite has been speculated to occur alongside ettringite, but the XRD pattern did not permit positive identification. No gypsum was detected in any of the samples.

The increased concentration of Ca in some weathered samples compared to unweathered hopper ash may be due to capillary movement of solutions coupled with evaporation at the surface. Accumulation of calcite could possible result in a surface crust by processes analogous to those involved in pedogenic calcrete formation. The presence of this calcite layer may be important to ash dam hardening. The positive identification of only two secondary minerals, calcite and ettringite, in weathered ashes may have been due to the fact that only in such Ca-enriched material is it possible to detect the secondary minerals by XRD.

5.3 Factors which affect the degree cementation

Preparation of fly ash briquettes cured for 24 hours under ambient conditions produced very little secondary mineral growth. The small size of the briquettes may have resulted in excessive evaporation possibly preventing the conditions needed for crystallisation of secondary phases detectable under the electron microscope. Although calcite was detected in the briquettes, the only indication of secondary mineral formation under SEM was the appearance of a very small quantity of amorphous material coating the ash spheres. The effects of longer curing times and different environments (water content, CO_2 concentration and temperature) still remain to be investigated.

5.4 Modification of hardening by $Ca(OH)_2$ addition to fly ash

Initial modulus of rupture results for fly ash briquettes indicated that the CaO content provides a possible means of predicting relative strength. The addition of $Ca(OH)_2$ to Sasol fly ash increased the short-term strength of the briquette. The strength increase with different quantities of $Ca(OH)_2$ added was consistent with that which would have been predicted from the relationship (mentioned earlier) between the modulus of rupture and CaO content of three of the ashes (Kriel excepted). These results confirmed the importance, mentioned in the literature, of the free lime content in determining hardening.

A number of questions remain or have been raised by this study which could form the basis of fruitful additional investigation.

- Longer-term hardening experiments (lasting months rather than a few days) should be conducted with a more rigorous examination of water content, temperature and CO_2 concentration as factors possibly relating to strength development.
- Artificially hardened ashes from these experiments should then be examined for chemical, mineralogical and morphological evidence of secondary mineral precipitation.

- Intermittent extraction and analysis of pore solutions from wetted ashes equilibrated over the same period as that of the hardening experiments would facilitate tracking of the hardening reactions in terms of mineral saturation and precipitation or dissolution reactions. The chemical analysis of these solutions should be expanded to include not only all major ions but also Al and Si.
- Expanding the collection of ash samples to include other power stations would facilitate attempts to relate key variables such as CaO content to strength development.
- Careful field studies of ash dams are needed to find out the importance of capillary flow and surface evaporation of pore water in producing a concentrate from which a calcrete-like crust would be expected to develop. Such a study would essentially be pedological in nature, given the strong parallel which such processes have in soil formation.

References

Adriano, D.C., Page, A.L., Elseewi, A.A., Chang, A.C., and Straughan, I. (1980). Utilisation and disposal of fly ash and other coal residues in terrestrial ecosystems: A review. Journal of Environmental Quality, **9,** 333-344.

Aitcin, P.C., Autefage, F. Carles-Gibergues, F., and Vaquier, A. (1986). Comparative study of the cementitious properties of different fly ashes. In: Malhotra, V. ed. Proceedings of the 2nd International Conference on Fly Ash, Silica Fume, Slag, and Natural Pozzolans in Concrete, Madrid, 1986. American Concrete Institute Special Publication 91, 1, 91-114.

Allison, J.D., Brown, D.S. and Novo-Gradac, K.J. (1991). A geochemical assessment model for environmental systems: Version 3.0 user's manual. Washington, DC: US EPA.

Alonso, J.L. and Wesche, K. (1991). Characterisation of fly ash. In: Wesche, K. ed. Fly ash in concrete: properties and performance. Chapman and Hall, New York.

American Society for Testing and Materials (1993). ASTM C 618. Standard specification for fly ash and raw or calcined natural pozzolan for use as a mineral admixture in Portland cement concrete. In: Annual Book of ASTM Standards. ASTM, Philadelphia, PA.

American Society for Testing and Materials (1993b). Atterberg limits. In: Annual Book of ASTM Standards (ed.). Soil and Rock Dimension and Geosynthetics. ASTM, Philidelphia, PA.

Bayvel, L.P. (1986). Methods and instruments for ensemble particle sizing by light scattering. South African Journal of Science, **82**, 14-18.

Bezuidenhout, N. (1995). Chemical and mineralogical changes associated with leachate production at Kriel power station ash dam. Unpublished MSc Thesis, University of Cape Town, SA.

Bosch, G.L. (1990). The mineralogy and chemistry of pulverised fuel ash produced by three South African coal-burning power stations. Unpublished MSc Thesis, University of Cape Town, SA.

Cabrera, J.G. and Gray, M.N. (1973). Specific surface, pozzolanic activity and composition of pulverised fuel ash. Fuel, **52**, 213-219.

Cabrera, J.G., Hopkins, and C.J., Woolley, G.R. (1986). Evaluation of the properties of British pulverised fuel ashes and their influence on the strength of concrete. In: Malhotra, V.M. ed. Proceedings of the 2nd International Congress of fly ash silica fume, slag, and natural pozzolans in concrete, Madrid. American Concrete Institute Special Publication 91, **1**, 115-44.

Carlson, C.L. and Adriano, D.C. (1993). Environmental impacts of coal combustion residues. Journal of Environmental Quality, **22**, 227-246.

Carter, D.L., Mortland, M.M., and Kemper, W.D. (1986). Specific surface area. In: Klute, A., (ed.). Methods of soil analysis, Part 1: Physical and mineralogical methods, 2nd ed. American Society of Agronomy. Soil Science Society of America, USA.

Clifton, J.R., Brown, P.W., and Frohnsdorff, G. (1978). Reactivity of fly ashes with cement. In: Cement research progress 1977, Ch. 15, 321-341. American Ceramic Society, Columbus, Ohio.

Centre for Civil Engineering Research and Codes, (1992). Fly ash as addition to concrete. Rotterdam.

Cohen, B. (1997).Cement-based solidification of ferro-alloy solid wastes. Unpublished PhD Thesis, University of Cape Town, SA.

Coles, D.G., Ragiani, R.C., Ondov, J.M., Fisher, G.L., Silberman, D. and Prentice, B.A. (1979). Chemical studies of stack fly ash from a coal-fired power plant. Environmental Science and Technology, **13**, 455-459.

Crammond, N.J. (1985). Quantitative X-ray diffraction analysis of ettringite, thaumasite and gypsum in concretes and mortars. Cement and Concrete Research, **15**, 431-441.

Diamond, S. (1983). On the glass present in low-calcium and in high-calcium fly ashes. Cement and Concrete Research, **8**, 1107-1113.

Diamond, S and Lopez-Flores, F. (1981). On the distribution between physical and chemical characteristics between lignitic and bituminous fly ashes. Proceedings, Symposium on Effects of Fly Ash Incorporation in Cement and Concrete. Diamond, S. (ed.). Materials Research Society, Boston, 34-44.

Drever, J.I. (1988). The geochemistry of natural waters. 2nd ed., Prentice Hall, New Jersey.

Dudas, M.J. (1981). Long-term leachability of selected elements from fly ash. Environmental Science and Technology, **7**, 840-843.

Eglington, M.S. (1987). Concrete and its chemical behaviour. Thomas Telford Ltd., London.

Falcon, R.M.S. (1978). Coal in South Africa, Part III. The application of petrography to the characterisation of coal. Minerals Science and Engineering, **10**, 28-52.

Falcon, R.M.S., and Snyman, C.P., (1986). An introduction to coal petrography: Atlas of petrographic constituents in the bituminous coals of Southern Africa. Geological Society of South Africa. Review paper no.2.

Fisher, G.L., Chang, D.P.Y., and Brummer, M. (1975). Fly ash collected from electrostatic precipitators: microcrystalline structures and the mystery of the spheres. Science, **192**, 553-555.

Fourie, A.B., Blight, G.E., Bhana, Y., Harris, R., and Barnard, N. (1997). The geotechnical properties of dry dumped and hydraulically placed power station fly ash. Proceedings of the 2nd International Conference on Mining and Industrial Waste Management, Johannesburg.

Frohnsdorff, G. and Clifton, J.R. (1981). Fly ashes in cements and concrete: technical needs and opportunities. Washington: U.S. Department of Commerce, National Bureau of Standards.

Griffin, R.A. and Jurinak, J.J. (1973). Estimation of activity coefficients from the electrical conductivity of natural aquatic systems and soils extracts. Soil Science, **116**, 26-30.

Hassett, D.J., Hassett, D.F., and Brobjorg, J.N. (1988). Control of trace element solubility in coal fly ash leachates. 311-312. In: Proceedings of the 11th Annual Madison Waste Conference, Madison, WI.

Helmuth, R. (1987). Fly ash in cement and concrete. Portland Cement Association, Skokie, Illinois.

Hodgson, F.D. and Grobbelaar, R. (1996). Pozzolanic characteristics and rain-water infiltration at the Kendal fly ash dump. Confidential research report to ESKOM, 1-23.

Hubbard, F.H. and Dhir, R.K. (1984). A compositional index of the pozzolanic potential of pulverised fuel ash. In: Journal of Materials Science Letters, **3**, 958-960.

Hubbard, F.H., Dhir, R.K., and Ellis, M.S. (1985). Pulverised fuel ash for concrete: compositional characterisation of United Kingdom PFA. Cement and Concrete Research, **15**, 185-189.

Hullett, L.D., Weinberger, A.J., Northcutt, K.J., and Ferguson, M. (1980). Chemical species in fly ash from coal-burning power plants. Science, **210**, 1356-1358.

Jarrige, A. (1971). Les cendres volantes. Paris: Editions Eyrolles.

Jawed, I., and Skalny, J. (1981). Hydration of tricalcium silicate in the presence of fly ash. In: Proceedings of Symposium N on effects of fly ash Incorporation in Cement and Concrete, Boston, 60-70.

Joshi, R.C. and Rosauer, E.A. (1973). Pozzolanic activity in synthetic fly ashes: II, pozzolanic behaviour. Ceramic Bulletin, **52**, 459-463.

Lea, F.M. (1971). The chemistry of cement and concretes. Edward Arnold, London.

Lesch, W. (1987). The mineral and glass content of South African fly ash, Unpublished M.Sc. Thesis, University of Stellenbosch, SA.

Lesch W. and Cornell D.H. (1987). The mineralogy and morphology of fly ash from South African power stations, Ash- a valuable resource, CSIR, session-13, 13p.

Lindsay, W.L. (1979). Chemical equilibria in soils. John Wiley and Sons, New York.

Linton, R.W., Williams, P., Evans, C.A. and Natusch, D.F.S. (1977). Determination of the surface predominance of toxic elements in airborne particles by ion microprobe mass spectrometry and auger electron spectroscopy. Analytical Chemistry, **49**, 1514-1520.

Luke, W.I. (1961). Nature and distribution of particles of various sizes in fly ash. US Army Engineers, Waterways Experiment Station, Technical Report No. 6-583.

Malhotra, V.M. and Ramezanianpour, A.A. (1994). Fly ash in concrete, 2nd ed., CANMET, Ottawa.

Massazza, F. (1998). Pozzolana and pozzolanic cements. In: Hewlett, P.C. (ed.). Lea's chemistry of cement and concrete, 4th ed., 471-631.

Mather, B. (1984). The glass in low calcium fly ash. Cement and Concrete Research, **14**, 887-890.

Mattigod, S.V., Rai, D., Eary, L.E. and Ainsworth, C.C. (1990). Geochemical factors controlling the mobilisation of inorganic constituents from fossil fuel combustion residues: I. Review of the major elements. Journal of Environmental Quality, **19**, 188-201.

Mehta, P.K. (1994). Testing and correlation of fly ash properties with respect to pozzolanic behaviour. Electric Power Research Institute, Report CS314. Palo Alto, CA.

Morris, G.K. (1997). Energy minerals; Coal. In: Metals and Minerals; Annual review, 1997. Mining Journal LTD., London.

Norrish, K. and Hutton, J.T. (1969). An accurate X-ray spectrographic method for the analysis of a wide range of geological samples. Geochimica et Cosmochimica Acta, **33**, 431-453.

Odler, I. (1998). Hydration, setting and hardening of Portland cement. In: P.C. Hewlett (ed.). Lea's chemistry of cement and concrete, 4th ed., 241-297.

Padia, A.S., Sarofim, A.F., and Howard, J.B. (1976). The behaviour of ash in pulverised coal under simulated combustion conditions. Paper presented at the Spring Meeting of the Central States Section, Columbus, Ohio.

Potts, P.J. (1992). A handbook of silicate rock analysis. Blackie, Glasgow.

Raask, E. (1968). Cenospheres in pulverised-fuel ash. Journal of the Institute of Fuel, **13**, 339-344.

Raask, E. and Bhaskar, M.C. (1975) Pozzolanic activity of pulverised fuel ash. Cement and Concrete Research, **5**, 363-376.

Ravina, D. (1980). Optimised determination of PFA (fly ash) fineness with reference to pozzolanic activity. Cement and Concrete Research, **10**, 573-580.

Reeve, R.C. (1982). Modulus of rupture. pp.466-471. In: C.A. Black (ed.). Methods of Soil Analysis, Part 1. American Society of Agronomy, Madison, Wisconsin.

Rhoades, J.D. (1996). Salinity: Electrical conductivity and total dissolved solids. In D.L. Sparks (ed.) Methods of Soil Analysis, Part 3. Methods of chemical analysis. p. 420.

Schwab, A.P. (1995). Application of chemical equilibrium modelling to leachates from coal ash. pp.143-161. In: Loeppert, R.H., Schwab, A.P. and Goldberg, S. (eds.). Chemical equilibrium and reaction models, SSSA special publication number 42, Madison, Wisconsin.

Singer, J.K., Anderson, J.B., Ledbetter, M.T., McCave, I.N., Jones, K.P.N., and Wright, R. (1988). An assessment of analytical techniques for the size analysis of fine-grained sediments. Journal of Sedimentary Petrology, **58**, 534-543.

Smit, J.P. (1998). Communication C2666 M: Stabilisation of soluble waste in bricks manufactured at Secunda. Confidential Report, MINTEK.

Standard Test Methods (1979). The determination of the liquid limit of soils by means of the flow curve method.

Takemoto, K. and Uchikawa, H. (1980). Hydration of pozzolanic cement. In: Proceedings of the 7th international congress on the chemistry of cement, **1**, s.iv.2/1-iv.2/29.

Taylor, H.F.W. (1997). Cement Chemistry. Academic Press, London.

Thorne, D.J. and Watt, J.D. (1965). Composition and pozzolanic properties of pulverised fuel ashes. II. Pozzolanic properties of fly ashes, as determined by crushing strength tests on lime mortars. Journal of Applied Chemistry, **15**, 595-604.

Townsend, W.N. and Gillham, E.W.F. (1975). Pulverised fuel ash as a medium for plant growth. pp.287-304. In: The ecology of resource degradation and renewal, M.J. Chadwick and G.T. Goodman (eds.). Blackwell Scientific, Oxford.

Valenti, G.L., Sabatelli, V., Marchese, B., (1978). Hydration kinetics of tricalcium silicate solid solutions at early ages. Cement and Concrete Research, **8**, 61-72.

Van Olphen, H. (1977). An introduction to clay colloid chemistry. 2nd ed., Wiley-Interscience, New York.

Watt, J.D. and Thorne, D.J. (1965). Composition and pozzolanic properties of pulverised fuel ashes. I. Composition of fly ashes from some British power stations and properties of their component particles. Journal of Applied Chemistry, **15**, 585-594.

Watt, J.D. and Thorne, D.J. (1966). The composition and pozzolanic properties of pulverised fuel ashes. III. Pozzolanic properties of fly ashes as determined by chemical methods. Journal of Applied Chemistry, **16**, 33-39.

Wesche, K. (1991). Fly ash in concrete: properties and performance. Chapman and Hall, London.

White, R.E. (1997). Principles and practice of soil science: the soil as a natural resource. 3rd ed., Blackwell Science, London.

Willis, J.P. (1987). Variations in the composition of South African fly ash, Ash – a valuable resource, 2-6 February 1987, CSIR, Vol. 3.